PAGE, AZ

OCTOBER 6-8, 2017

PTYS594A: PLANETARY GEOLOGY FIELD STUDIES
LUNAR AND PLANETARY LABORATORY
UNIVERSITY OF ARIZONA

Letter from the Editor

Hello everyone! This semester we are heading to Page, Arizona to explore slot canyons and Horseshoe Bend. We're going on a boat, so that's pretty rad.

Don't forget your field books, colored pencils, compasses, and hand-lenses because we'll be sketching, striking, and dipping on this quick three-day field trip.

Sarah Peacock

Participants

Bramson, Ali
Brock, Laci
Cambioni, Saverio
Ganesh, Indujaa
Garnello, Anthony
Hamilton, Christopher
Komacek, Tad
Lo, Daniel
O'Brien, Patrick
Peacock, Sarah
Pearson, Kyle
Seifert, Laura
Spitale, Joe
Steinrueck, Maria
Sutherland, Adam
Tigges, Mattie

Table of Contents

Schedule

Friday, October 6

7:00 am	Pick up rental vehicles, meet in the car park behind the Flandreau Planetarium, and load the trucks.
8:00 am	Depart for the Sunset Crater Volcano National Monument. The estimated drive is 4 hours and 30 minutes (including time to pick up Anthony Garnello).
12:30 pm	Arrive at Sunset Crater Volcano National Monument. Meet at the visitor center, have lunch, explore the local trails, and hear presentations from: *1. Thaddeus Komacek: San Francisco Volcanic Field* *2. Mattie Tigges: Volcanoes – Lava* *3. Saverio Cambioni: Quarrying and Power*
3:00 pm	Depart Sunset Crater Volcano National Monument and drive to Cameron. Estimated Driving Time 45 minutes.
3:45 pm	Arrive in Cameron and hear a presentation from: *4. Uranium Mining and the Navajo People: Adam Sutherland*
4:15 pm	Depart Cameron for Campsite, which is 20 minutes passed the Glen Canyon Dam. Estimated driving time 1 hour 30 minutes.
5:45 pm	Arrive at the campsite. Sunset is at 6:01 pm.

Saturday, October 7

8:00 am Depart the campsite. The main group will be dropped off in Page (at the Colorado River Discovery Visitor's Center) and the drivers will take all five vehicles to Lees Ferry Boat Ramp, returning in one vehicle, and leaving the other four there to bring the group back to Page at the end of the day.

8:30 am The main group arrives at the Colorado River Discovery Visitor's Center.

9:30 am Drivers arrive at the Lees Ferry Boat Ramp.

10:30 am Drivers at the Colorado River Discovery Visitor's Center.

11:00 am Group departs for the boat ride. On the trip we will hear presentations from:

5. *Daniel Lo: Basin and Range*
6. *Indujaa Ganesh: Navajo Sandstone*
7. *Maria Steinrueck: River Systems*
8. *Ali Bramson: Tectonics/Faulting*

3:00 pm Group arrives at Lees Ferry Boat Ramp.

3:30 pm Departs for Glen Canyon Dam. Estimated driving time 1 hour.

4:30 pm Arrive at Glen Canyon Dam for a 30 minute stop.

5:00 pm Depart for the campsite. Estimated driving time 20 minutes.

5:20 pm Arrive at the campsite. Sunset is at 6:01 pm.

Sunday October 8

8:00 am Depart campsite and go to Horseshoe Bend. Estimated driving time 30 minutes.

8:30 am Arrive at Horseshoe Bend and hear presentations from:

9. *Sarah Peacock: Horseshoe Bend*
10. *Laci Brock: Dinosaurs, Birds, & Fish (oh my!)*
11. *Anthony Garnello: Ecological Theory and Practice in the Grand Canyon*

9:45 am Depart Horseshoe Bend for the Waterholes Canyon Trailhead. Estimated driving time 5 minutes.

9:50 am Arrive at the Waterholes Canyon trailhead and conduct a field based exercise as well as hear presentations from:

12. *Christopher Hamilton: General – The Grand Staircase*
13. *Patrick O'Brien: Physics of Aeolian Processes*
14. *Laura Seifert: Aeolian Morphology of the Colorado*
15. *Kyle Pearson: Slot Canyons*

2:00 pm Depart from the Waterholes Canyon Trailhead and drive to Flagstaff. Estimated driving time 2 hours and 30 minutes.

4:30 pm Arrive in Flagstaff, where Anthony Garnello and Christopher Hamilton will be dropped off and then continue on to outskirts of Phoenix for dinner. Estimated driving time 2 hours.

6:30 pm Stop outside of Phoenix of dinner for approximately 30 minutes.

7:00 pm Continue to Tucson. Estimated drive time 2 hours.

9:00 pm Arrive in Tucson and return vehicles. Estimated drive time 2 hours.

Maps

Our overall route extends from Tucson, AZ (A) to Page, AZ (B). Along the way to Page we will strop at the Sunset Crater National Monument, just north of Flagstaff, and at Cameron. The campsite location is approximately 20 minutes past the Glen Canyon Dam, down a gravel road branching from US 89 N.

Locations of Interest near Page, AZ. The turn off for the campsite is marked by an arrow

Routes to camping locations 1 and 2. Well will approach the fork from the north

Draft version modified September 9, 2017
Preprint typeset using LaTeX style emulateapj v. 12/16/11

SAN FRANCISCO VOLCANIC FIELD

Thaddeus D. Komacek

1. INTRODUCTION

The San Francisco peaks are a volcanic field in northern Arizona, just north of Flagstaff. Fig. 1 shows the view of the peaks that we will have on our drive up from Flagstaff toward Page on U.S. 89. The name of the peaks comes from Franciscan Friars, who were conducting missionary work with local Najavo people and named the mountains in honor of Patron Saint Francis of Assisi in 1629 (U.S. Forest Service Website). Note that the Navajo tribe has a different name for the peaks, "Dook'o'ooslííd," which can be translated as "the mountain whose summit never thaws," as the summit is at 3,851 m (12,633 feet) elevation. Additionally, there are a myriad of names for each of the individual peaks, and notably the highest point (Humphrey's peak) is named after Brig. Gen. Andrew Atkinson Humphreys, a captain with the Ives expedition to survey wagon roads and a railroad throughout the region who later became Chief of the Army Corps of Topographical Engineeers.

Fig. 2 shows a digital elevation model of the volcanic field, which covers over $4,600$ km^2 (1,800 square miles) and has more than 600 vents (U.S. Forest Service Fact Sheet 017-01). This volcanic field is less than 6 Myr old, and includes the youngest volcano in the state, Sunset Crater, which erupted less than $1,000$ years ago. The San Francisco peaks themselves are the remains of an eroded stratovolcano, termed San Fransisco Mountain. Surrounding these peaks are the hundreds of volcanic vents, manifested as both cinder cones (e.g. Sunset Crater, SP Crater) and lava domes (e.g., Elden Mountain, very near the city of Flagstaff). Fig. 3 is a digital elevation model (looking from the northeast) nicely showing the relative size and placement of these volcanoes.

Fig. 1.— Image of San Francisco Peaks as seen from U.S. Route 89. From Wikimedia commons.

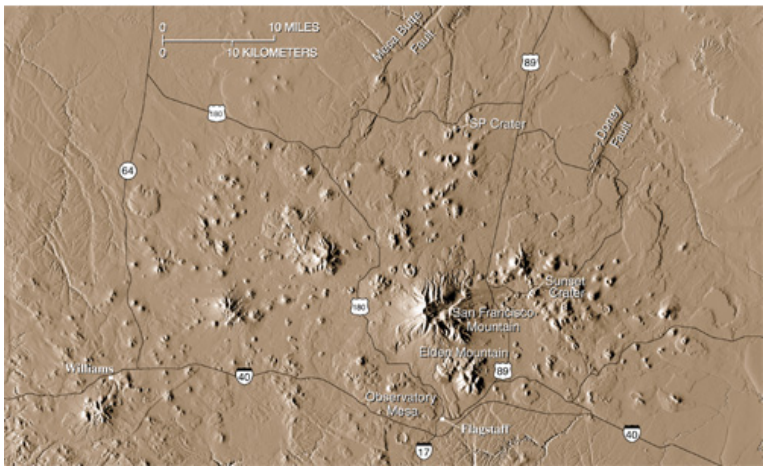

Fig. 2.— A digital elevation model of the San Francisco volcanic field, from U.S. Forest Service Fact Sheet 017-01. Lava flows can be seen near vents, and there are $\gtrsim 600$ vents in the region (all < 6 Myr old). One can also see tectonic features (Mesa Butte and Doney faults) in the north and northeastern parts of the image.

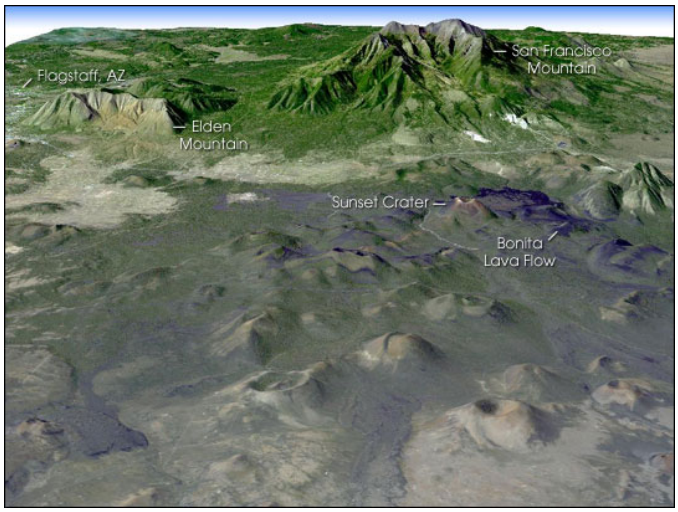

FIG. 3.— Digital elevation model showing the relative size and position of Sunset Crater to San Francisco Mountain and Mt. Elden. From the NASA Earth Observatory.

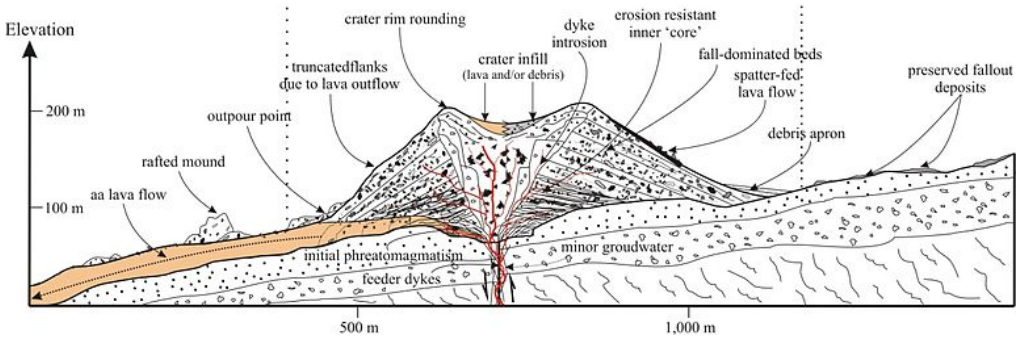

FIG. 4.— Schematic cross section through a cinder cone, from Kereszturi and Nemeth (2012).

2. TYPES OF VOLCANOES

Most of the vents in the San Francisco volcanic field are basaltic cinder cones. Cinder cones are formed of loose pyroclastic material formed by lava fountaining or exploding outward from a single vent (Sigurdsson et al. 1999). Fig. 4 shows a sample cross section of a cinder cone, showing the typical volcanic deposition processes related to their formation and their geomorophology. Cinder cones are often found on the flanks of larger volcanoes (stratovolcanoes and shield volcanoes). For example, recall the field trip (for those that attended) to Hawai'i, where we found a myriad of cinder cones on the flanks of Mauna Kea during the drive up to the observatory.

San Francisco Mountain was the only stratovolcano in the San Francisco volcanic field, formed between $0.5 - 1$ Mya (U.S. Forest Service Fact Sheet 017-01). The famous "inner basin" that the San Francisco peaks surround has been formed since that time. The exact formation of the inner basin is unknown, but possibilities include an eruption similar to the recent eruption of Mt. St. Helens or slower erosional processes such as glacial scouring. Regardless of its relevance for the formation of the inner basin, glacial scouring is seen on the slopes of the San Francisco Peaks, especially along the northeast (which is the direction from which the inner basin is most visible).

The San Francisco volcanic field is of course not solely basaltic in composition, as there is a combination of cinder cones and stratovolcanoes that are formed by more viscous lava. The field also includes lava domes, which are formed by lava with high viscosity and hence high silica content (e.g. dacite, rhyolite). Due to the large viscosity of these lavas, they form domes with very steep sides. Lava domes can be formed by both internal inflation ("endogenous" domes) and lava added to the flanks ("exogenous" domes). Both types of domes are found in the San Francisco volcanic field: Mt. Elden (near the town) is an exogenous dome, while Mt. Sugarloaf (near the inner basin) is thought to be endogenous (U.S. Forest Service Fact Sheet 017-01).

3. FORMATION: INLAND VOLCANISM

Perhaps surprisingly, the San Francisco volcanic field is thought to have formed due to a mantle plume, or volcanic "hot spot." Due to subduction of the pacific plate under the north american plate, the north american plate is moving westward with respect to the mantle. As a result, the crust of northern Arizona is also moving westward with respect to the mantle. Hence, the San Francisco volcanic field is aging from west to east. That is, vents on the westward side (near Williams, AZ) are the oldest, and those on the eastward side (e.g. Sunset Crater) are the youngest. This

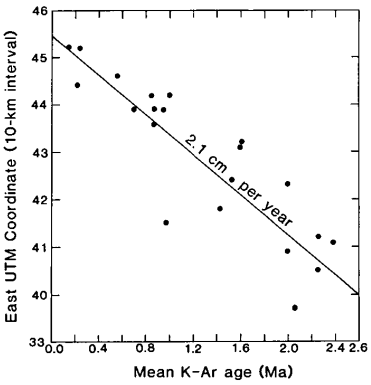

FIG. 5 K-Ar ages of volcanic rocks (x-axis) compared to geographical location (y-axis) for young rock samples in the San Francisco volcanic field. The linear fit (with an $R^2 = 0.76$) indicates that the eastward migration rate of volcanism in the field is 2.1 cm/yr. From Tanaka et al. (1986).

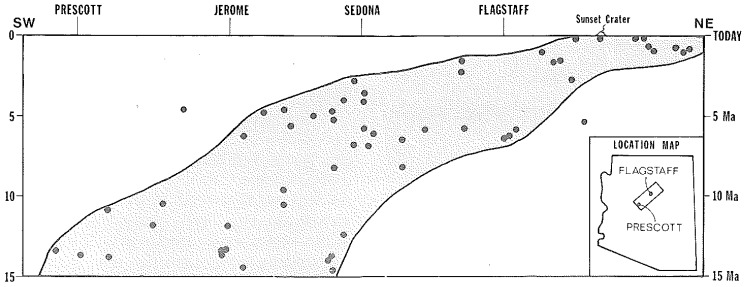

FIG. 6.— Ages of volcanic rocks (y-axis) compared to their geographic positions (from Prescott to Flagstaff, x-axis). Active volcanism has been moving from Prescott to Flagstaff over the past 15 Myr. From Reynolds et al. (1986).

has been borne out through K-Ar dating of silicic rock samples, see Fig. 5. This "belt" of volcanoes extends ≈ 50 miles from west to east (U.S. Forest Service Fact Sheet 017-01), and may correlate with even older volcanic rocks near Prescott, see Fig. 6. Of course, this volcanic field is still active, but it is expected that future eruptions will be both small and not near the city of Flagstaff.

Though the general mechanism of the volcanic field moving from west to east is easily understood using a mantle plume, it is not clear *a priori* what caused the San Francisco Mountain stratovolcano to form. Additionally, it is not clear without deatiled study how the mantle plume is generated – is it a large-scale plume from the D" layer (that is, the bottom of the mantle), or local heating due to subduction of the pacific plate? Tanaka et al. (1986) showed that the latter is more realistic, with the lava chemistry pointing towards origination as partial melt from the base of the lithosphere. This is also borne out through strontium isotopic measurements (Brookins and Moore 1975). The partial melt that led to the formation of the volcanic field is likely caused by shear heating at the base of the lithosphere, where asthenospheric flow viscously dissipates energy, heating up the base of the lithosphere and causing partial melting (Tanaka et al. 1986). Using this mechanism, the formation of the large San Francisco Mountain can be explained through a possible "bump" at the bottom of the lithosphere allowing for an enhancement in viscous dissipation and localized increase in partial melt, leading to more vigorous volcanism.

4. PLANETARY CONNECTIONS

On Earth, stratovolcanoes are made of magma that is of intermediate composition, which requires a combination of mafic (low viscosity) and felsic (high viscosity) material. Magma with intermediate composition naturally forms at plate boundaries between the mafic oceanic crust and felsic continental lithosphere on Earth, but such plate boundaries do not exist on other planets in the solar system. As a result, one might naively think that stratovolcanoes do not occur on planets without plate tectonics, which includes all bodies in the solar system besides Earth. However, though stratovolcanoes on Earth have intermediate composition, they need not have such a composition on other planets. For a volcano to be deemed a stratovolcano, there just needs to be a combination of lava flows and pyroclastic deposits (Walker 1993). Given that mafic magma systems can lead to both effusive eruptions (with lava flows) and explosive eruptions (with pyroclastic deposits), stratovolcanoes could form in basaltic magma systems such as those on Mars.

Stewart and Head (2001) present geomorphologic evidence from Mars Orbiter Laser Altimeter (MOLA) altimetric data that Zephyria Tholus (a hill on Mars) is stratovolcanic in origin (see Figs. 7 and 8). They also find six other features near Zephyria Tholus that appear to be stratovolcanoes. These features have sizes similar to Earth stratovolcanoes, but shallower flank slopes. However, it is expected that pyroclastic eruptions on Mars would lead to volcanoes with shallower slopes (Wilson and Head 1994), so the flank slopes are still consistent with stratovolcanoes. Additionally, these features appear to be Noachian in age, which is contributing evidence toward a stratovolcanic origin. Though these are apparent stratovolcanoes, they are not coincident with a subduction zone. Hence, the explanation for these stratovolcanoes (if they are truly stratovolcanoes) cannot lie in plate tectonic-like motions on early Mars, but

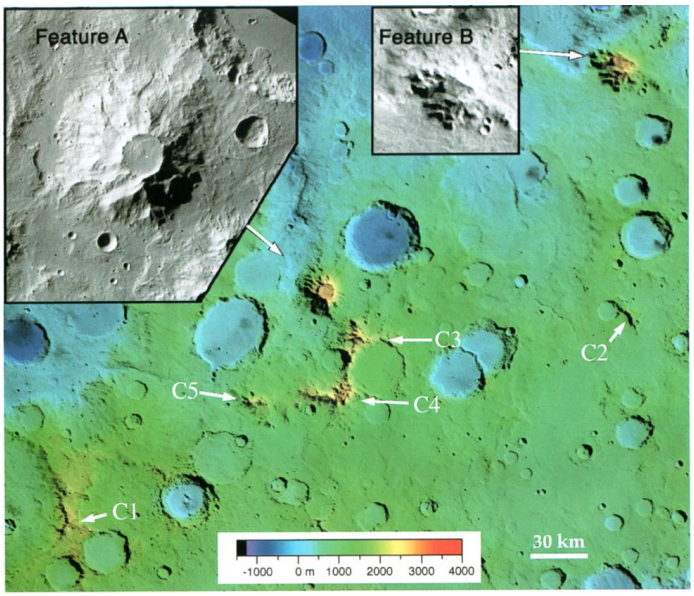

FIG. 7.— Viking image overlain with MOLA topography for the region surrounding Zephyria Tholus (feature A) and Nplh (feature B). Additionally, features C1-C5 show other dome-shaped features that have similar topography to features A and B. From Stewart and Head (2001).

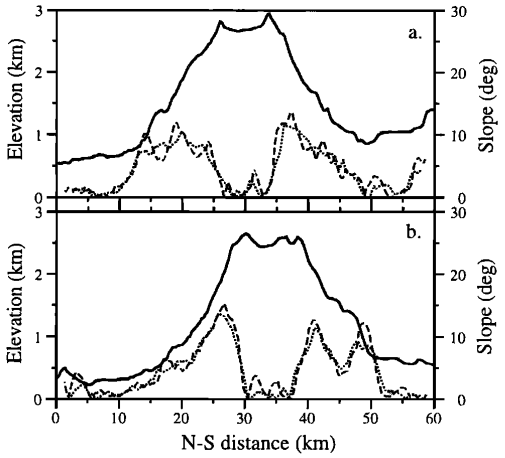

FIG. 8 MOLA summit profile of Zephyria Tholus (A) and Nplh (B). Elevation is solid lines, slopes dashed lines (3 km baselines are dashed lines, 5 km baselines are dotted lines). From Stewart and Head (2001).

from a different mechanism. Potentially, viscous heating due to interactions between a hot young athenosphere and lithosphere (similar to that mentioned above by Tanaka et al. 1986) could play a role in the formation of these ancient Martian stratovolcanoes.

REFERENCES

U.S. Forest Service Website. History of the San Francisco Peaks. URL https://www.fs.usda.gov/detail/coconino/about-forest/about-area/?cid=stelprdb5340115.

U.S. Forest Service Fact Sheet 017-01. The San Francisco Volcanic Field, Arizona. URL https://pubs.usgs.gov/fs/2001/fs017-01/.

G. Kereszturi and K. Nemeth. *Updates in Volcanology - New Advances in Understanding Volcanic Systems*, chapter Monogenetic Basaltic Volcanoes: Genetic Classification, Growth, Geomorphology and Degredation. 2012.

H. Sigurdsson, B. Houghton, H. Rymer, J. Stix, and S. McNutt. *Encyclopedia of Volcanoes*. Academic Press, 1999.

K.L. Tanaka, E.M. Shoemaker, G.E. Ulrich, and E.W. Wolfe. Migration of volcanism in the San Francisco volcanic field, Arizona. *Geological Society of America Bulletin*, 97:129, 1986.

S.J. Reynolds, J.W. Welty, and J.E. Spencer. Volcanic history of Arizona. *Arizona Bureau of Geology and Mineral Technology Fieldnotes*, 16(2), 1986.

D.H. Brookins and R.B. Moore. Strontium isotope initial ratios from the San Francisco volcanic field, Arizona. *Isochron/West*, (12):1, 1975.

E.M. Stewart and J.W. Head. Ancient Martian volcanoes in the Aeolis region: New evidence from MOLA data. *Journal of Geophysical Research*, 106:17505, 2001.

G.P.L. Walker. *Magmatic Processes and Plate Tectonics*, chapter Basaltic-volcano systems, page 3. Number 76. Geological Society Special Publication, 1993.

L. Wilson and J.W. Head. Mars: Review and analysis of volcanic eruption theory and relationships to observed landforms. *Review of Geophysics*, 32:221, 1994.

Mattie Tigges

Volcanoes: Lava

Two different types of lava: Pahoehoe (dark) flows over A'a (light)

Types of basaltic lava
Pahoehoe ("*paw-hoey-hoey*"): Forms on land, smooth, ropy look

A'a ("*ah-ah*"): Forms on land, chunks of angular basalt, formed when lava flows rapidly

Pillow ("*pill-oh")*: Forms underwater

Sunset Crater
Cinder cone (340m high)
Ejected material went about 259m up- Statue of Liberty is 93m tall. Yikes!

About 25% of the magma erupted as lava flows
Bonito extends ~2.5km NW
Kana-a extends ~9.6km NE

10m high FOUNTAIN OF LAVA (of the pahoehoe sort)

Bonito Lava Flow and Sunset Crater

Lava's effect on landscape and cool ish left behind
Soil: devoid of plant life for ~400 years, growth started ~500 years ago
It takes a long time for soil to recover!
Bonito flow preserved a big ol' crack
10km long!
Squeeze ups! Nice!
Lava tubes and ravines from collapsed tubes!

Oh yeah, volcanoes and lava affect people too: eruption scares!
2015: a website with satellite images showed steam rising from Sunset crater. It was actually a wildfire. Oops.

Squeeze up: so waow, much yes

Saverio Cambioni

Introduction

The area surrounding Antelope canyon is part of the Navajo Nation, extendig into the states of Utah, Arizona and New Mexico, covering over 27,000 square miles.

- Energy and natural resource revenues, including earnings from forest products and agricultural enterprises, are (and are expected to remain) major contributors to the Navajo economy even as it diversifies.
- Leases for mineral and petroleum exploration or extraction currently total 400,000 acres, or about 2.5 percent of the reservations land area.
- The Navajo Nation practices environmental protection in the prudent development of its mineral and stone resources.[1]

Prudence goes along with the respect of Navajo traditions, in particular for what concerns the sacred lands and rivers.

- Traditional Navajos and Hataałii make offerings to both the mountains and rivers for the well-being of the Navajo People.
- As explicitly indicated in the *Natural Resources Protection Act*, mining, quarrying or other any type of economic activity are subjected to special laws (prohibited) in the sacred areas.

Quarrying

A quarry is a place from which dimension stone, rock, construction aggregate, riprap, sand, gravel, or slate has been excavated from the ground.

- A quarry is the same thing as an open-pit mine from which minerals are extracted.
- The only non-trivial difference between the two is that open-pit mines that produce building materials and dimension stone are commonly referred to as quarries. The word quarry can also include the underground quarrying for stone, such as Bath stone. [3]

Quarrying is restricted by law all over the the sacred mountains are the boundaries of Navajoland.

- The four mountains are located in the four cardinal directions, with two additional mountains toward the east symbolizing the entrance to Navajoland.
    - The east (ha'a'aah) mountain is Sisnaajiní - Blanca Peak near Alamosa, Colorado;
    - The southern (shádi'ááh) mountain is Tsoodził - Mt. Taylor by Grants, New Mexico;
    - The west (e'e'aah) mountain is Dook'o'oosłííd - San Francisco Peaks near Flagstaff, AZ;
    - Tthe northern (náhook-s) mountain is Dibé Ntsaa - Mount Hesperus, near Durango, Colorado.

Figure 1: Navajolands with the sacred mountains and rivers

Between the many quarrying activities in the Navajo area, the extraction of nearly pure quartz sands is getting more and more important[4]:

- Pure quartz sands have become increasingly important for oil and gas production and have appropriate properties for use in hydraulic fracturing ("frac sands").
- A main player was the Preferred Sands plant and quarry which was active in 2015 (last year of the survey), with employment of 53 workers according to the U.S. Department of Labor.

If we consider all the mineral extraction activities, we should for sure include mining of uranium and coal.

- Many private entities, including Cyprus Amax (a successor-in-interest to Vanadium Corporation of America and Climax Uranium Company) and Western Nuclear, mined approximately thirty million tons of uranium ore on or near the Navajo Nation between 1944 and 1986.
- Tribal members have worked over long periods in the coal and uranium mining industries. Many Navajo people worked in and near the mines, often living and raising families in close proximity to the mines and mills.
- Uranium mining have ceased in Navajo lands but the effects are still felt today.[5]
- In the past, the exploitation of Navajo resources has been a harsh point of conflict between Federal government and Navajo Nation leaders, especially for what concerns Uranium extraction for the Manhattan project and in the Cold War (see Native American section for more details).

Modern strategy of the Navajo Nation to avoid wild quarrying and mining is a combination of environmental laws and landscape conservation laws.

- Some patterns design natural mining and quarrying opportunities.
- Navajos works to include these patterns under the national park regulation, which prevents from wild activities (e.g. Antelope Canyon). [6]

Power generation

The main power station is the Navajo Generating Station.

- This is a net coal-fired powerplant located on the Navajo Indian Reservation, near Page, AZ.
- This plant provides electrical power to customers in Arizona, Nevada, and California.
- It also provides the power for pumping Colorado River water for the Central Arizona Project, supplying about 1.5 million acre feet (1.85 km3) of water annually to central and southern Arizona (so to Tucson and Phoenix as well).

Year	GW·h
2011	16,952
2012	15,888
2013	17,132
2014	17,297
2015	13,573
2016	12,059

Figure 2: On the left, the Navajo Generating Station seen from the nearby Lake Powell, from where the cooling water is pumped. On the right, energy production by coal-firing in the different years.

The power plant is part of the Navajo Power Project, consisting of the Navajo Generating Station (NGS) along with the Kayenta mine, Black Mesa & Lake Powell (BM&LP) Railroad, and 800 miles (1,300 km) of 500 kV transmission lines.

- The site was close to a source of competitively priced fuel and a reliable source of surface water for cooling. Indeed the site is three miles (5 km) south of Lake Powell on 1,786 acres (723 ha) of land leased from the Navajo Nation.
- Northern Arizona and the Colorado Plateau have consistently met National Ambient Air Quality Standards (NAAQS) established to protect public health.
- NGS and Kayenta Mine payments in 2012 accounted for about a quarter of the Navajo Nation's revenues, and 65% of the Hopi Tribe's revenues.
- In addition to payments that help fund the Navajo central government and more than 100 local entities, the power plant and coal mine are key employers in northern Arizona.

The plant produces also byproducts for industrial application:

- The plant sells about 500,000 tons of fly ash per year for use in the manufacture of concrete and Flexcrete insulating block building product.
- Bottom ash and gypsum, a byproduct of the scrubber operation, are dewatered in the removal process; and, along with any fly ash not sold, are landfilled on-site as solids.

The cumulative economic impact on the state of Arizona as a whole for the time period 2011 - 2044 was expected to be $20 billion in gross state product, or about $330 million per year in disposable income and $20 million per year in state tax revenues, also assuming all three units continued running.

As of 2017 permission to operate as a conventional coal-fired plant is anticipated until 2017-2019 and to December 22, 2044 if extended.

- In February, its operators announced they wanted to close the plant in 2019, a quarter-century earlier than expected.
- The recent fracking boom has pushed prices of natural gas so low, coal is no longer competitive in some markets. [6]

Glen Canyon Dam is a concrete arch-gravity dam on the Colorado River in northern Arizona, United States, near the town of Page. It forms Lake Powell, one of the largest man-made reservoirs in the U.S. with a capacity of 27 million acre feet (33 km^3). The dam is used to:

- Control the capacity of the river, which was very unpredictable in the past and caused major damages (flood of part of California's Imperial Valley and creation of the Salton Sea in 1904);
- Provide carry-over water storage for times of drought.
- Allow hydroelectricity generation. It is the second-biggest producer of hydroelectric power in the Southwestern United States, after Hoover Dam. Moreover, it regulates the flow for two additional hydroelectric dams, at Marble Canyon and Bridge Canyon (Colorado River Storage Project).

Its capabilities are:

- A total capacity of 1,320 megawatts from eight 165,000 kilowatt generators.
- Between 1980 and 2013, Glen Canyon Dam generated an average of 4,717 gigawatt hours (GWh) per year, enough for about 400,000 homes. The highest was 8,703 GWh in 1984, and the lowest was 3,299 GWh in 2005.
- Drought conditions in the 21st century have reduced the amount of hydropower available from Glen Canyon Dam.

Because of its tremendous ecological effect on the Colorado River, the Glen Canyon Dam has been subject to decades of criticism from the environmental movement:

- Being located in a high desert climate amid porous geology, Lake Powell causes huge evaporation and seepage losses. The Glen Canyon Institute estimates that 860,000 acre feet (1.06 km^3) is lost from the reservoir in an average year.
- About 100 million US tons (90,700,000 metric tons) of sediment are trapped behind the dam annually, changing the flows of the Colorado and its tributaries.

- Huge effect on local fluvial flora and fauna ("death zone for native fish") [7]

Figure 3: Aereal view of the Glen Dam and the Lake Powell

References

[1] Navajo nation website, http://www.navajoadvantage.com/pages/natrlrs.htm

[2] Significant Traditional Cultural Properties of the Navajo People, http://www.hpd.navajo-nsn.gov

[3] Wikipedia page, https://en.wikipedia.org/wiki/Quarry

[4] Silica-Sand Deposits in Arizona, http://repository.azgs.az.gov

[5] International expert group meeting on indigenous peoples and protection of the environment, United nation report, 2007

[6] Wikipedia page, https://en.wikipedia.org/wiki/Navajo_Generating_Station

[7] Wikipedia page, https://en.wikipedia.org/wiki/Glen_Canyon_Dam

Adam Sutherland

Uranium Mining and the Navajo People

- 92% of U mines are on the Colorado plateau.
- 521 abandoned mines exist on the Navajo Reservation.
- In some places around the mines, the cancer rate is 200 times the norm.
- Mining company and government response is lacking.

The Navajo People

- Largest reservation in the US, population of 180,000
- One of the only reservations to keep their original land.
- Reservation was expanded multiple times after the civil war.

Formation of Uranium Deposits

- Nearly all of the uranium-vanadium Carnotite mines in the Monument Valley district occurred in the Shinarump Sandstone Member of the Triassic Chinle Formation.
- The deposits in the Shinarump Member occur in paleochannels scoured into the underlying Moenkopi Formation. Sometimes reaching into the Permian De Chelly Sandstone underlying the Moenkopi.
- Ore deposits are associated with carbonized wood in the sandstone.

Collapsed Breccia Pipe:

- Easier to mine. Cheaper. Totally vertical. North and south of the grand canyon. Not on reservation land. 1000-2000 ft deep shaft.
- Collapse breccia pipes are vertical cylindrical columns of broken sedimentary rock, in caverns in underlying limestone.
- Uraninite accumulated within the permeable column of broken rock, forming a cylindrical and vertical uranium deposit.

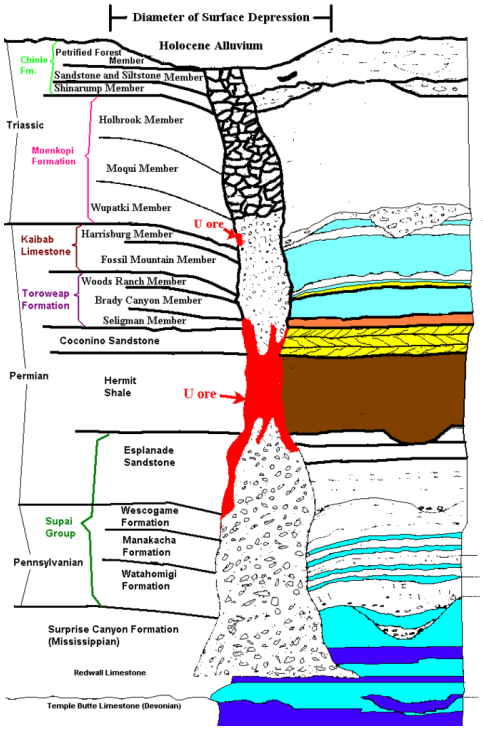

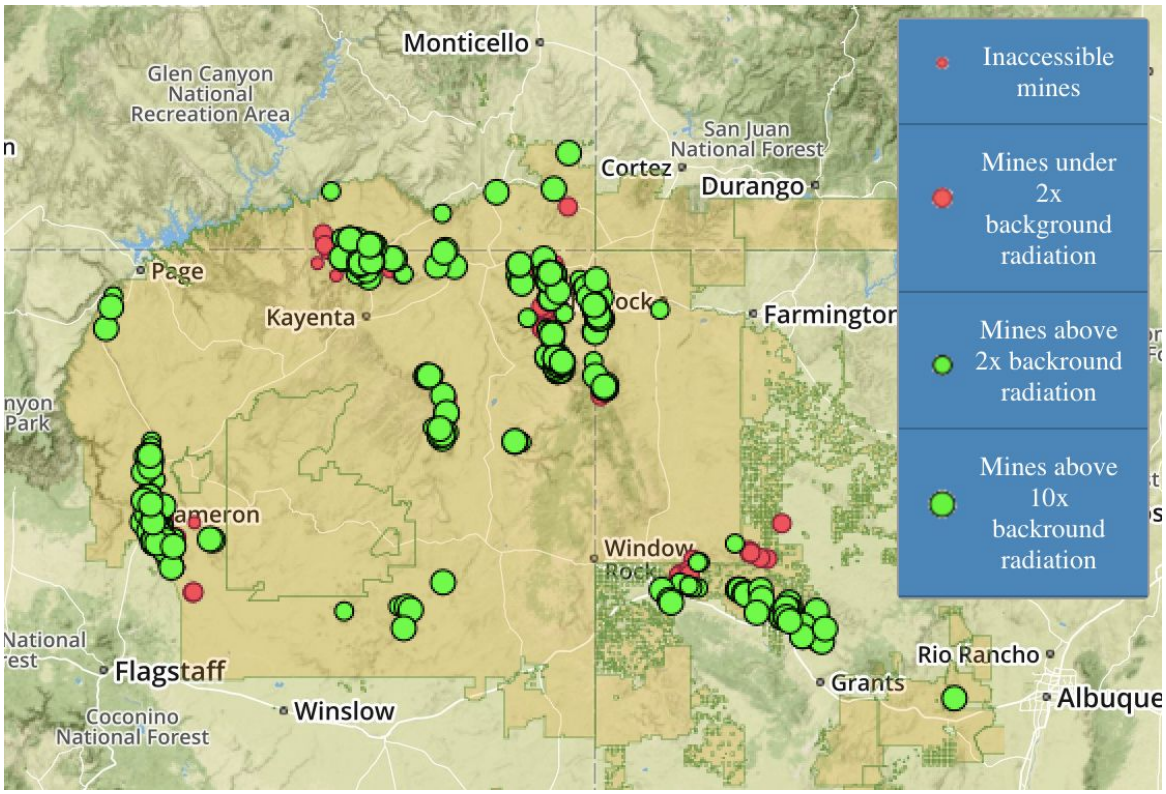

Uranium Mining History

- Carnotite was mined for vanadium before the nuclear age.
- Vanadium was used to lighten steel on Model T Fords and bicycles.
- Mining for Uranium started in the late 1940s
- Majority of the mining was in Monument Valley. Cameron district had the second most.

- Mining stopped in the Monument Valley district in 1969, after producing 8.7 million pounds of uranium oxide, the most in Arizona.
- Mining operations continued in smaller scale in other locations until 2005 the Navajo Nation declared a moratorium on uranium mining on the reservation, for environmental and health reasons.

Most Navajo miners at the time were not informed of the dangers and were not provided with proper safety gear. Especially for the radon gas in the mines, which led to lung cancer rates 27 times higher than normal for miners. Kidney damage was the other large side effect, affecting the people who lived in the towns near by just as much as the miners.

- Most of the ore went to nuclear weapons.
- Not just a problem for those who mined, but a problem for their relatives as well.
- Children who grew up near the mines after decommissioning.
- The mining contaminated water sources. Sometimes the only sources in the area. People now drive over 50 miles to get water once a week.

Radiation exposure was not considered an illness until the 1990s, so many miners could not get compensation. EPA created in 1970. No federal oversight for decades, leading to massive contamination. Many miners were not informed of the risks, even when they were required to be informed by law. Language barriers and racism further exacerbated the problem.

Church Rock Uranium Mill Spill

- A New Mexican Uranium mill dam spilled over contaminating waterways for 80 miles in 1979.
- Largest radioactive incident in American history.
- NM governor refused to ask the federal government for support, so cleanup efforts were limited.

Effects today

- Rates for certain cancers 200 times above average for mining communities.
- More than 10% of wells above federal levels for radiation.
- Some lawsuits have been won, such as a recent settlement for $1 billion from a mining company. But many mining companies no longer exist. Out of 521 mines, the government only knows who is responsible for 78 of them.
- The *Radiation Exposure Compensation Act* attempted to compensate miners and downwinders.
- Compensation is hard to prove after such long times. Lack of good research on long term effects of uranium exposure.
- Some other more recent acts attempt to help with the cleanup but only target the most affected mines. Current funding rates would take 100 years for the clean up.
- Current uranium rates in children's blood is above national levels.

Breccia mining was planned for north of the grand canyon but abandoned after the prices of uranium fell post Fukushima

Highlights the caution needed for health and the environment concerns when exploring other worlds.

References:

1. Lauren Renteria. *Contamination from decades of uranium mining lingers on Navajo land*, Arizona Sonora News Service http://arizonasonoranewsservice.com/contamination-from-decades-of-uranium-mining-lingers-on-navajo-land/
2. *Uranium Mines in Navajo country and Beyond*, SRIC http://www.sric.org/uranium/docs/Navajo_AUM_Maps_Photos_101013rev.pdf
3. *Navajo Nation: Cleaning Up Abandoned Uranium Mines*, EPA https://www.epa.gov/navajo-nation-uranium-cleanup
4. Sen. Kennedy, Edward M., *S.1865 - Radiation Exposure Compensation Act of 1979*, https://www.congress.gov/bill/96th-congress/senate-bill/1865
5. Brandon Loomis, The Republic. *Abandoned uranium mines continue to haunt Navajos on reservation*. Parts 1-3. http://www.azcentral.com/story/news/arizona/investigations/2014/08/04/uranium-mining-navajos-devastating-health-effects/13591333/
6. Karen J. Wenrich, *Uranium Mining in Arizona—High Grade and Safe*
7. William L. Chenoweth, *Summary of the uranium-vanadium ore production 1947-1969 Monument Valley district, Apache and Navajo Counties, Arizona*, AZGS, May 2014.
8. Francie Diep, *Abandoned Uranium Mines: An "Overwhelming Problem" in the Navajo Nation*. Scientific American, Dec 2010. https://www.scientificamerican.com/article/abandoned-uranium-mines-a/
9. *Cameron Area Abandoned Uranium Mines*, EPA Aug 2014

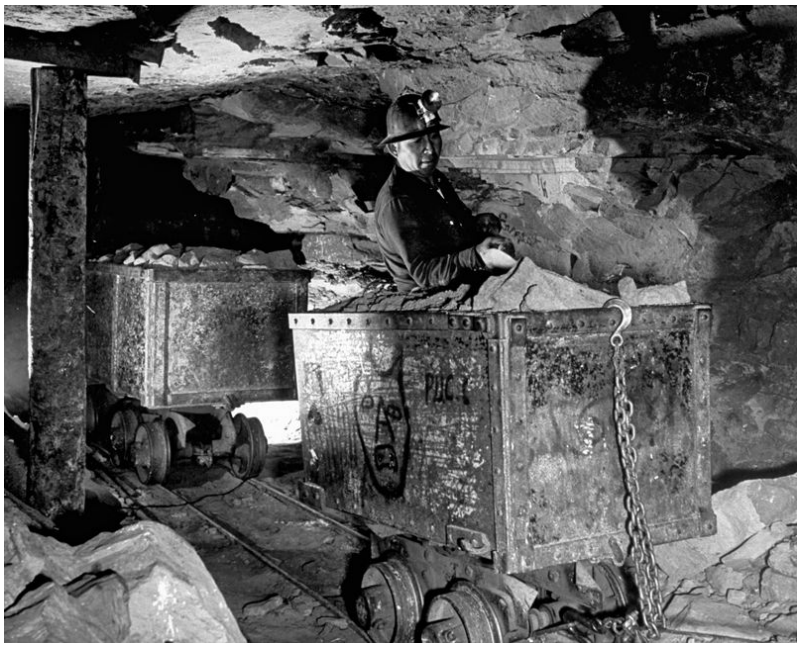

Basin and Range

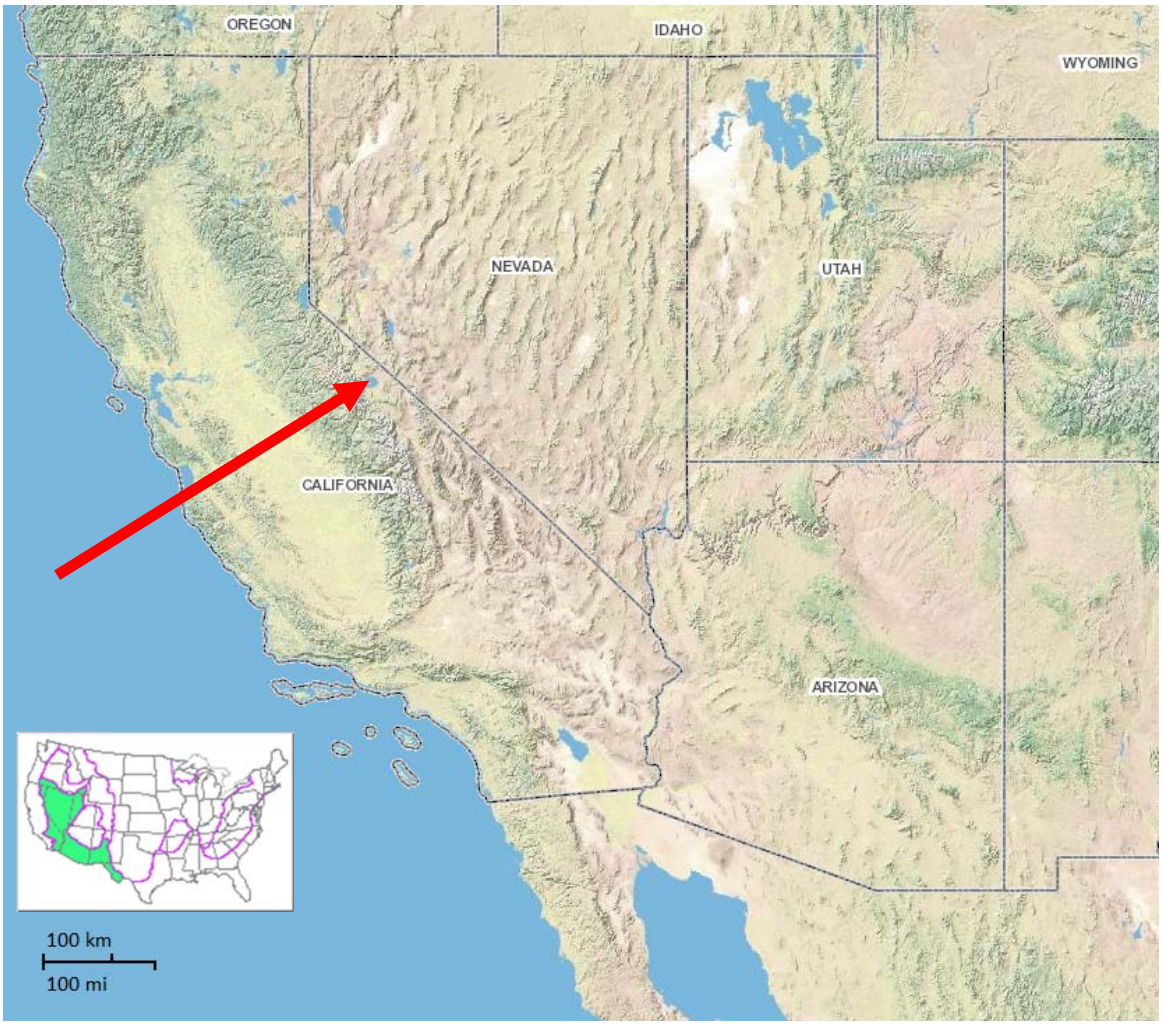

"Army of caterpillars marching towards Mexico" – Clarence Dutton [Image from USGS]

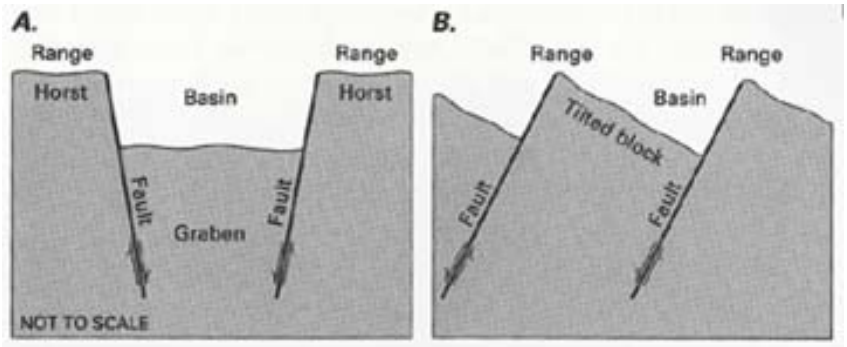

Effects of crustal extension: (A) Uplifting and subsidence, (B) Tilting [Image from USGS]

Basin and range topography is a term used to describe a landscape of alternating parallel mountain ranges and valleys formed from crustal extension. Tensional stresses result in the formation of normal faults perpendicular to the direction of stress. Between these normal faults are blocks of crust, which can subside to form basins, be uplifted to form mountain ranges, or tilted to form both valleys and mountain ranges. Unlike purely uplifting and subsidence, tilting along gently dipping normal faults (detachment faults) tend to create asymmetric faulting with one side steeper than the other. As the crust undergoes further extension, the uplifting, subsidence and/or tilting become more pronounced.

The archetypical basin and range topography can be found in the surprisingly-named Basin and Range Province that spans much of the inland western United States and northwestern Mexico. The Basin and Range Province is bordered on the west by the eastern fault scarp of the Sierra Nevada and spans over 500 miles (800 km) to its eastern border marked by the Wasatch Fault, the Colorado Plateau and the Rio Grande Rift. It extends north to the Columbia Plateau and south as far as the Trans-Mexican Volcanic Belt (close to the southern extent of the Gulf of Mexico). Thus, in Mexico, the Basin and Range Province is dominated by and largely synonymous with the Mexican Plateau.

The Basin and Range Province is home to many well-known mountain ranges and valleys. Major ranges include the Snake Range, the Panamint Range, the White Mountains, the Sandia Mountains and the Tetons. Valleys include Owens Valley, Death Valley and Snake Valley. Relief changes are drastic – White Mountain Peak in California stands 4344 m above sea level, while Badwater Basin in Death Valley is at –86 m. The series of mountain ranges also results in the development of extensive deserts in their rain shadows. Almost all North American deserts are located in the Province.

Total crustal extension in the Basin and Range Province is estimated to be about 100%. The mechanism driving its development still remains to be fully fleshed out however. Key ideas involve a long period of compression due to the subduction of the Farallon Plate under the west coast of the North American continental plate resulting in crustal thickening in the Sevier and Laramide orogenies. By ~30 Ma, most of the Farallon plate has been subducted under the North American plate, with the smaller Juan de Fuca, Cocos, Nazca, Explorer and Gorda plates remaining as “remnants”. The boundary between the Farallon and Pacific plate merged with boundary between the Farallon and North American plate, forming the San Andreas fault. Due to the different relative motions of the plates, the originally convergent Farallon-North American plate boundary then changed to the transform San Andreas fault. The strike-slip motion not only relieved the compressional stresses from the subduction of the Farallon plate, but the crustal shearing stresses also caused additional extensional stresses within the North American plate. Plate motion alone did not account for the high elevation of the Basin and Range region however. Subduction of the Farallon plate also resulted in high heat flow in the region, lowering the density of the lithosphere and causing isostatic uplift. In addition, the high heat flow weakened the lithosphere and promoted deformation. The exact link between subduction and heat flow remains unclear. Water liberated from the subducted plate is believed to contribute greatly to efficient vertical heat transfer through the crust.

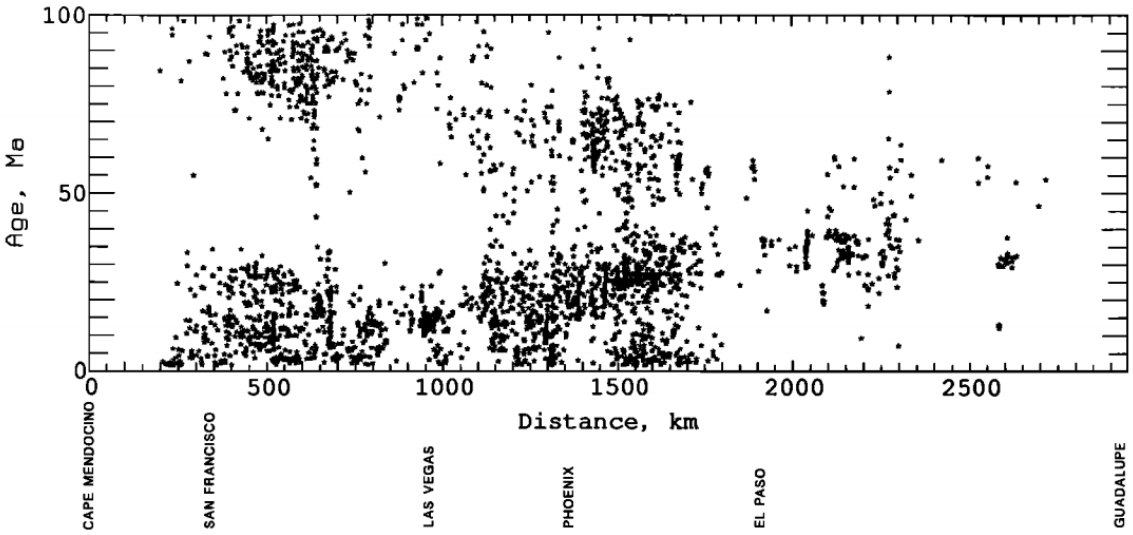

West-East-West migration of volcanic activity [Ward, 1991]

The high heat flow also manifested as extensive volcanism in the Basin and Range Province. Before the formation of the San Andreas fault, relatively shallow subduction of the Farallon plate resulted in eastward migrating arc volcanism. Subduction rates slowed drastically after the formation of the San Andreas fault, resulting in an increase of the subduction dip angle and the weakening of arc volcanism. However, crustal deformation from the change of compressional to extensional stresses resulted in resurgence of extensive volcanism towards the west.

Other than the Basin and Range Province in the US, basin and range topography also exists around the world. Northerly trending basins lace the Tibetan Plateau. These basins are more widely spaced than those in the western US, and are believed to reflect an earlier stage of the basin and range development. The landscape of western Turkey likewise is cut by easterly trending basins and neighboring ranges that were formed by crustal extension in the North-South direction. This morphology of basins and ranges extends westward beneath the Aegean Sea, with many islands in the Aegean being ranges that stand high enough to rise above the sea level.

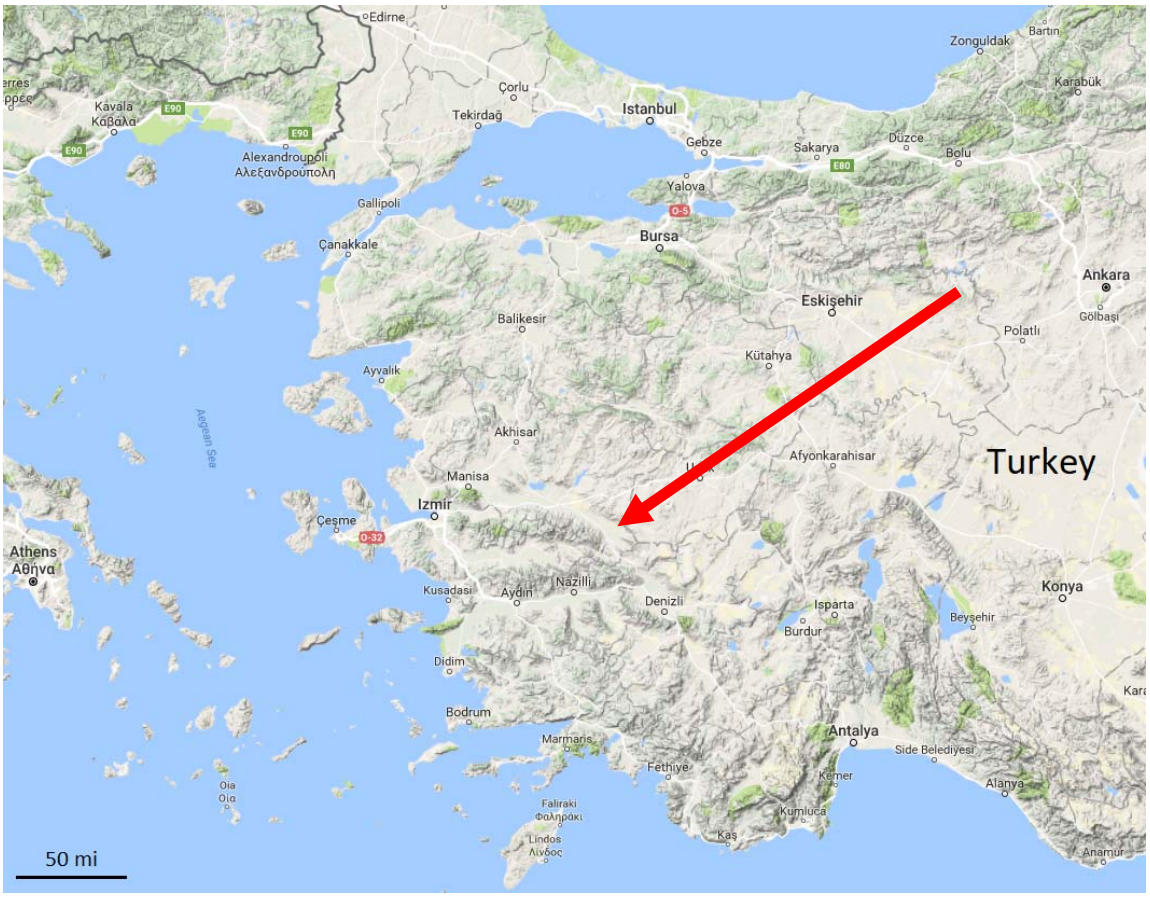

Basin and range topography in western Turkey [Image from Google Maps]

References

Tectonic basin. In Encyclopaedia Britannica. Retrieved 19 September, 2017.

Basin and Range Province. In Wikipedia. Retrieved 19 September, 2017.

Basin and range topography. In Wikipedia. Retrieved 19 September, 2017.

Sevier Orogeny. In Wikipedia. Retrieved 19 September, 2017.

Laramide Orogeny. In Wikipedia. Retrieved 19 September, 2017.

Farallon Plate. In Wikipedia. Retrieved 19 September, 2017.

Owens Valley. In Wikipedia. Retrieved 19 September, 2017.

White Mountain Peak. In Wikipedia. Retrieved 19 September, 2017.

Putirka K. and Platt B. (2012) *Basin and Range volcanism as a passive response to extensional tectonics*. Geosphere.

Ward P.L. (1991) *On plate tectonics and the geologic evolution of southwestern North America*. Journal of Geophysical Research 96 (B7): 12479–12496.

The Navajo Sandstone

The Navajo nugget sandstone formation is an outcrop of the Colorado Plateau (a classic example for layer-cake geology) which underlies Southern Utah, Northern Arizona and parts of Colorado and New Mexico. Along with Triassic Kayenta and Wingate sandstones, they make up the Glenn canyon group. The best exposures of the formation can be seen in the high canyon walls of the Zion National Park in Southern Utah.

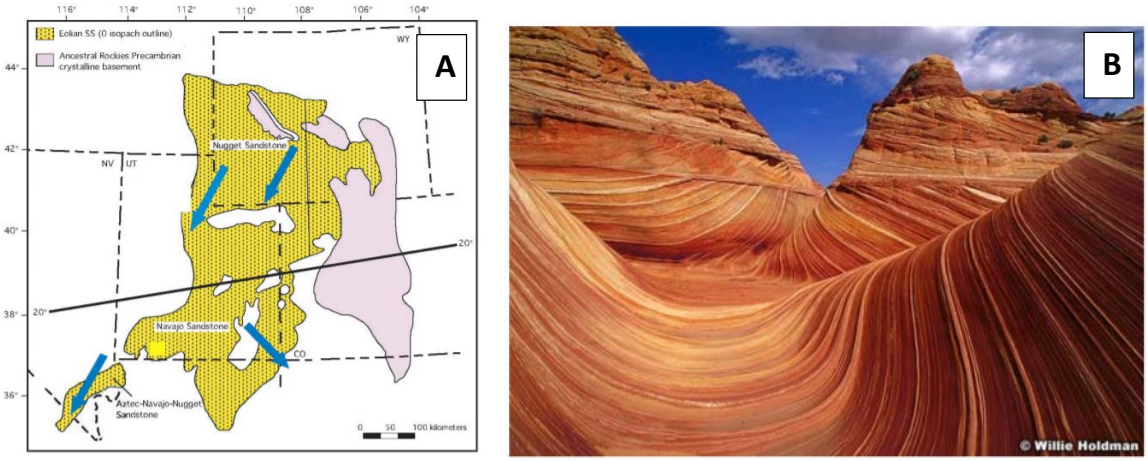

Figure – 1: A) The extent of the Navajo Sandstone in the southwestern U.S, from Chan and Archer (2000). B) A photograph of stratification in Navajo sandstone by Willi Holdman (http://www.willieholdman.com)

How did the Navajo sandstones form?

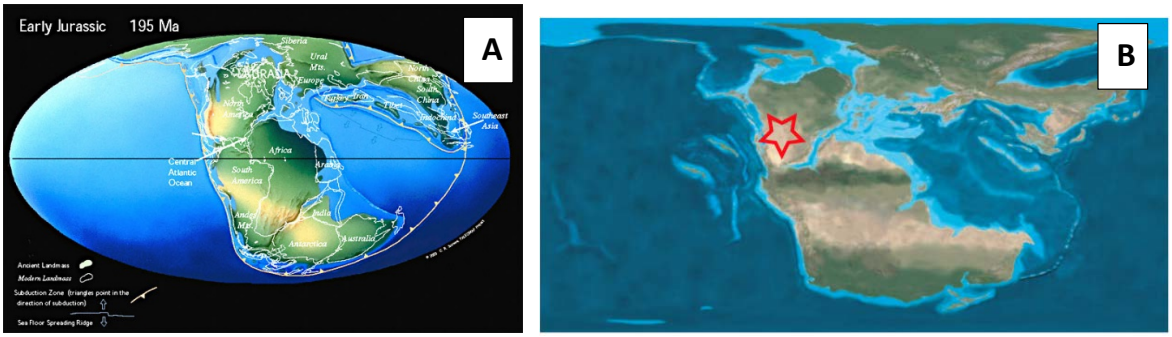

Figure – 2: A) Paleomap of the world by Christopher Scotese (www.scotese.com). B) The configuration of the plates during the Early Jurassic (ca 190 Ma). Star indicates approximate region of the Navajo Sand Sea (http://jan.ucc.nau.edu/~rcb7/globaltext2.html.)

The Navajo sandstones were deposited during the early Jurassic period (roughly 190 Mya ago) when most of Northern Arizona was a vast sea of sand larger than twice the current extent of

the Navajo sandstone (imagine Sahara Desert like environment). Aeolian action piled sand up the windward side of these dunes; when the pile gets too high, the deposited grains slide down the leeward side forming a thin depositional layer. Repetition of this event gave rise to several angled layers also called cross beds. The cross beds in the Navajo formation are large and could have formed in dunes easily as high as 100 feet. Lithification and cementation of the sand eventually resulted in the Navajo sandstone formation.

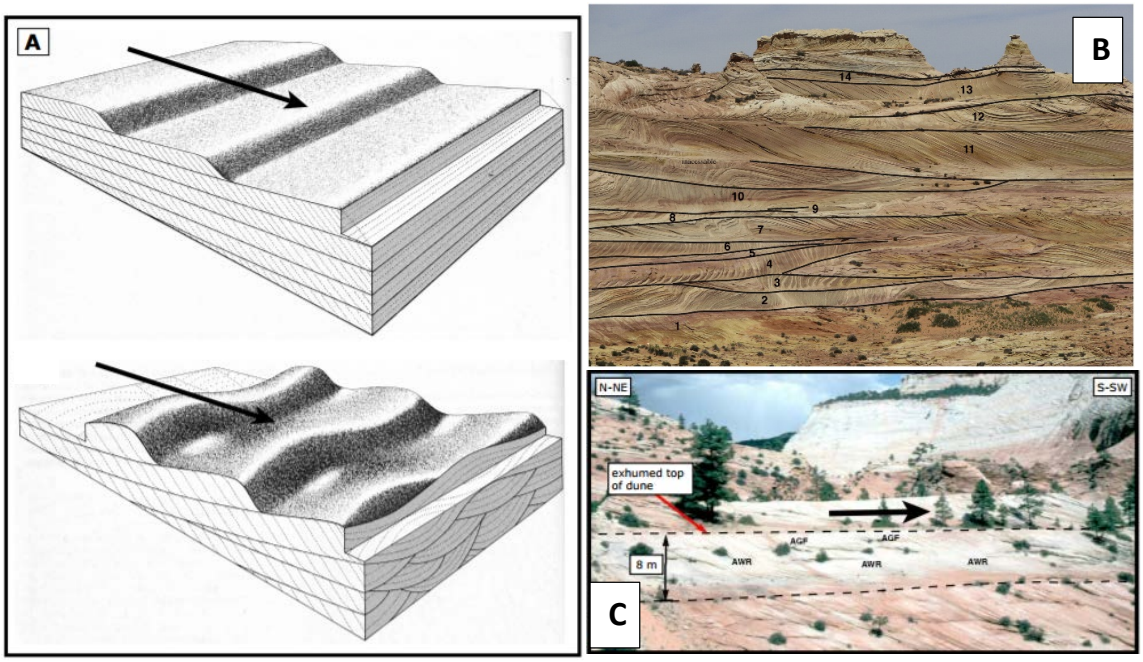

Figure – 3: A) Formation of cross beds in dunes; arrows indicate direction of wind flow, from Reineck and Singh (1975). B) Cross-beds in the Navajo sandstone, from Loope et al. (2003). C) Crossbeds demarcated by boundary surfaces which also delineate bleached sandstone from unbleached orange sandstone, from Chan and Archer (2000).

Geology of the Navajo sandstones

Lithology	The Navajo formations is made of smooth and light-colored sandstone monolith.
Geomorphology	Primary geomorphic features of interest are cliffs showing large scale cross bedding and cross stratification.
Composition	Sandstones typically comprise 85% – 90% quartz. The buff/grey to red color indicates the presence of calcite and iron oxide.
Fossils	Apart from a small number of preserved dinosaur skeletons which have been discovered in the Navajo sandstones of Northern Arizona, much of the formation is devoid of fossil record indicating paleoconditions too hostile to sustain life.

Analog for Mars

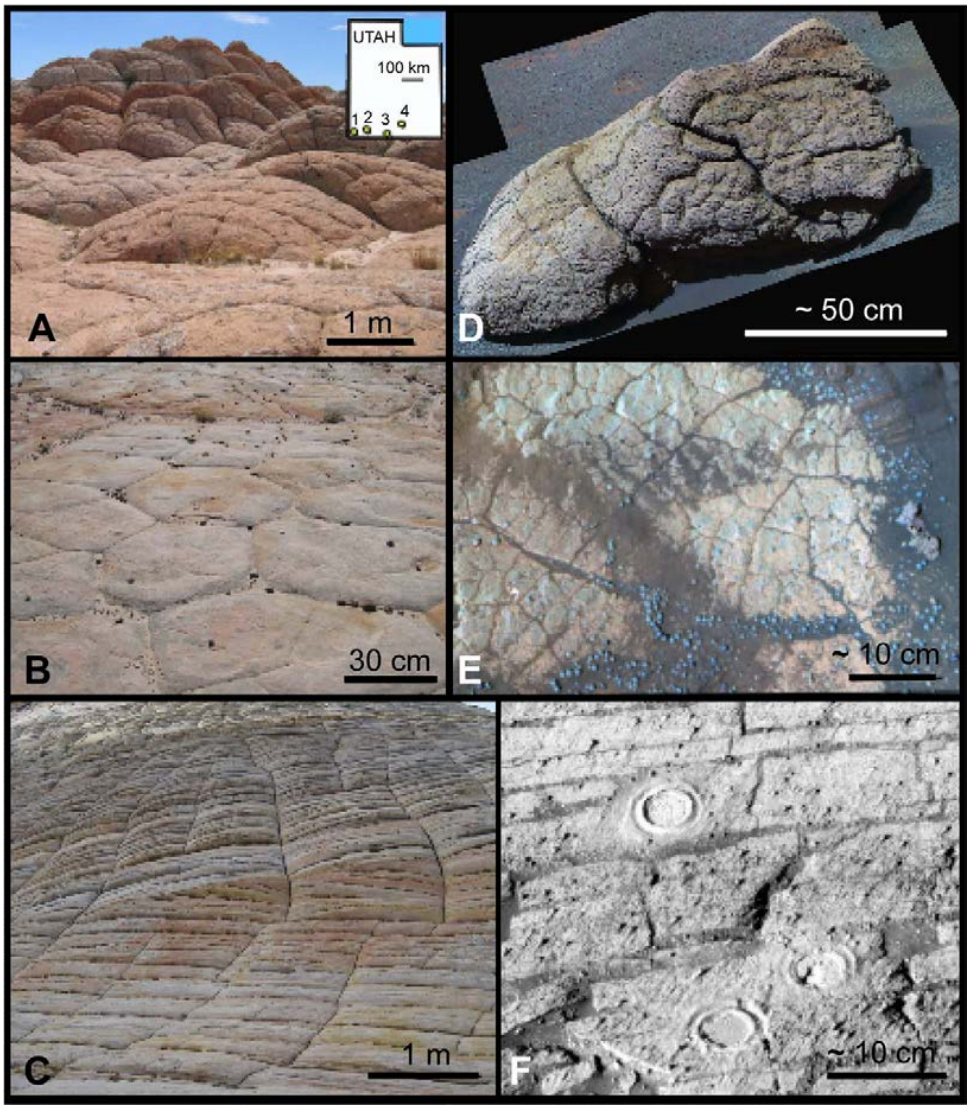

Figure – 4: Comparisons of terrestrial Navajo Sandstone (left, A to C) and Mars Burns formation (right, D to F) bedrock cracks. Localities of Jurassic Navajo Sandstone polygon patterns (upper right inset): 1—Snow Canyon, 2—Zion National Park, 3—Vermillion Cliffs near Utah–Arizona border, and 4—Grand Staircase Escalante National Monument. (A) Pervasive polygonal cracks (locality 3). (B) Polygons with scattered dark hematite concretions (locality 4). (C) Rectangular cracks perpendicular to eolian stratification. (locality 2). (D) Polygonal cracks in the Wopmay rock imaged by the MER Opportunity, Endurance Crater area of Meridiani Planum, Mars (Pancam false color photo,: NASA/JPL/Cornell). (E) Polygonal cracks in bedrock, Endurance Crater area (Pancam false color photo, NASA/JPL/Cornell). (F) Rectangular cracks perpendicular and parallel to bedding in stratified deposits (MER Opportunity image, photo credit: NASA/JPL/Cornell). Source: Chan et. Al. 2008.

The Navajo sandstone has been considered as a terrestrial analog for some of the sedimentary and weathering features imaged on Mars by the Mars Exploration Rover (MER) Opportunity in Meridiani Planum.

i. MER found haemetite spherules aka 'blueberries' on Mars for which iron concretions in the Navajo sandstone was proposed as a possible analog. The processes forming the concretions in the Navajo sandstones were found to be different from the spherule forming processes on Mars. Despite this, the Navajo concretion forming processes can serve as an analog for concretions on any of the terrestrial planets.
ii. The Burns formation in Meridiani Planum shows eolian cross-bedding like the ones on the Navajo formation.
iii. Opportunity imaged small scale polygonal crack patterns on Mars similar to the terrestrial cracks that occur in large porous sandstones in arid climates.
iv. MER also found small scale domal relief between the polygonal cracks in large outcrops as well as boulders. This is similar to the microrelief weathering patterns observed on Navajo sandstones.

References

1. Chan, M., and A. Archer, Cyclic eolian stratification on the Jurassic Navajo Sandstone, Zion National Park: Periodicities and implications for paleoclimate, in Geology of Utah's Parks and Monuments, edited by D. Sprinkel, J. T.C. Chidsey, and P. Anderson, 1 ed., pp. 606–617, Utah Geol. Assoc. Pub. 28, 2000.
2. Loope, D., and C. Rowe, Long-lived pluvial episodes during deposition of the Navajo Sandstone, J. Geol., 111, 223–232, 2003.
3. Loope, D., C. Rowe, and R. Joeckel, Annual monsoon rains recorded by Jurassic dunes, Nature, 412, 64–66, 2001.
4. Reineck, H.-E., and I. Singh, Depositional Sedimentary Environments with Reference to Terrigenous Clastics, Springer Verlag, Berlin, 1975.
5. Chan MA, Yonkee WA, Netoff DI, Seiler WM, Ford RL. Polygonal cracks in bedrock on Earth and Mars: Implications for weathering. Icarus. 2008 Mar 31;194(1):65-71.

River Systems

Maria Steinrueck

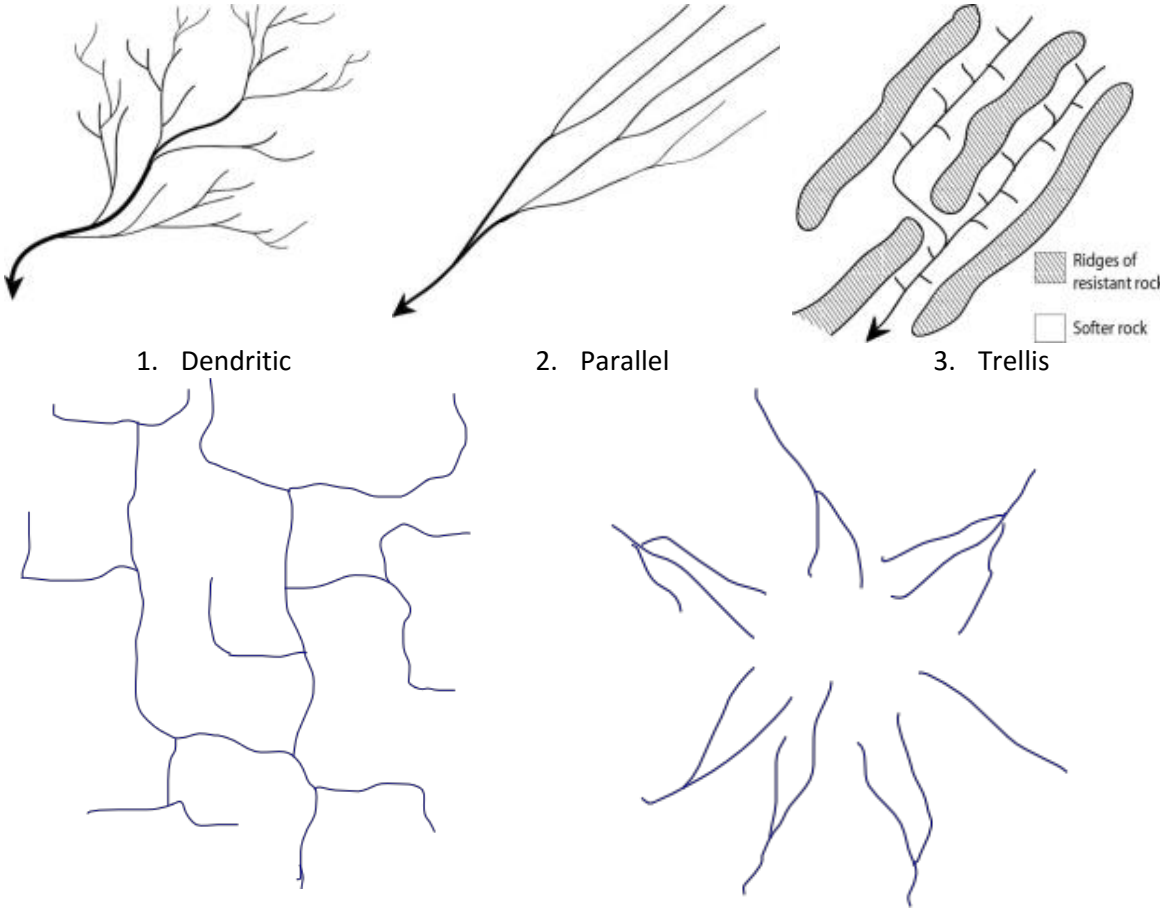

Figure 1 Classification of drainage patterns. (Credit: Wikipedia User Tshf aee (1-3), Eurico Zimbres (4-5))

Drainage Patterns

Depending on the underlying rock types and structure, different drainage patterns emerge.

Dendritic

The pattern resembles the branches of a tree – therefore the name, derived from the Ancient Greek δένδρον (*déndron* – tree). This pattern is formed when the underlying rock is uniformly resistant to erosion. It is the most common drainage pattern.

Parallel

This pattern typically emerges when there is a relatively steep, uniform slope across a large area. Streams run parallel and join each other at acute angles.

Trellis

Trellis drainage patterns are found in areas that have parallel ridges of erosion resistant rock. Short tributaries run downhill into the valley and join the main channel at an angle close to 90 degrees.

Rectangular

In areas with faults or bedrock joints, erosion happens preferentially along these faults or joints, resulting in a rectangular drainage pattern.

Radial

Radial drainage patterns emerge around a central elevation.

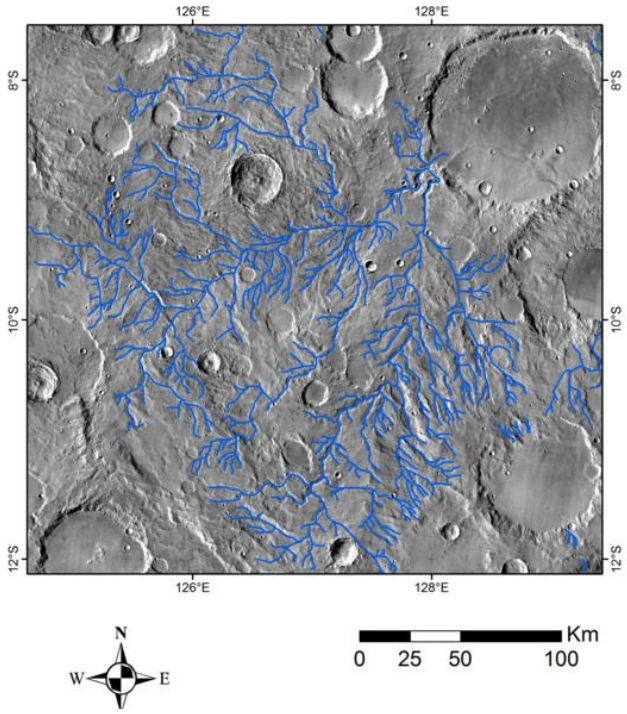

Figure 2 Map of valley network on Mars on top of an image from the THEMIS instrument of Mars Odyssey. (Credit: NASA/JPL/ASU/Brian Hynek)

Drainage basins

The *drainage basin* of a river (or bay or other body of water) is the area across which precipitation collects and supplies the river. In the US, the term *watershed* is often used synonymously with drainage basin, though in some other regions, watershed refers to the drainage divide (i.e. the boundary between two drainage basins).

The Colorado River Basin

The Colorado River Basin is the largest and most important drainage basin of the Southwest. It supplies water to over 30 million people and has a major impact on the economy of the Southwest. Today, the flow of the Colorado has been strongly regulated by dams. On its lower course, much of its flow has been diverted for agricultural purposes. This has led the river to dry up even before it reaches the Gulf of California.

River systems in the Solar System

Mars

Valley networks resembling drainage systems on Earth were first discovered in images of the Viking orbiters. They represent one of several lines of evidence for the presence of liquid water in the early history of Mars. Most of these valley networks were formed in the late Noachian to early Hesperian era (3.8 to 3.6 billion years ago).

Titan

Radar images of Titan show evidence of methane river systems. A large fraction of these river systems have rectangular drainage systems. This provides indirect evidence of faults and joints on Titan. For example, Burr et al. (2013) conclude from an analysis of drainage patterns that those rectangular patterns formed under tensional stresses. This indirect evidence of tectonics is highly valuable: As Titan's thick and strongly scattering atmosphere prohibits imaging at optical wavelengths, it is impossible to see faults directly.

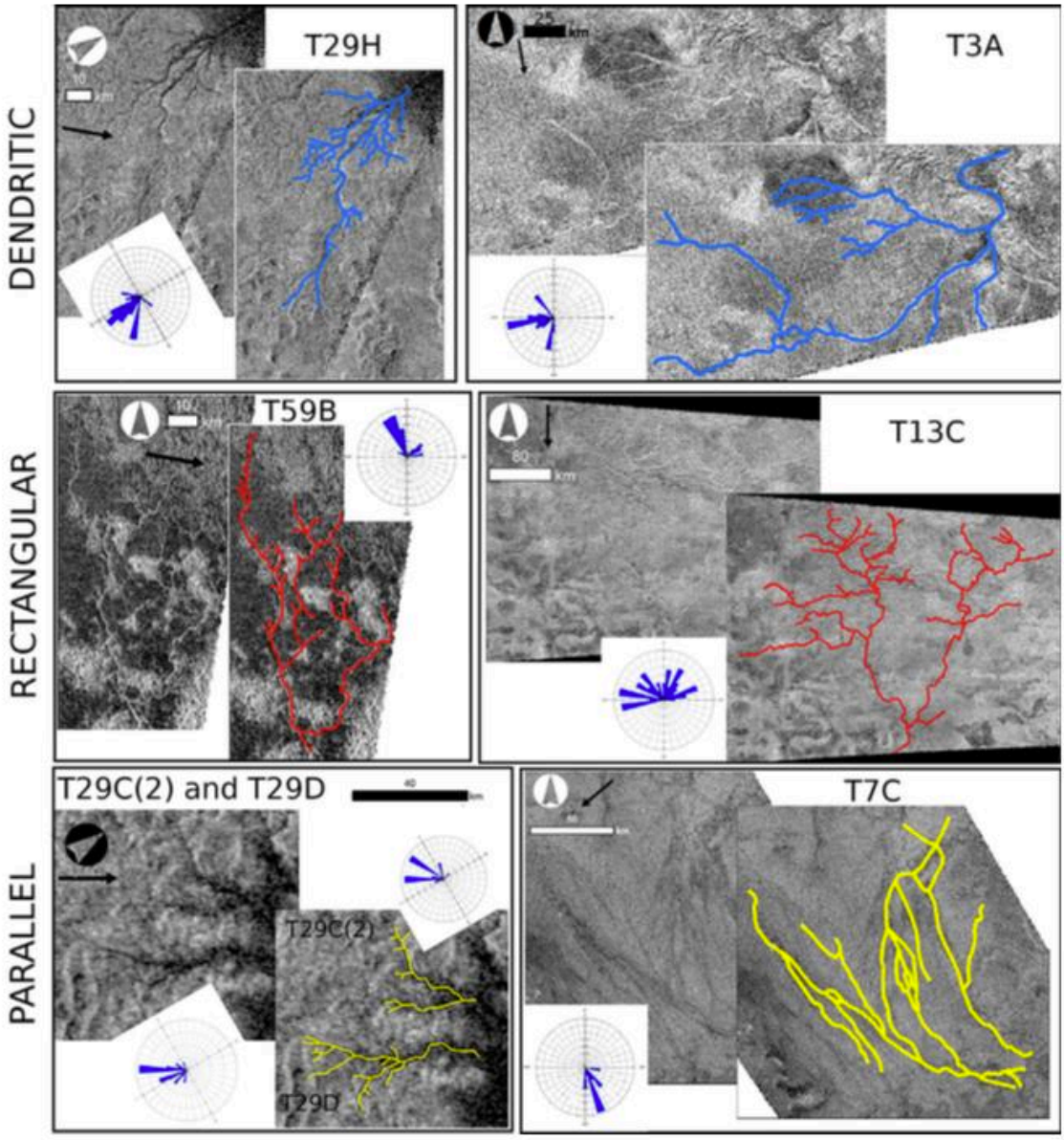

Figure 3 Drainage patterns on Titan as seen in data from Cassini's Synthetic Aperture Radar (SAR). (Credit: Burr et al., 2013)

References

1. http://www.earthonlinemedia.com/ebooks/tpe_3e/fluvial_systems/drainage_patterns.html (9/28/17)
2. http://www.tulane.edu/~sanelson/eens1110/streams.htm (9/28/17)
3. http://environment.nationalgeographic.com/environment/freshwater/change-the-course/colorado-river-map/ (9/29/17)
4. http://www.planetary.org/blogs/emily-lakdawalla/2013/what-mars-valley-networks.html (9/29/17)

5. http://www.planetary.org/blogs/emily-lakdawalla/2010/2542.html (9/28/17)
6. Burr, Devon M., Sarah A. Drummond, Richard Cartwright, Benjamin A. Black, and J. Taylor Perron. “Morphology of Fluvial Networks on Titan: Evidence for Structural Control.” Icarus 226, no. 1 (September 2013): 742–759.

Figure 4 Map of the Colorado River drainage basin (Credit: Wikipedia User Shannon1)

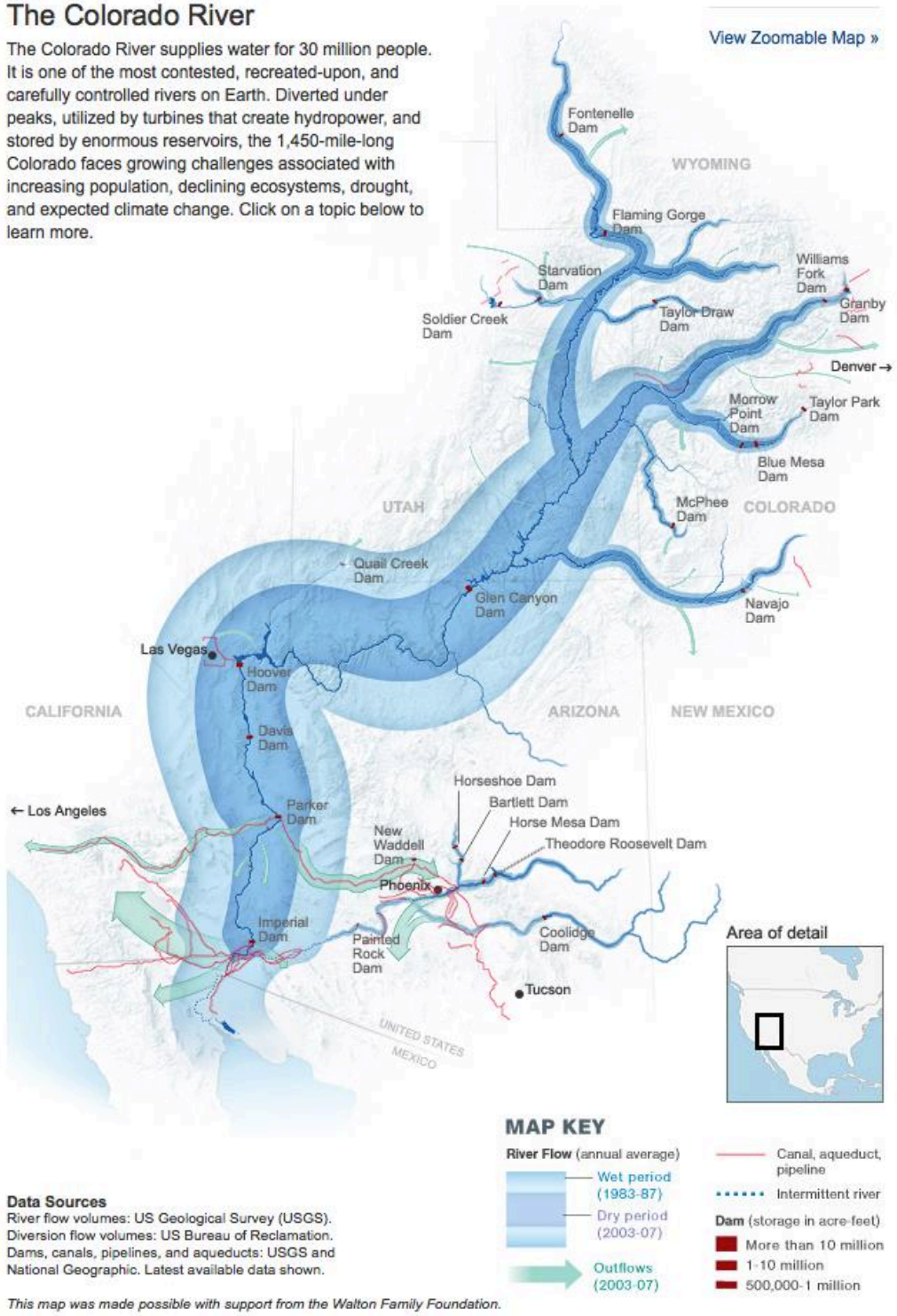

Figure 5 Map visualizing the flow volume, major tributaries and outflows of the Colorado River. (Credit: National Geographic)

Tectonics/Faulting

Ali Bramson

Tectonics: the deformation of crustal rocks and the forces that cause such deformation.

Types of tectonic forces based on the direction of the applied forces:

a. **Compressional**
b. **Tensional**
c. **Shearing**

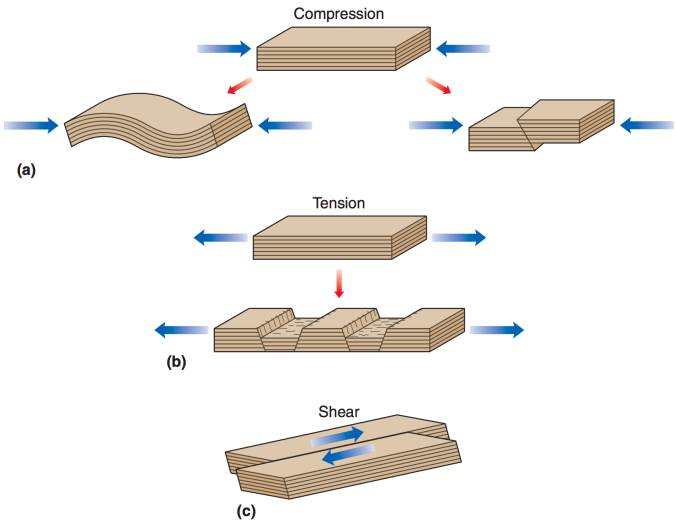

a. **Compressional Forces**
Compressional forces push rocks together, often shortening and thickening the crust or fracturing it depending on how brittle the rocks are and how fast the forces are applied. The deformation generally falls under either:

1. **folding** — the bending of ductile rocks; more likely to happen when forces are applied slowly and/or to rocks under high pressure at depth, which tend to be more ductile

Some types of folding:

- **anticlines**: convex folding, giving the layers an arch-like shape, causing the layers at the center to be older
- **synclines**: downward folding where layers at the bottom are younger
- **monocline**: step-like folding, in one dip direction
- **recumbent folds**: folds that have been overturned asymmetrically (due to the compressional forces being stronger in one direction than the other) to the point of being flipped backed over such that the layers are almost horizontal again

2. **faulting** — the brittle fracturing of rocks due to compressional forces. This causes one rock to be pushed up relative to the other, with the fracture where the movement happens called the "**fault**". Rocks closer to the surface tend to exhibit more brittle behavior, as well as rocks undergoing stress in a short amount of time. The fractured pieces of crust are called **fault blocks**.

Types of faulting from compressional forces:

- **reverse fault**: steep fault along which one side is pushed up
- **thrust fault/overthrust**: shallow fault causing one rock to be pushed on top of the rocks on the other side of the fault

Anticlines and Synclines (symmetric folds- top diagram) and recumbent folds (asymmetric folds) in the progression of features due to folding depending on the amount of asymmetry in the compressional forces applied (bottom diagram)

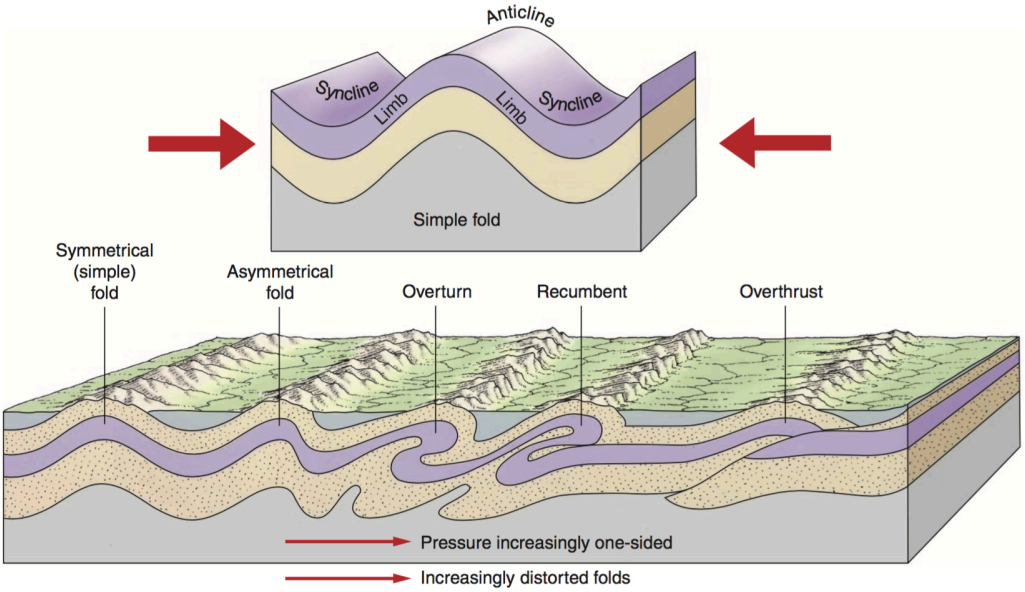

Reverse Fault

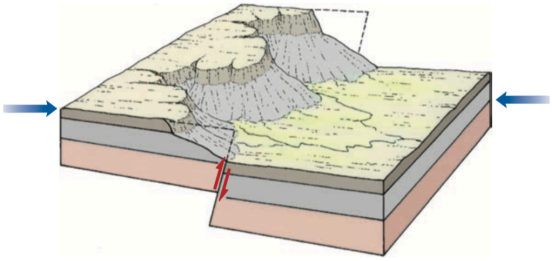

Thrust Fault

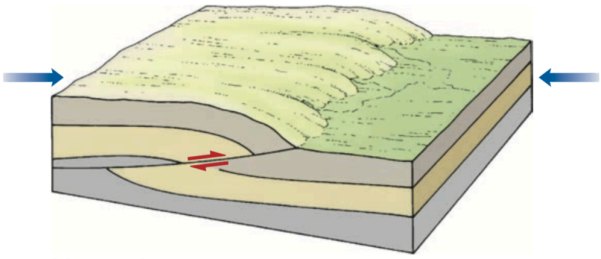

b. **Tensional Forces**

Tensional forces stretch and thin rocks due to the forces being applied in opposite directions, which causes faulting (you generally don't get folding from tensional stresses).

faulting – same definition as above but now one block slides downward along the fault (**normal fault**) to make up for extension of the crust. You often get terrain with parallel normal faults causing alternating fault blocks that are down-dropped and pushed up (e.g. *Basin and Range province*), known as **graben and horst**:

- **graben**: fault blocks that have been appeared to be down-dropped between two normal faults (often form *basins*)
- **horst**: fault blocks that appear to be shifted upward from two parallel normal faults (often form mountain *ranges*)

Other types of faulting from tensional forces:

- **tilted fault blocks**: fault block where one side is uplifted and the other side is tilted downward
- **rift valleys**: long, narrow area of down-dropped blocks along normal faults

Normal Fault

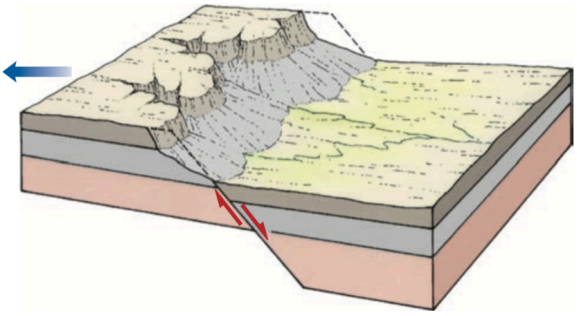

Horst and Graben

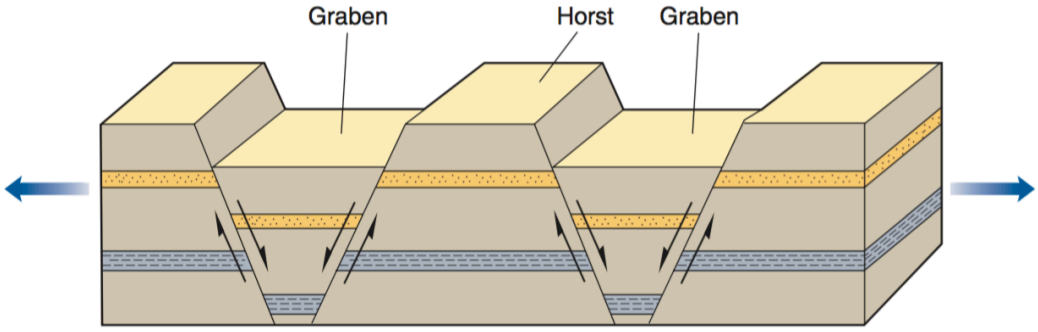

Tilted fault block

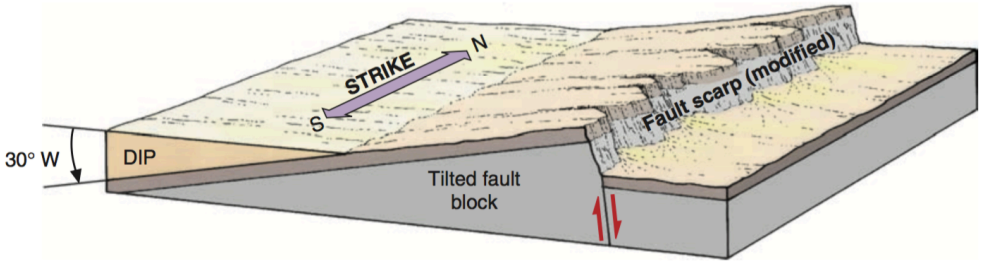

Rift Valley

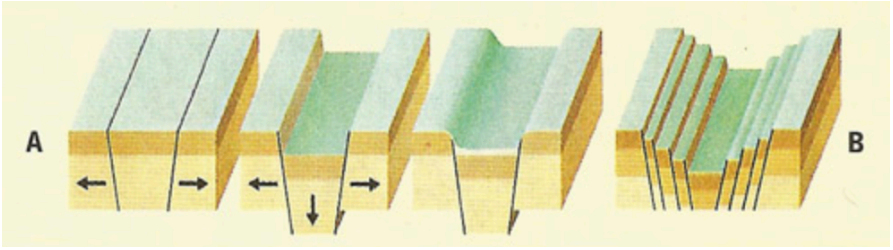

Image from [2]: Long version of a graben (A), or a series of parallel faults (B)

The term **scarp** (or escarpment) refers to the steep cliffs caused by movement of crust along faults.

c. **Shear Forces**
The faults above occur from vertical movements between blocks (dip-slip faults), however, shear forces cause **strike-slip faults** (also known as a **lateral fault**) in which horizontal motion occurs parallel to the fault. This motion can be described in two ways, depending on the direction that one block appears to move compared to the other (from the perspective of standing on side looking at the other across the fault).
Types of strike-slip faults:

1. **Right lateral faulting**
2. **Left lateral faulting**

Strike-Slip Fault (left lateral)

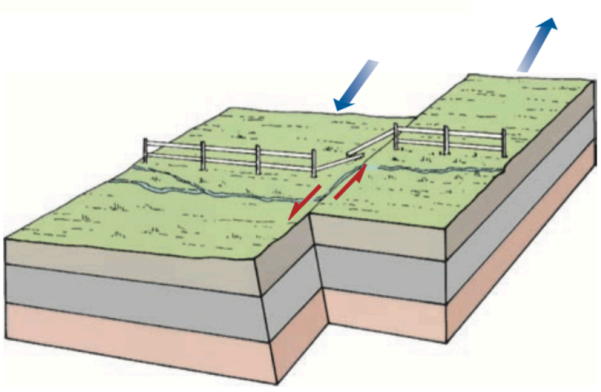

Instantaneous movement from a fault generally causes millimeters to meters of movement, which can add up over time if faulting continues in the same area. In the case of the largest and longest-active faults, *millions of years of displacement can cause vertical movement on the order of 10s of kilometers and horizontal movements can be up to 100s of kilometers of total displacement*. Some of the largest instantaneous displacements measured include *6 meters of horizontal movement* along the San Andreas Fault during an earthquake in 1906 and *10 meters of vertical displacement* during an earthquake in Alaska in 1964.

<u>One word of caution to keep in mind about tectonic terminology vs. topography:</u>
"Words like *mountain, ridge, valley, basin,* and *fault scarp* are geomorphic terms that describe the surface topography, while *anticline, syncline, horst, graben,* and *normal fault* are structural terms that describe the arrangement of rock layers."

See example on next page from [1]: "Structural upfolds do not always comprise topographic mountains, nor do all downfolds form valleys. (a) The structure is an anticline, but the surface landform is a plain of low relief. (b) Here, the erosionally resistant center of a downfold (a syncline) supports a mountain peak. (c) A valley has been eroded into the crest of an anticline."

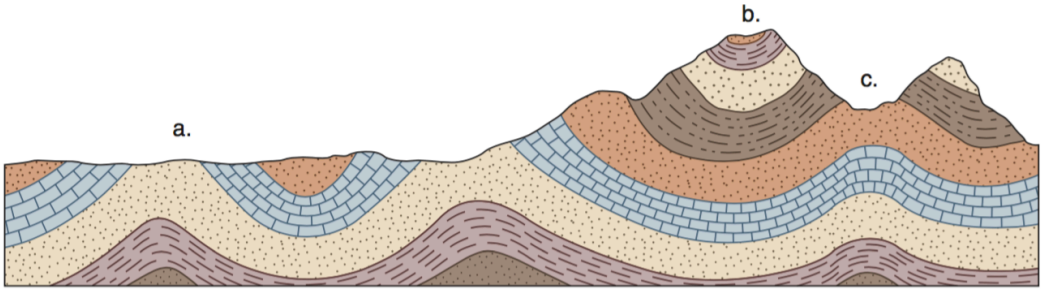

ACTIVITY: IDENTIFY THE FEATURE!

1

Courtesy Sheila Brazier

2

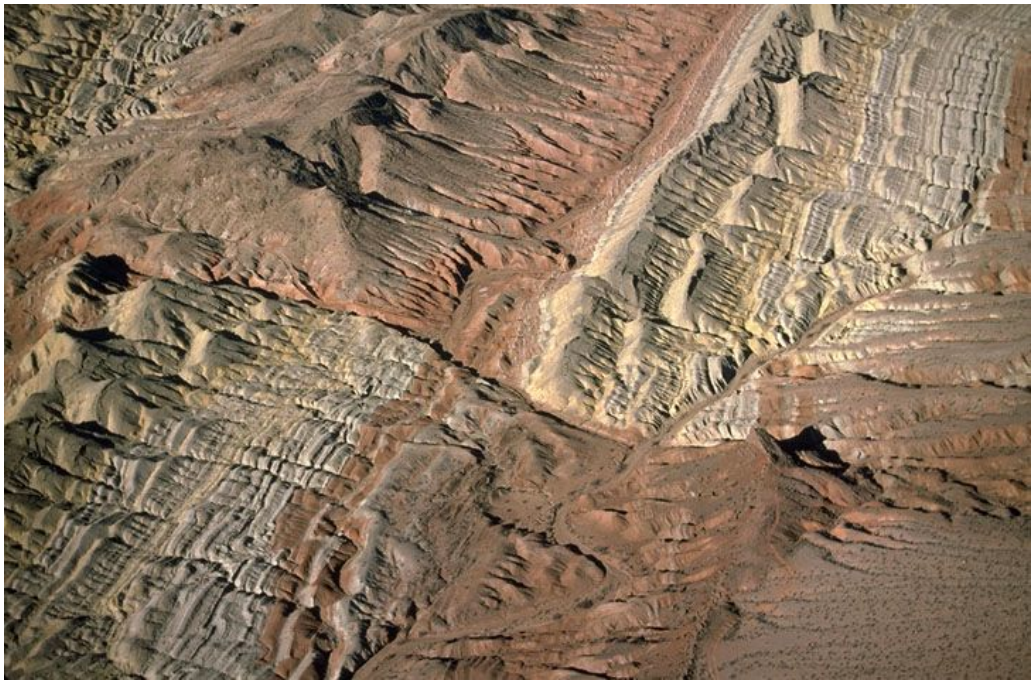

3

4

Planetary Analogs

Valles Marineris (“The Grand Canyon of Mars”) is generally agreed upon to be tectonic in origin, though debate exists about the kind of tectonics involved - from a large rift valley originated from extensional stresses imparted on the crust by the formation of the Tharsis volcano to vertical subsidence and collapse [6]. It has also been speculated that the canyon is along a strike-slip fault formed at a plate boundary and that it signifies that Mars has plate tectonics [7].

Some scarp faces of Valles Marineris have triangular “faceted spurs” [8] which on Earth are due to normal faulting and subsequent erosion of these scarps.

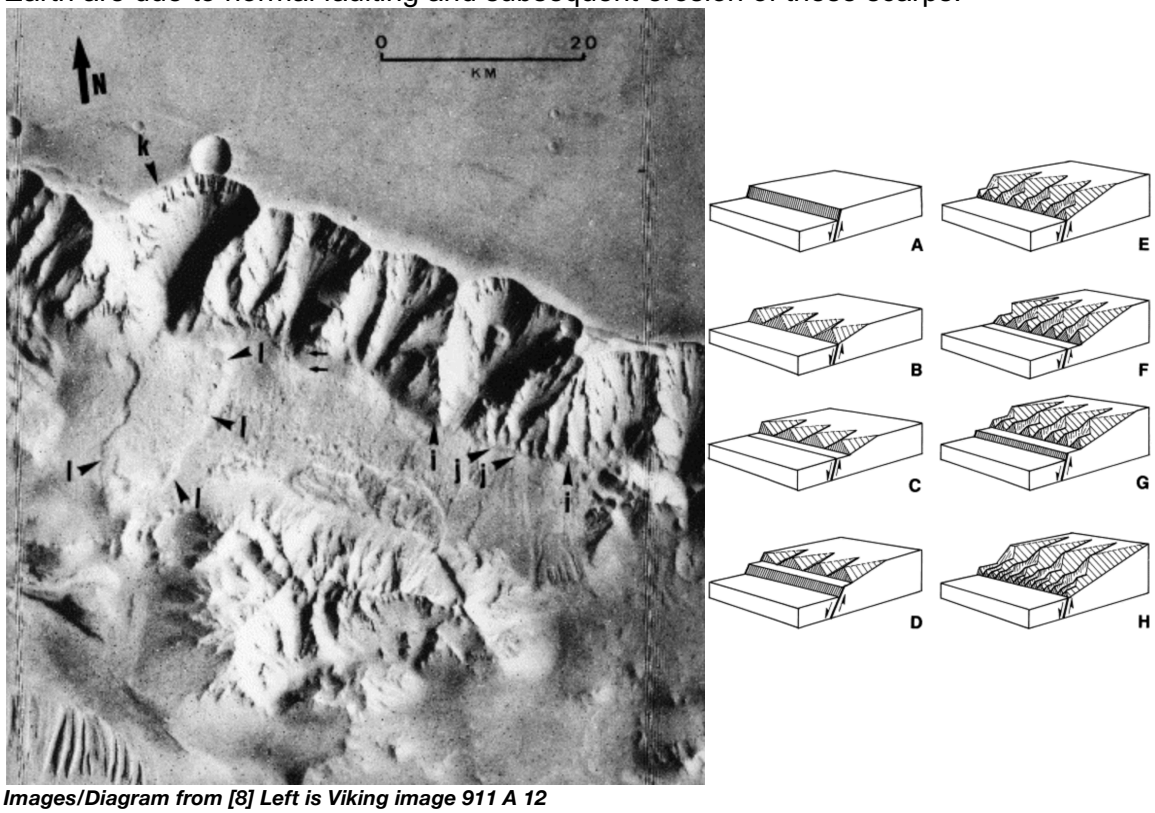

Images/Diagram from [8] Left is Viking image 911 A 12

Similar erosion on the scarp faces exists of the Comb Ridge, Utah monocline [9]

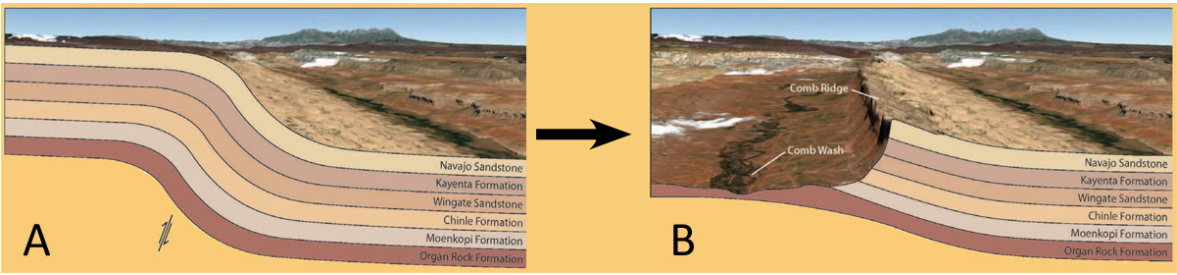

Block diagram of the monocline at Comb Ridge [10]

Images from MESSENGER found small (10s of meters wide) fault scarps associated with graben on the surface of Mercury, suggesting that the planet is still tectonically active (impacts would have erased these small of features if they were super old) from the stresses of the cooling and therefore contraction of the crust of the planet [11].

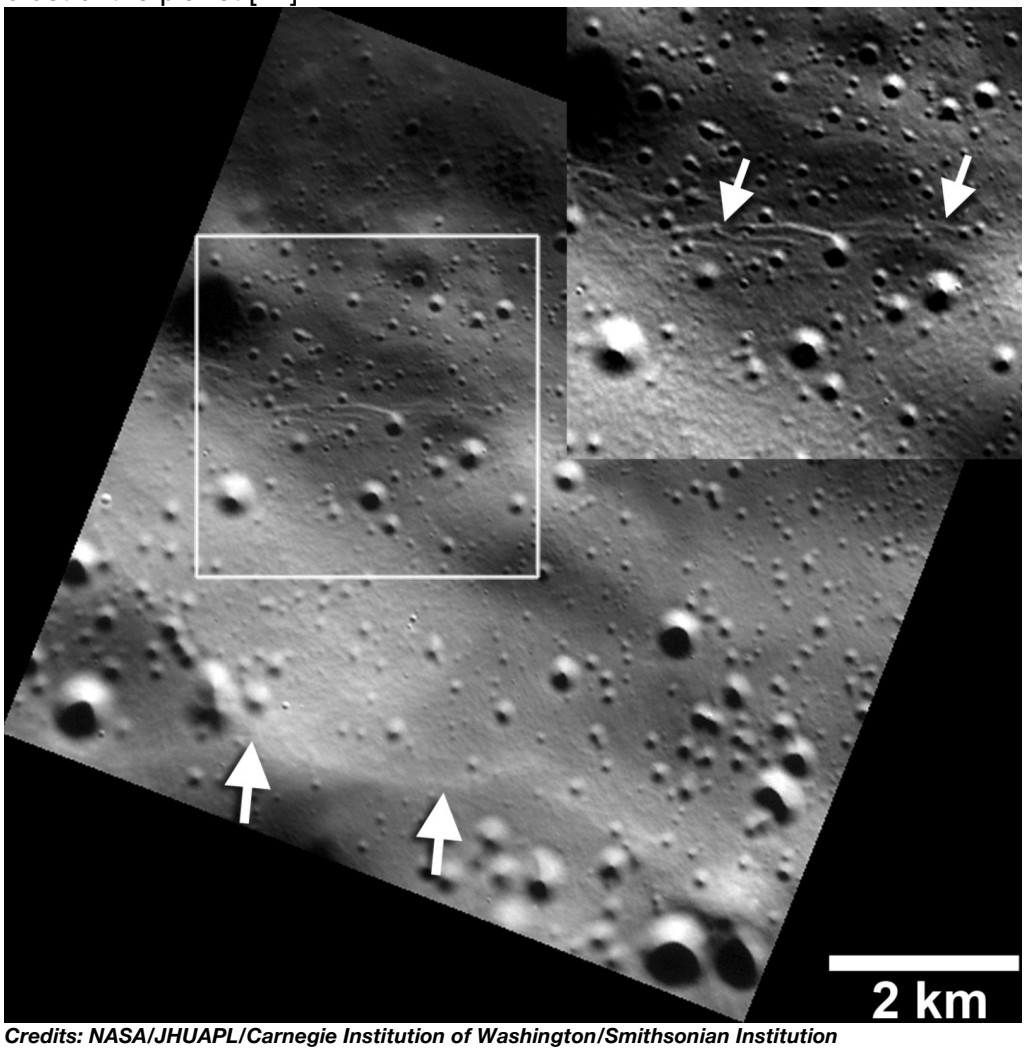

Credits: NASA/JHUAPL/Carnegie Institution of Washington/Smithsonian Institution

The trailing hemisphere of Dione (moon of Saturn) shows a network of extensional faults related to Dione's endogenic activity and thermal history [12].

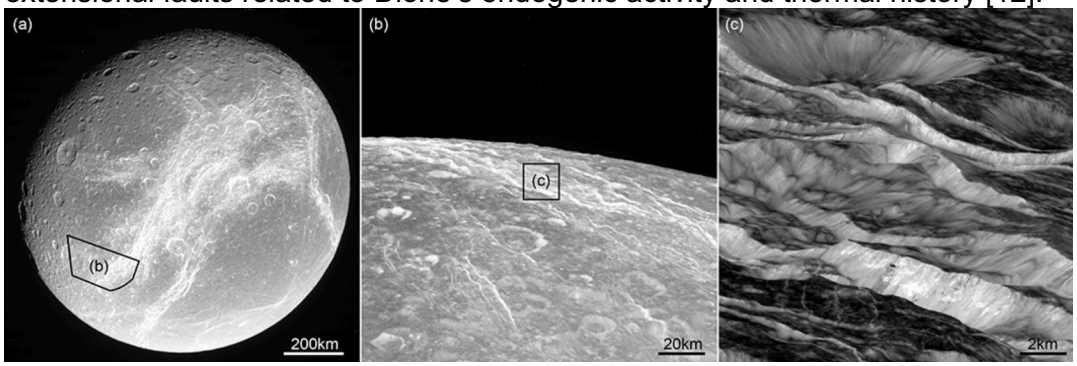

Figure from [12] of Cassini images showing faults on Dione

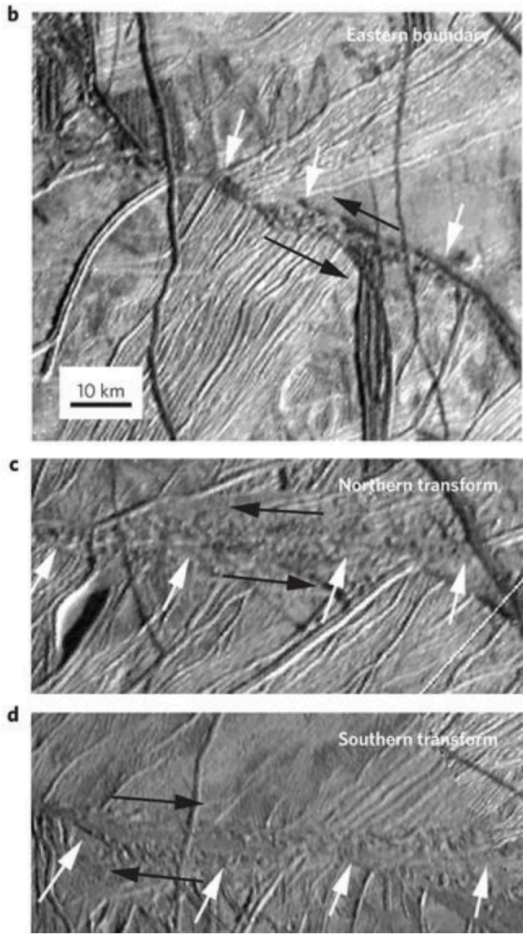

Many icy satellites are also known to be tectonically active. Europa particularly has lots of tectonic activity (perhaps even plate tectonics [13]) from tidal stresses that cause fractures in the icy shell that then allow younger material to come up to the surface [14], perhaps analogous to terrestrial mid-ocean spreading centers.

Sources:
Unless otherwise noted, the content of the report (particularly the basics of tectonics and terminology) comes from [1].

[1] Physical Geography by Robert E. Gabler, James F. Petersen, L. Michael Trapasso and Dorothy Sack. Cengage Learning, 2008, 672 pages
Chapter 14 Tectonic Forces, Rock Structure, And Landforms (pgs. 391–402)

[2] The Worlds of David Darling, Encyclopedia of Alternative Energy, entry on Rift Valley, http://www.daviddarling.info/encyclopedia/R/rift_valley.html

[3] https://i.pinimg.com/736x/25/4a/1b/254a1b05a9da9ca133f2af0159a19eb5--earth-science-aerial-view.jpg
[4] myweb.facstaff.wwu.edu/talbot/cdgeol/Structure/Fold/Folds1/Recumbent.html

[5] https://www.geologyin.com/2015/02/types-of-folds-with-photos.html

[6] Andrews-Hanna (2012) The formation of Valles Marineris: 1. Tectonic architecture and the relative roles of extension and subsidence, JGR-Planets, 117, E3, https://doi.org/10.1029/2011JE003953.

[7] Yin (2012) Structural analysis of the Valles Marineris fault zone: Possible evidence for large-scale strike-slip faulting on Mars, Lithosphere, 4 (4): 286-330, https://doi.org/10.1130/L192.1

[8] Peulvast et al. (2001) Morphology, evolution and tectonics of Valles Marineris wallslopes (Mars), Geomorphology, 3-4, 329-352, https://doi.org/10.1016/S0169-555X(00)00085-4.

[9] http://bluffutah.org/comb-ridge/

[10] https://geology.utah.gov/

[11] Watters et al. (2016) Recent tectonic activity on Mercury revealed by small thrust fault scarps, Nature Geoscience, 9, 743–747, doi:10.1038/ngeo2814

[12] Hirata (2016) Timing of the faulting on the Wispy Terrain of Dione based on stratigraphic relationships with impact craters, JGR-Planets, 121, 11, 2325-2334, doi:10.1002/2016JE005176

[13] Kattenhorn & Prockter (2014) Evidence for subduction in the ice shell of Europa, Nature Geoscience, 7, 762-767, doi:10.1038/ngeo2245.

[14] Greenberg et al. (2002), Tidal-tectonic processes and their implications for the character of Europa's icy crust, Reviews of Geophysics, 40, 2, 1-33, doi: 10.1029/2000RG000096.

Answers to the “Identify the Feature” activity:

1. Death Valley is an example of tilted fault block. This has created a basin 282 feet below sea level (fun fact: this is the lowest elevation in North America) [1]

2. Right-lateral strike-slip fault in southern Nevada [3]

3. Recumbent fold in Cornwall, England [4]

4. Syncline that makes up Sideling Hill in the Appalachian Mountains. This roadcut in western Maryland clearly shows the folding of strata. [5]

General Overview

Orient yourself! From the point of view of the above picture, in front of you is the Colorado River curving around a sandstone escarpment. Beyond the bend are the Paria Plateau and Vermillion Cliffs, to the right, the Colorado River leads up to Lake Powell, behind you is the city of Page, and to the left is the Navajo Nation.

About 200 million years ago (Jurassic era) the sand here was part of the largest system of sand dunes on the North American continent – stretching from Arizona to Wyoming and is over 2000 feet thick in some areas. These "sand seas" are known as ergs. This enormous erg was eventually hardened by water and minerals into the uniform, smooth Navajo sandstone layer.

The height of the sandstone making up Horseshoe Bend from river to rim is 1000 feet. After the Navajo Sandstone hardened, other layers of sandstone, mudstone, and different sedimentary layers piled on top of it. Then, after a couple of million years, water in the form of rain, ice, floods, and streams, worked to erode away the different layers. Today the Navajo Sandstone is once again exposed, and its sand is slowly wearing away.

Meanders and Oxbow Lakes

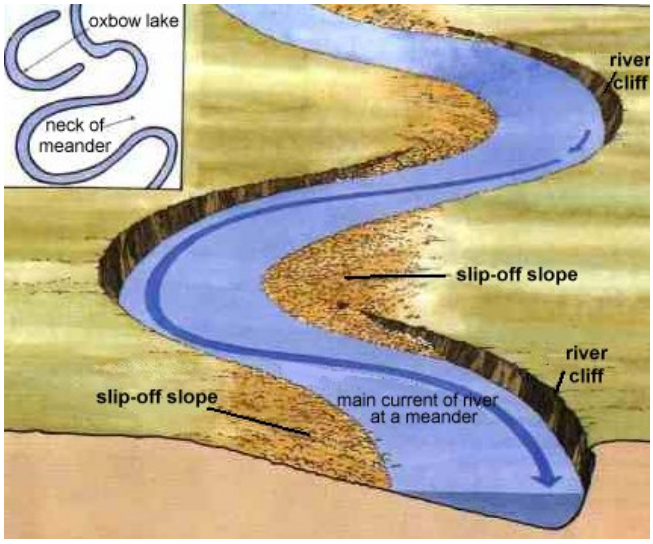

Meanders are a series of curves found in rivers or streams. The distance around the inside of the meander is less, so the current there flows more slowly compared to the faster current along the outside of the meander. The results of this are that the outside curve often undercuts a bluff while the inside commonly deposits a slip-off slope (sedimentary material on the inside bank of the meander). This process continues until erosion cuts a shorter path for the water. Eventually, the water runs across the constantly thinning neck of a meander and forms an oxbow lake. The cause of meandering is not perfectly understood, but is typically associated with a decreased slope and the interaction between flow, slope, and streambed resistance.

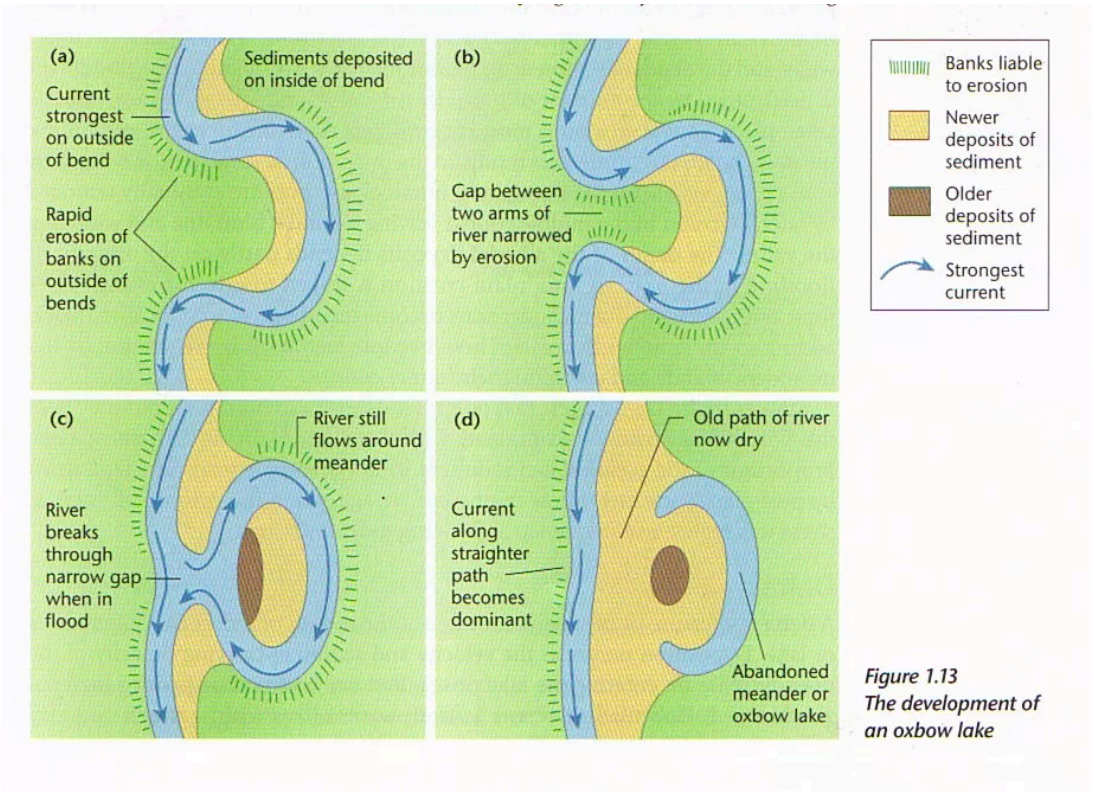

Figure 1.13
The development of an oxbow lake

Incised Meanders

An incised meander is when a meander cuts into bedrock. There are two types of incised meanders:

Ingrown Meander (Right): when the incision is slower and more lateral erosion occurs. The valley continues to grow horizontally and vertically with an asymmetric slope in its walls. There are steep cliffs on the outer bends and gentle slip-off slopes on the inner bends.

Entrenched Meander (Below): when the incision is rapid and vertical erosion dominates. The cross-section has symmetrical, near-vertical walls with little horizontal growth.

Entrenched meanders are generally rare, but seem to be common in low-sloped reaches of large plateaus, like the Colorado Plateau. They are characterized by vertical walls on both sides of the channel, with no slip-off slopes on the inside of bends -indicating that there was once a rapid downward cutting.

Both Horseshoe Bend and the Goosenecks of the San Juan River demonstrate these characteristics. They formed as a result of the uplift of the Colorado Plateau 5 million years ago. As the plateau lifted and shifted, the rivers that meandered across the ancient landscape cut down through the softer sandstone instead of eroding laterally to find the new base level.

Planetary Connection: Mars

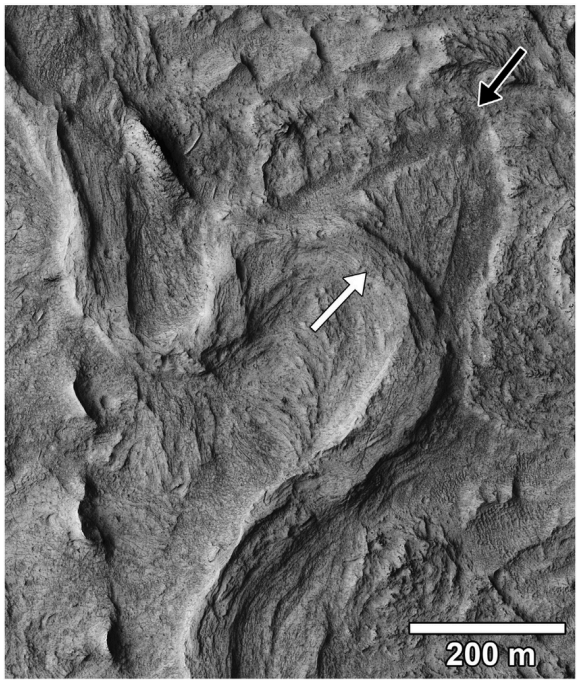

The paleo-meanders in the Aeolis Dorsa region of Mars show that meandering channels can develop in the absence of vegetation. Three possible mechanisms other than vegetation could contribute to the bank cohesion required to promote meandering: permafrost, abundant mud, and chemical cementation.

The black arrow point to the apex of a former abandoned meander loop. The white arrow points to a chute cutoff. (Image: HiRISE)

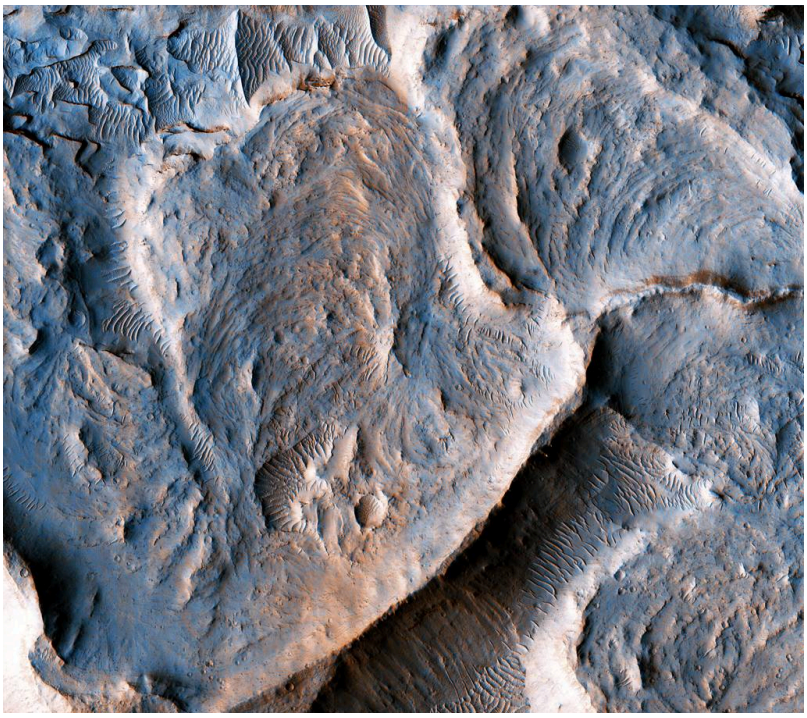

This is a portion of an inverted fluvial channel in the region of Aeolis/Zephyria Plana, at the Martian equator. The series of curvilinear lineations, or scroll-bars, are a result of the continuous lateral migration of a meander. On Earth, they are more common in mature rivers. The presence of scroll bars suggests that the water flow in this channel may have been sustained for a relatively long time. (Image: HiRISE)

Scroll-bars indicate progressive point bar accretion associated with lateral and translational bend migration.

[1] Matsubara, Y., et al. 2014. Geomorphology, 08, 031; [2] 'Entrenched Meanders' by Michael Oard; [3] National Park Service; Glen Canyon National Recreation Area; [4] 'A Guide to the Geology of the Flagstaff Area' by John Bezy, AZGS

DINOSAURS, BIRDS, & FISH (OH MY)
PAGE, ARIZONA

Laci Brock
PTYS 594 FALL 2017

PALEOGEOGRAPHY

During the Late Cretaceous Period (100.5-66 Ma), the region that is now Page, AZ looked quite different. A large sea breached what we know as the United States, known as the Western Interior Seaway. Figures 1-3 below show how the Seaway progressed during the end of this period in Earth's history. Interestingly, North America had the greatest diversity of dinosaur species during this time such as plesiosaurs, mosasaurs, theropods (e.g., tyrannosaurs), ceratopsians (e.g., pentaceratops), and hadrosaurs.

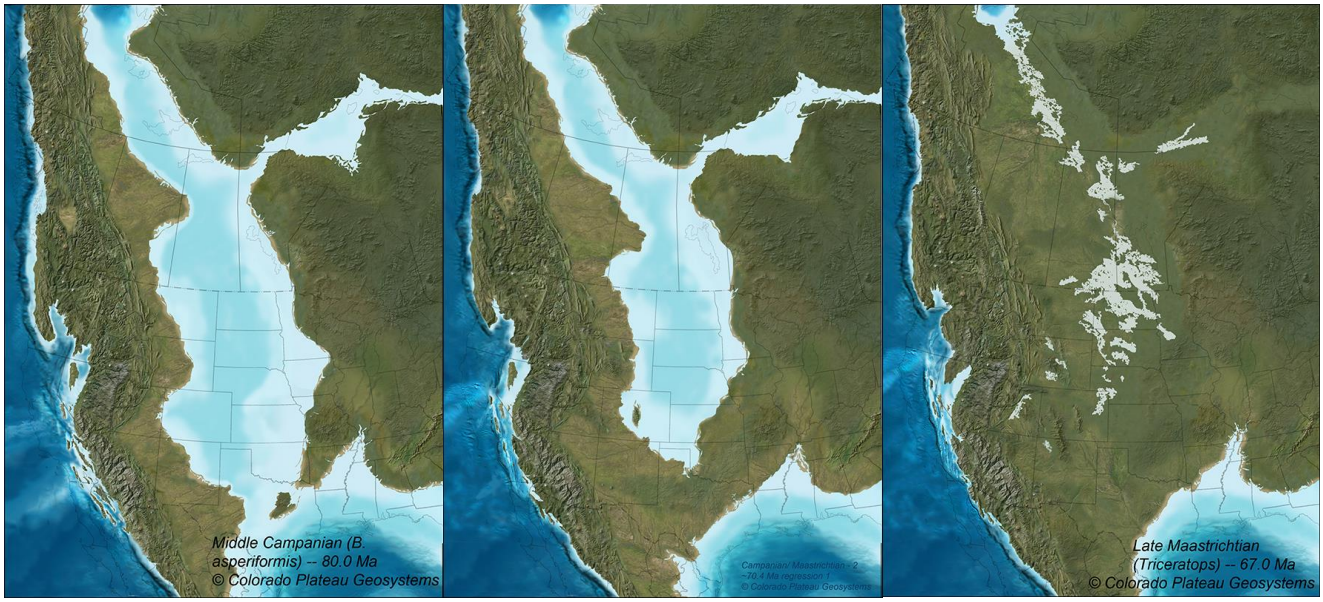

Figures 1-3 (from left): Paleogeographic reconstructions of the Southwestern United States during a timespan when the Western Interior Seaway was present (80-65 Ma). Images courtesy of Dr. Ron Blakey.

THERIZINOSAUR

A notable dinosaur species was recovered near Big Water, Utah (18 miles NW from Page) in the year 2000. It began as the discover as a single toe bone, but this eventually led the Museum of Northern Arizona (MNA) to excavate a nearly complete skeleton. Previously, this region was known for marine deposits and fossils (e.g., plesiosaurs) because it was submerged under the Seaway. MNA was able to excavate more of the skeleton and determined it was a sickle-clawed Therizinosaur, which had previously only been uncovered in China and Mongolia. One of the MNA members on this excavation included my former advisor, Dr. David Gillette, the Chair of Vertebrate Paleontology.

Figure 4-5 (from left): (4) Dr. Dave Gillette at the Big Water excavation site uncovers one of the sickle claws. (5) Final skeleton of the Therizinosaur discovered in Southern Utah previously on display at MNA.

BIRDS, FISH, MAMMALS

The diverse, large open water habitat of Lake Powell and the Colorado River provides a migration corridor for aquatic and riparian birds. Bird surveys were conducted beginning in 1994 and continue to the present day due to the influx of species in this area. Approximately 315 different species of birds have been documented in this region. Some rarities include the endangered Mexican spotted owl, bald eagles, and the Southwestern willow flycatcher. Water bird species have increased over the years, from 32 species before 1963 to 83 in 2007. Common species include: dabbling ducks, waders, shorebirds, herons, and gulls.

Despite the high species count, breeding is uncommon in the region. Only 80 native breeding species have been confirmed in the area. This is due to the harsh climate, unsuitable structures (e.g., slick cliff and rock faces), and a low shrub vegetation. Furthermore, the lake is poor in nutrients and tends to fluctuate, which does not provide stability. The habitat in this year has existed for less than 50 years and changes with the level of the lake.

Figures 6-7 (from left): American coot and Western grebe, some of the most common water fowl found on Lake Powell.

Several mammalian species can be found in and around the Lake Powell area. Smaller creatures, such as kangaroo mice and pack rats are found in burrows in the area. A few species of bats are also common nocturnal visitors, as well as the black-tailed jackrabbit. Larger species include the desert bighorn sheep and bison. Keystone predators in the area are similar to those found in Tucson. Bobcats, mountain lions, and coyotes can call be seen in the area.

Interestingly, the Colorado River basin is home to 14 native species of fish, 4 of which are considered endangered. More than 40 non-native species of fish have been introduced to the area due to tourism and sport fishing. Invasive species have contributed to a decline of native species in the region as well as the negative contributions caused by water development, flood control, power generation, and recreation.

The endangered species of fish include the Colorado Pikeminnow, Razorback Sucker, Bonytail, and Humpback chub (pictured below, in order). All four of these fish evolved in the Colorado River basin 3-5 million years ago and exist nowhere else on Earth. Each fish is ~2-3 feet in length.

Figures 8-11 (from left): Four endangered fish species of the Colorado River basin. The pikeminnow is the largest minnow in North America, whereas the bonytail is the rarest of the four species.

PLANETARY CONNECTION

Endemic species are most likely to develop on geographically and biologically isolated areas. For example, on Earth, regions conducive to the development of endemic species include remote islands (such as Hawaii or the Galapagos), but they can also develop in isolated areas of land, or bodies of water far from other lakes/sources of water.

Figure 12: An endemic honeycreeper, the `I`Iwi found on the big island of Hawaii in Hakalau Forest.

The endemic fish species of the Colorado River Basin provide an analogue for how life could develop outside of Earth. Such ecological niches could exist on other bodies in the Solar System, and Europa has been a prominent example of this via theories that suggest life may exist in the icy moon's subsurface ocean. This would be especially true if there were smaller "lakes" separate from the ocean, which is illustrated in the figures below.

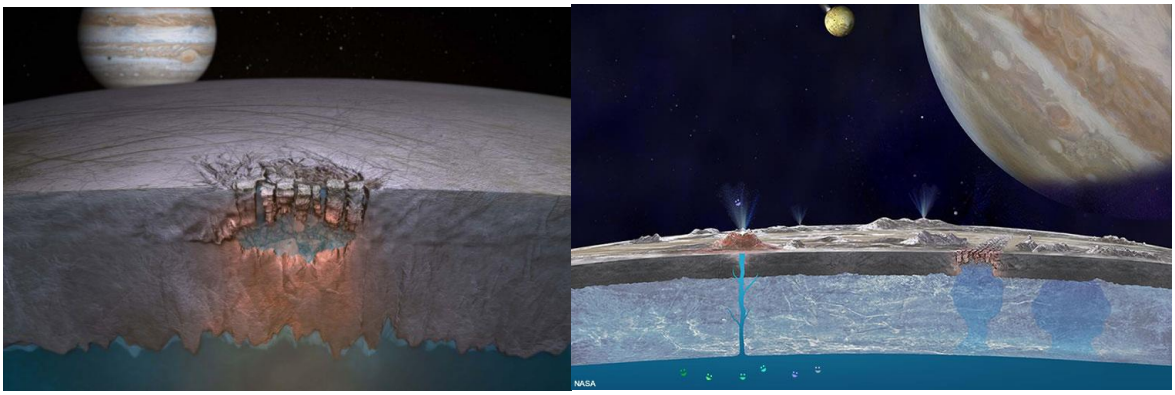

Figures 13-14: These images show regions that may be conducive to life on Europa below the surface where radiation is less harsh.

National Park Service
U.S. Department of the Interior

Glen Canyon National Recreation Area
Rainbow Bridge National Monument

Checklist of Birds Found in Glen Canyon National Recreation Area

Osprey

KEY

STATUS

W= winter resident (lower case = secondarily so)
M =migrant (lower case = secondarily so)
S = summer resident (lower case= secondarily so)
Y= year around resident
*= breeding confirmed
(*)= breeding suspected
C= casual
Esc= escaped
Exp= experimental population

HABITAT

R = riparian
A = aquatic (lake, ponds and rivers)
D = desertscrub (blackbrush, shadscale, sagebrush etc.)
P = pinyon-juniper woodland
T = talus and cliffs
W = widespread
H = human developed

ABUNDANCE

A = abundant, in large numbers
C = common , always seen but not in large numbers
FC = fairly common, very small numbers or not always seen
U = uncommon, seldom seen but not a surprise
S = sparse, always a surprise but not out of normal range
X = accidental, stray not to be wholly expected again

This checklist includes the species of birds presently known to have occurred in Glen Canyon National Recreation Area or nearby developed areas. The abundance and habitat symbols suggest when, where, and how readily a bird can usually be found.

The surprising number of species on this list is due in part to the large size of the recreation area (over 1.2 million acres) and to the variety of habitat types. Desert scrublands, lush streamside vegetation, pinyon-juniper woodlands, and vast areas of steep, rocky terrain all occur here. And there is water - Lake Powell and its side canyons, the Colorado and San Juan Rivers, and numerous springs and seeps.

Much of the recreation area has been largely unexplored by birders. Many of Lake Powell's side canyons remain a mystery, as do the pinyon-juniper woodlands, sagebrush flats, and extensive grasslands of the Hans Flat area. For combined productivity and accessibility, however, Lees Ferry is Glen Canyon's premier birding location. Here is the only readily accessible riparian (streamside) habitat along the Colorado River for over 150 miles in either direction. Lonely Dell Ranch, also at Lees Ferry, is famous for its spring and fall migrants. From late fall through winter, the boat launch area is *the* spot from which to observe waterfowl. And in spring and fall, the chances of spotting a California Condor at Navajo Bridge are very good.

To report unusual sightings, or for further information, contact:

Resource Management Division
Glen Canyon National Recreation Area
P.O. Box 1507
Page, AZ 86040

		Status	Habitat	Winter	Spring	Summer	Fall
	FINCHES AND ALLIES						
	BLACK ROSY-FINCH	W	T	U	U		U
	CASSIN'S FINCH	W	P		S	S	
	HOUSE FINCH	Y*	R,P,H	C	C	C	C
	RED CROSSBILL	Y*	P		S	S	
	PINE SISKIN	W	R,P		U	U	U
	LESSER GOLDFINCH	S*	R,H	S	C	C	C
	AMERICAN GOLDFINCH	W	R	F	F	X	F
	EVENING GROSBEAK	W	P	S	S	S	S
	OLD WORLD SPARROWS						
	HOUSE SPARROW	Y*	H	C	C	C	C

		Status	Habitat	Winter	Spring	Summer	Fall
	BLACK-CHINNED SPARROW	S*	P			S	
	VESPER SPARROW	M	D		C	U	C
	LARK SPARROW	S*	D,P		C	C	F
	BLACK-THROATED SPARROW	S*,w	D	S	A	A	S
	SAGE SPARROW	W,y*	D	F	F	F	F
	LARK BUNTING	M,w	D	S	S	S	S
	SAVANNAH SPARROW	M	D	S	C	C	C
	GRASSHOPPER SPARROW	C	R				X
	FOX SPARROW	C	R		S		S
	SONG SPARROW	W	R	C	C		C
	LINCOLN'S SPARROW	M,w	R	U	C		C
	SWAMP SPARROW	M,W	R	S	S		
	WHITE-THROATED SPARROW	W	R,h	S	S		S
	HARRIS'S SPARROW	W	H	S	S		S
	WHITE-CROWNED SPARROW	W,m	R,D	A	A	S	A
	GOLDEN-CROWNED SPARROW	C	R	S			
	DARK-EYED JUNCO	W	R,D,P	A	A		A
	CHESTNUT-COLLARED LONGSPUR	M	H				S
	GROSBEAKS AND ALLIES						
	ROSE-BREASTED GROSBEAK	M	R		S	S	S
	BLACK-HEADED GROSBEAK	S*	R		C	C	C
	BLUE GROSBEAK	S*	R		C	C	C
	LAZULI BUNTING	M,s*	R		C	C	C
	INDIGO BUNTING	S	R		S	S	S
	DICKCISSEL	M	H		S		S
	MEADOWLARKS, BLACKBIRDS, ORIOLES						
	BOBOLINK	M	H		S		S
	RED-WINGED BLACKBIRD	Y*	R	C	C	C	C
	WESTERN MEADOWLARK	M	D	F	F	F	F
	YELLOW-HEADED BLACKBIRD	M	R		C	C	C
	BREWER'S BLACKBIRD	M,w	R	F	C	F	C
	COMMON GRACKLE	S,M	R	S			
	GREAT-TAILED GRACKLE	Y*	R,H	C	C	C	C
	BROWN-HEADED COWBIRD	M,s*	W		C	C	C
	HOODED ORIOLE	S*	H		U	U	
	BALTIMORE ORIOLE	C	R				X
	BULLOCK'S ORIOLE	M,S*	R,H		C	C	C
	SCOTT'S ORIOLE	S*	P			U	

		Status	Habitat	Winter	Spring	Summer	Fall
	WAXWINGS						
	CEDAR WAXWING	M,w	R		F		F
	SILKY FLYCATCHERS						
	PHAINOPEPLA	S	R		U		
	WOOD-WARBLERS						
	TENNESSEE WARBLER	M	R		X		
	ORANGE-CROWNED WARBLER	M,w	R,P	S	F	S	C
	NASHVILLE WARBLER	M	R,P			U	U
	VIRGINIA'S WARBLER	M,s*	R,P		C	C	C
	LUCY'S WARBLER	S*	R		C	C	
	NORTHERN PARULA	M	R				X
	YELLOW WARBLER	M,S*	R		C	C	C
	BLACK-THROATED BLUE WARBLER	M	H				S
	YELLOW-RUMPED WARBLER	M,W	R,P	C	C	U	C
	BLACK-THROATED GRAY WARBLER	S*,m	P,r		C	C	U
	TOWNSEND'S WARBLER	M	P		S		F
	HERMIT WARBLER	M	P				S
	PRAIRIE WARBLER	C	H	X			X
	BLACKPOLL WARBLER	C	H				X
	BLACK-AND-WHITE WARBLER	C	P			X	
	AMERICAN REDSTART	C	R		S	S	
	PROTHONOTARY WARBLER	C	R		X		
	WORM-EATING WARBLER	C	R		X		
	NORTHERN WATERTHRUSH	M	R		U		
	MACGILLIVRAY'S WARBLER	M	R		U	F	F
	COMMON YELLOWTHROAT	M,s*	R		C	C	C
	WILSON'S WARBLER	M	R,P		C	C	C
	YELLOW-BREASTED CHAT	S*	R		C	C	F
	TANAGERS						
	SUMMER TANAGER	S	R		S	S	
	SCARLET TANAGER	C	R		X	X	

		Status	Habitat	Winter	Spring	Summer	Fall
	TOWHEES, SPARROWS, JUNCOES						
	GREEN-TAILED TOWHEE	M,c-w*	D	X	F	F	C
	SPOTTED TOWHEE	W,s*	P,R	C	C	C	C
	RUFOUS-CROWNED SPARROW	Y*	T,D	F	F	F	F
	AMERICAN TREE SPARROW	W	R				S
	CHIPPING SPARROW	M,s*	P,D		C	C	C
	CLAY-COLORED SPARROW	M	R,D		S		S
	BREWER'S SPARROW	M,w	D	S	C	C	C
	LOONS						
	PACIFIC LOON	W	A	S	S		S
	COMMON LOON	W	A	F	F	S	F
	YELLOW-BILLED LOON	W	A	S	S		
	GREBES						
	PIED-BILLED GREBE	W	A	F	F	U	F
	HORNED GREBE	W	A	F	F	U	F
	RED-NECKED GREBE	W	A	S	S		
	EARED GREBE	W,m	A	C	C	C	C
	WESTERN GREBE	W,m*	A	A	C	C	A
	CLARK'S GREBE	M	A		U	U	U
	PELICANS						
	AMERICAN WHITE PELICAN	M,c-w	A	S	F	F	F
	BROWN PELICAN	C	A		S	S	
	CORMORANTS						
	DOUBLE-CRESTED CORMORANT	W,m	A	U	U	S	U
	BITTERNS AND HERONS						
	GREAT BLUE HERON	W,m,s*	A	C	C	F	F
	GREAT EGRET	M	A		S		
	SNOWY EGRET	M	A		C	C	C
	LITTLE BLUE HERON	C	A				S
	CATTLE EGRET	M	A		F		F
	GREEN HERON	M,s	A		U	U	
	BLACK-CROWNED NIGHT-HERON	M	A		F	F	F
	IBISES						
	WHITE-FACED IBIS	M	A	X	C	C	C
	ROSEATE SPOONBILL	M	A		S	S	

		Status	Habitat	Winter	Spring	Summer	Fall
	AMERICAN VULTURES						
	TURKEY VULTURE	S,m*	W	C	C	C	
	CALIFORNIA CONDOR	exp	W	S	S	S	S
	SWANS, GEESE, AND DUCKS						
	GREATER WHITE-FRONTED GOOSE	W,M	A	S			S
	SNOW GOOSE	W,M	A	S			S
	ROSS'S GOOSE	W,M	A	S	S		
	CANADA GOOSE	y*,M,W	A	C	C	S	C
	TUNDRA SWAN	M	A	U			U
	TRUMPETER SWAN	M	A	X			
	WOOD DUCK	M	A	U	U	S	S
	GADWALL	W,M	A	C	C	F	C
	EURASIAN WIGEON	W	A	S	S		
	AMERICAN WIGEON	W,M	A	A	A	F	A
	MALLARD	Y*	A	C	C	C	C
	BLUE-WINGED TEAL	M	A	S	F	C	C
	CINNAMON TEAL	M	A	S	C	C	C
	NORTHERN SHOVELER	M,w	A	C	C	C	C
	NORTHERN PINTAIL	M,w	A	C	C	F	F
	GREEN-WINGED TEAL	M,W	A	C	C	F	C
	CANVASBACK	M,w	A	U	U	S	U
	REDHEAD	M,w	A	C	C	U	C
	RING-NECKED DUCK	M,W	A	C	C	F	C
	GREATER SCAUP	W,m	A	F	F		?
	LESSER SCAUP	W,M	A	C	C	F	C
	SURF SCOTER	M,w	A	S	S	S	S
	WHITE-WINGED SCOTER	M	A	S	S		
	LONG-TAILED DUCK	W	A	S	S		S
	BUFFLEHEAD	M,W	A	C	C	S	C
	COMMON GOLDENEYE	W,m,s	A	A	A	S	C
	BARROW'S GOLDENEYE	W	A	C	C	X	C
	HOODED MERGANSER	M,w	A	U	U		U
	COMMON MERGANSER	W,m,s*	AA	C	C	F	C
	RED-BREASTED MERGANSER	W,m	A	F	F		F
	RUDDY DUCK	M,w,s	A	U	C	F	C

Ecological Theory and Practice in the Grand Canyon

Grand Canyon National park contains several major ecosystems. Due to the 8000 feet of elevation encompassed within the Park, five of the seven Life Zones and three out of the four desert types found in North America can be found here! Not familiar with Life Zones? Well, let me inform you: Back in the late 19th Century an American naturalist named Clinton Hart Merriam studied the spatial and latitudinal distribution of plants from the bottom of the Grand Canyon to the top of Humphreys Peak. Essentially, Clinton organized the seeming inherent nature of plant and animal groupings to change with elevation, coining the term Life Zones (Figure 1). These Life Zones were designed to conceptually capture the following: changes observed in these communities with increases in latitude and constant elevation mirror the changes observed in maintaining latitude and increasing elevation (Merriam, 1890). In other words, the observable changes in plant community from the base of the Canyon to the North Rim approximate the changes in vegetation observable by trekking from Sonora, Mexico, to Canada. For you Tucson folk, think the biomes you drive through up on your way to the Mt. Lemmon summit.

Figure 1) Arizona Biomes, adapted from Merriam 1890.

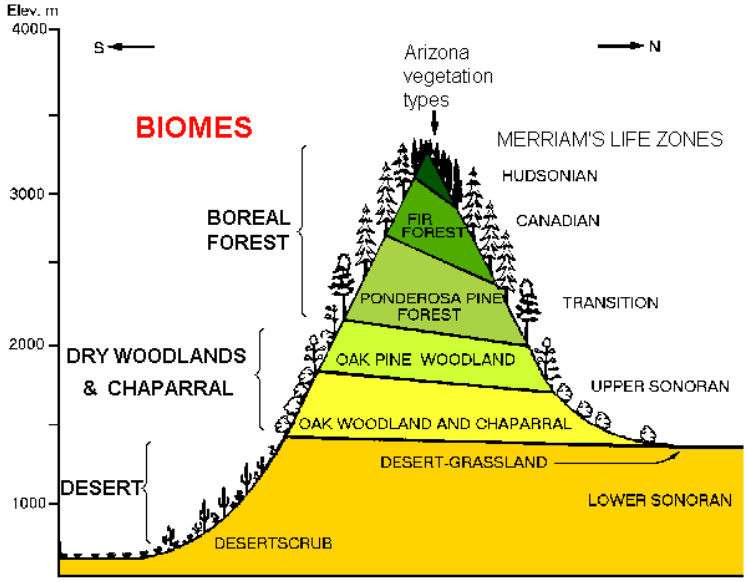

(www.geo.arizona.edu)

While the actions of erosion by wind and water change the landscape on the scale of thousands of years, changes in landscape ecology from human intervention are often immediately observable. For example, historical initiatives by land managers to preserve natural areas often involve predator control. Aimed at enhancing the experience for hunters and park visitors, natural predators within these parks were systematically exterminated, and in some cases their numbers were replaced with the transplantation of additional ungulate herbivores. In the case of the Kiabab mule deer surrounding the Grand Canyon, this land management technique occurred between 1910-1922, and has since become a keystone example of the complexity of ecological food webs.

Predominant theories in ecological food web modeling were designed to explain the expected outcome of the removal of top predators from a food chain. One asserts that the removal of survival pressure from the basal herbivore level of the food chain will cause unchecked and exponential-level population growth. Having removed these natural predators (in this example, wolves, bobcats, mountain lions), herbivores experienced very rapid population growth, which placed major and unprecedented predatory pressure on the supporting plant community. Rate of plant consumption by mule deer wasn't sustainable, and their primary food source collapsed, causing a bottom-up trophic cascade that decimated the deer populations. This event has been widely cited and detailed by environmentalists since the 1920's (Leopold, 1943), including by Rachel Carson in her hard-hitting environmental novel *Silent Spring*.

Even more exciting, this example has been the center of debates about ecological theory, particularly during the evolution of ecological theory in the mid-1960's. The US National Park Service adopted the mindset that primary producers (plants) were the dominant controls in food webs, and that ungulate herbivores were expected to stabilize with the proper management and removal of predators. In fact, the 1921 Kiabab mule deer collapse example was deemed "fake news" by Caughley (1970), who supposed that the population collapse happened from the removal of livestock in the area, who otherwise would compete for food sources. A team of researchers set out to explore this event using the age structure of aspen (*Populus tremuloides*), which constitute the primary source of deer browse, and an explosion of Kiabab deer population would be visible through the absence of a normal aspen cohort for that period (Binkley 2006). Their results showed a dramatic reduction in aspen stands during the early 1920's, along with another dip in aspen cohort numbers during another period of mule deer population explosion in the mid 1950's (Figure 2).

Figure 2) Density of Aspen (*Populus tremuloides)* on the Colorado plateau since 1800.

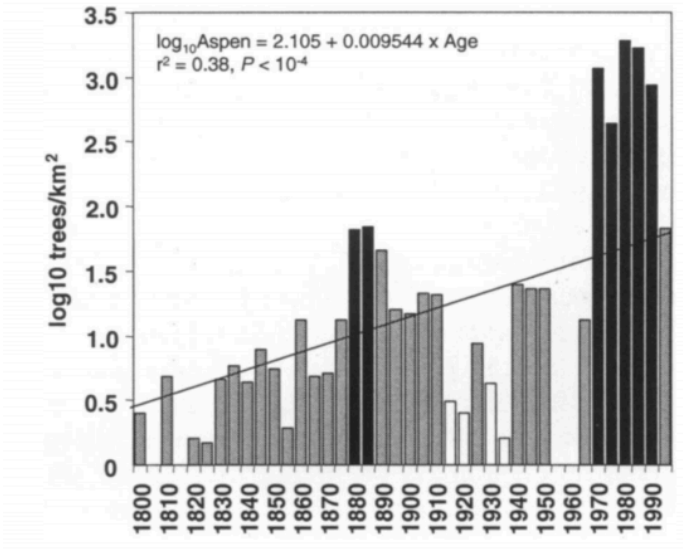

Figure taken from Leopold 1943.

These results support bottom-up controls over Kiabab mule deer population, which were eventually incorporated into most land management techniques (see the re-introduction of the Mexican Gray wolf, Brown 2001).

In short, early 1920's Grand Canyon Superintendent Miner Tillotson was not a perfect person; there were many things he wished he didn't do, including supporting the practice of killing predators in the park. But he continued learning, and never meant to do those things to the ecological structure of the park. And so he had to say before he left his post as superintendent that the practice of predator killing was over. That he just wanted us to know the importance of herbivory control in maintaining the balance of the natural system, and in doing so, he had found a reason for these predators. Tillotson had changed who he used to be, inadvertently stumbling onto a reason to start over new, and that reason was the majestic Kiabab mule deer.

Binkley, D., Moore, M., Romme, W., & Brown, P. (2006). Was Aldo Leopold Right about the Kaibab Deer Herd? *Ecosystems, 9*(2), 227-241.

Brown, W. (2001). Restoring the Mexican gray wolf to the mountains of the southwest. *Large Mammal Restoration : Ecological and Sociological Challenges in the 21st Century /,* 169-186.

Caughley G. 1970. Eruption of ungulate populations, with emphasis on Himalayan thar in New Zealand. Ecology 51:53 71

Leopold A. 1943. Deer irruptions. Wise Conserv Bull 8:3-11.

Lyrics, M. 2004. The Reason, Hoobastank, *Don't Touch my Mustache*. (10).

Merriam, C. H. (1890) Results of a biological survey of the San Francisco Mountains region and desert of the Little Colorado in Arizona. Department of Agriculture, Div. Ornithology and Mammalogy. North American Fauna 3: 1-136.

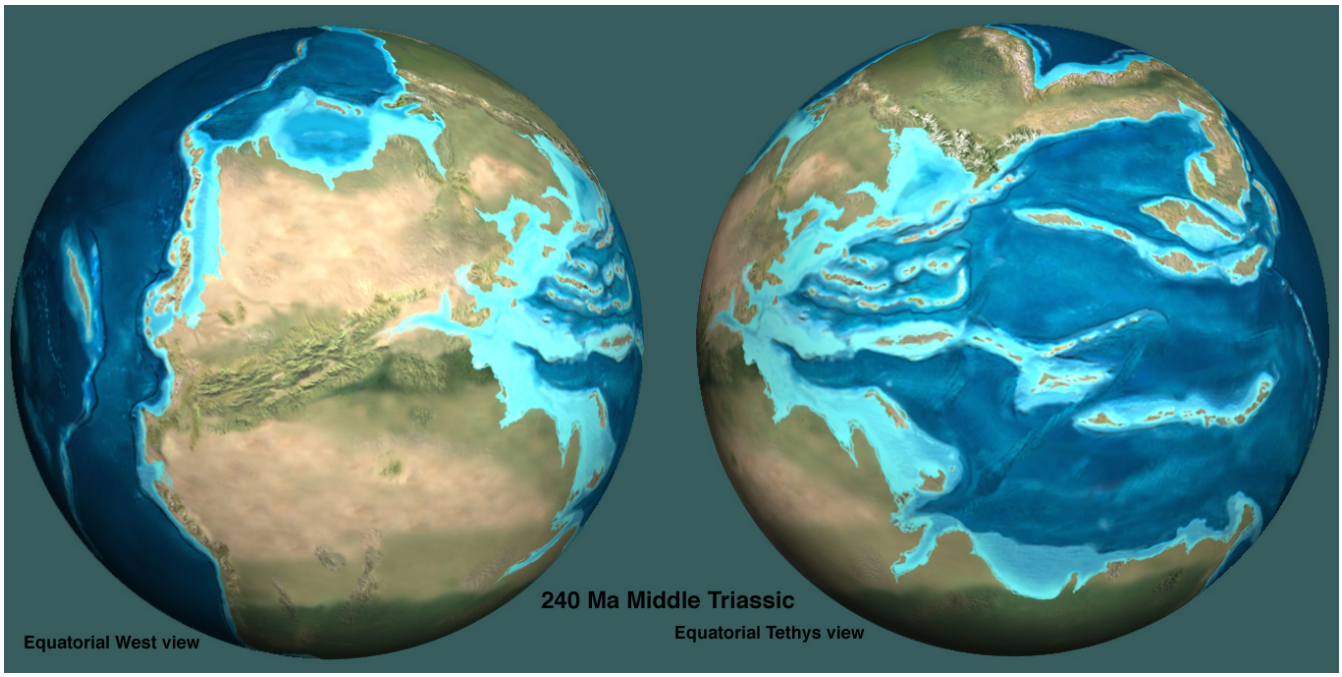
240 Ma Middle Triassic
Equatorial West view
Equatorial Tethys view

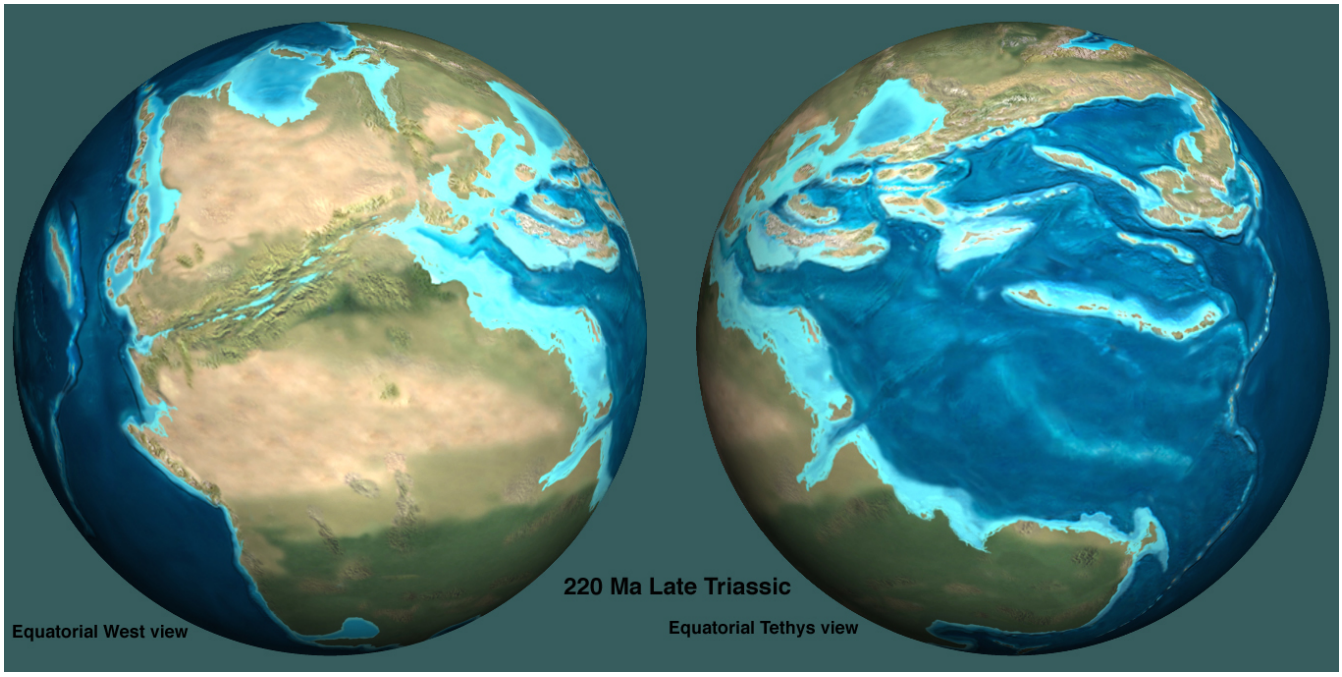
220 Ma Late Triassic
Equatorial West view
Equatorial Tethys view

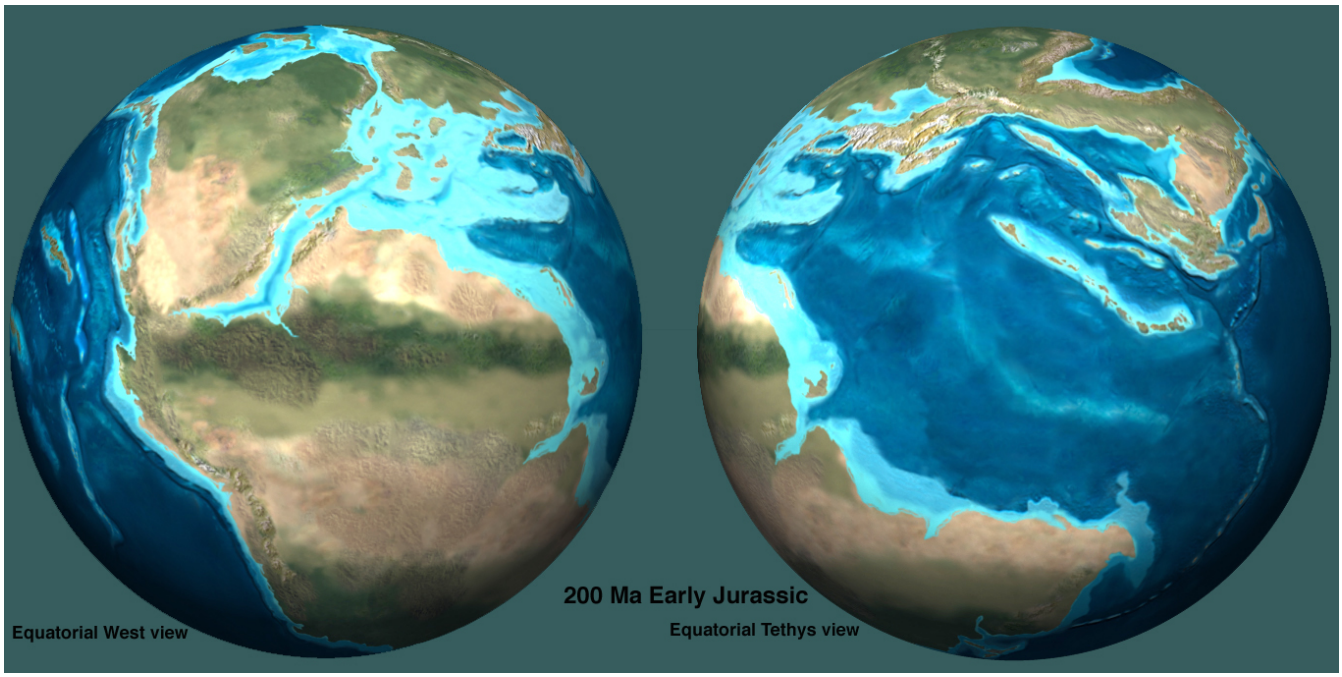
200 Ma Early Jurassic
Equatorial West view
Equatorial Tethys view

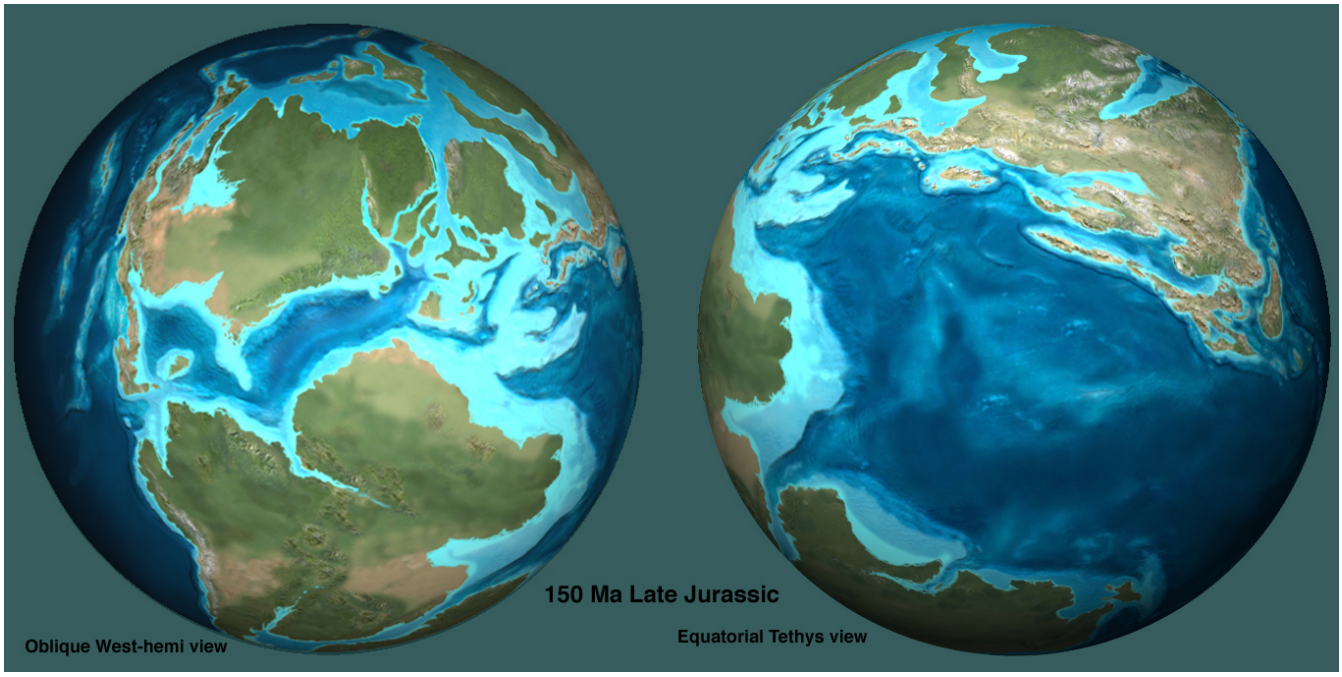
150 Ma Late Jurassic
Oblique West-hemi view
Equatorial Tethys view

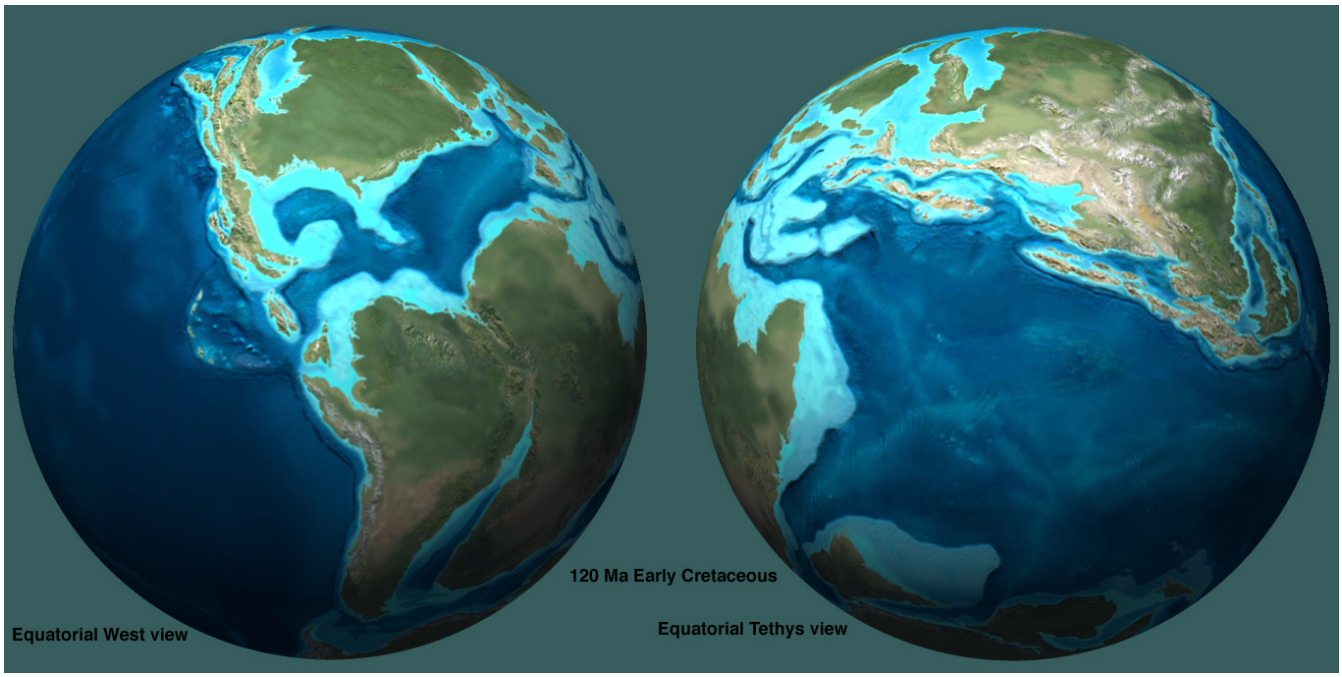
120 Ma Early Cretaceous
Equatorial West view
Equatorial Tethys view

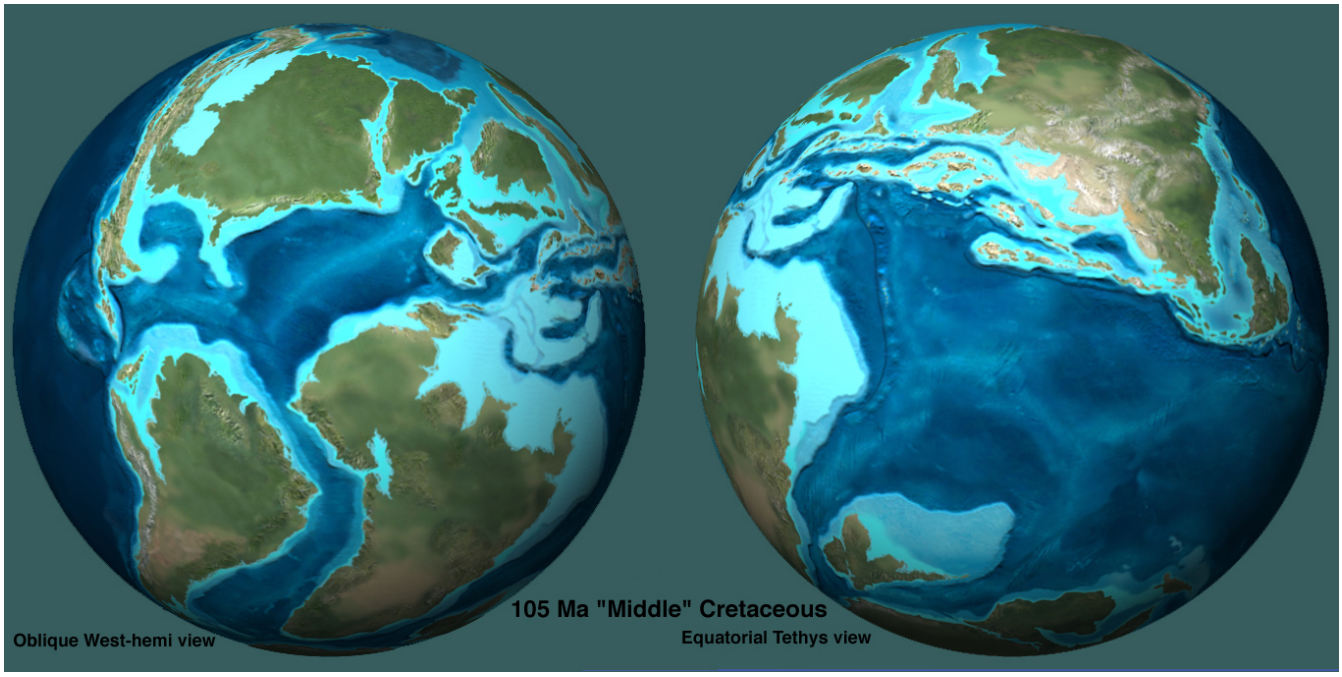
105 Ma "Middle" Cretaceous
Oblique West-hemi view
Equatorial Tethys view

Millimeters (mm)	Micrometers (μm)	Phi (ϕ)	Wentworth size class	
4096		-12.0	Boulder	
256		-8.0	Cobble	Gravel
64		-6.0	Pebble	
4		-2.0	Granule	
2.00		-1.0	Very coarse sand	
1.00		0.0	Coarse sand	
1/2 0.50	500	1.0	Medium sand	Sand
1/4 0.25	250	2.0	Fine sand	
1/8 0.125	125	3.0	Very fine sand	
1/16 0.0625	63	4.0	Coarse silt	
1/32 0.031	31	5.0	Medium silt	
1/64 0.0156	15.6	6.0	Fine silt	Silt
1/128 0.0078	7.8	7.0	Very fine silt	
1/256 0.0039	3.9	8.0	Clay	Clay
0.00006	0.06	14.0		

Sorting:

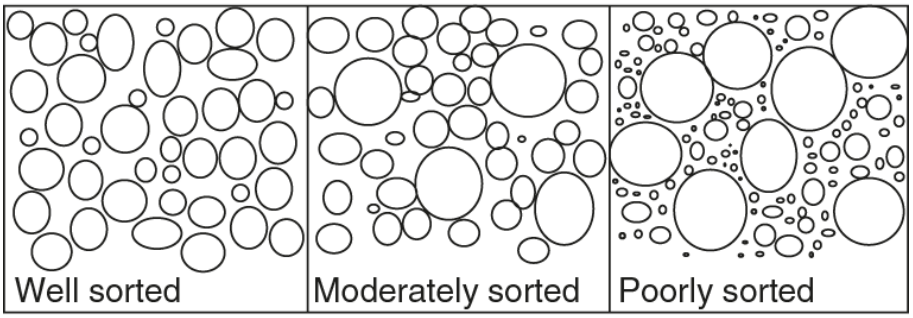

Rounding:

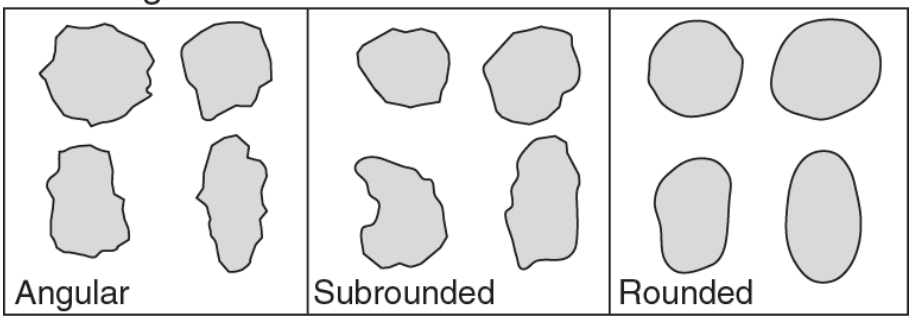

Visual estimates of proportions of mixtures

1% black

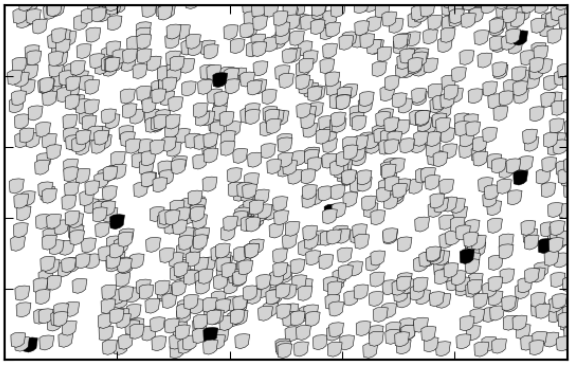

2% black

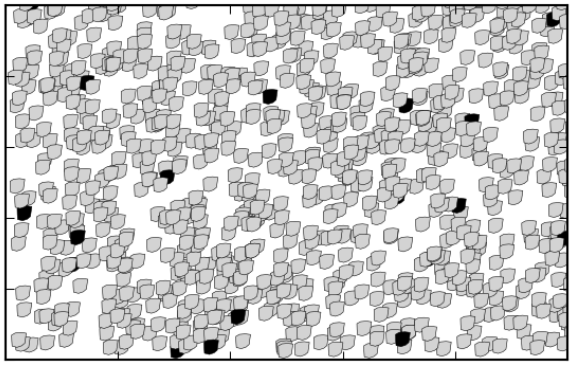

5% black

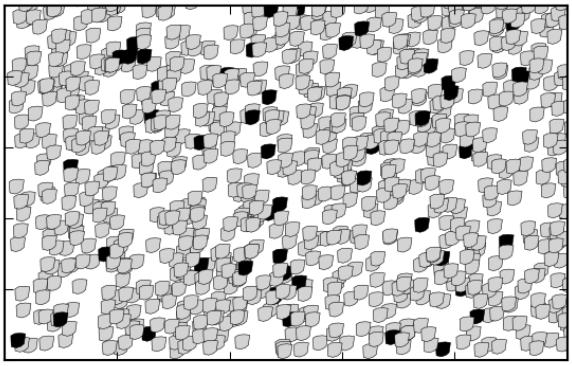

10% black

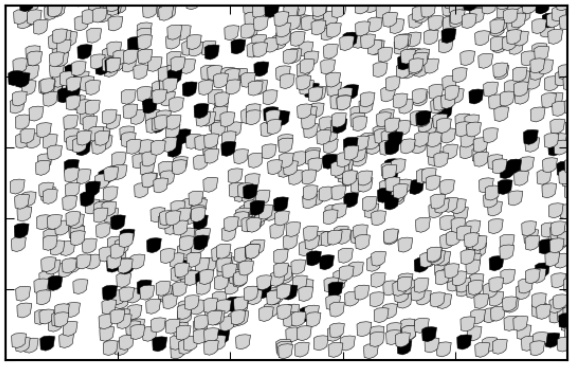

20% black

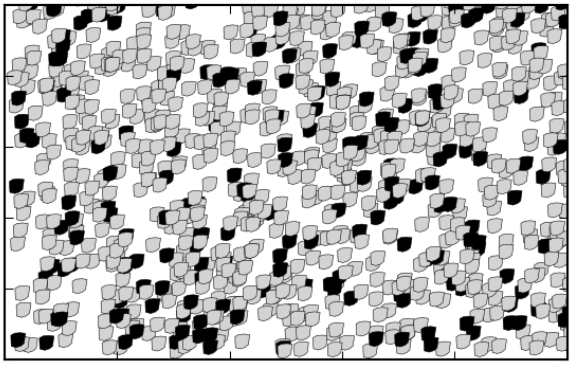

30% black

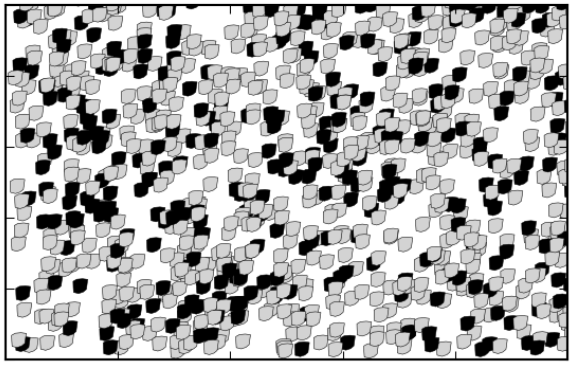

50% black

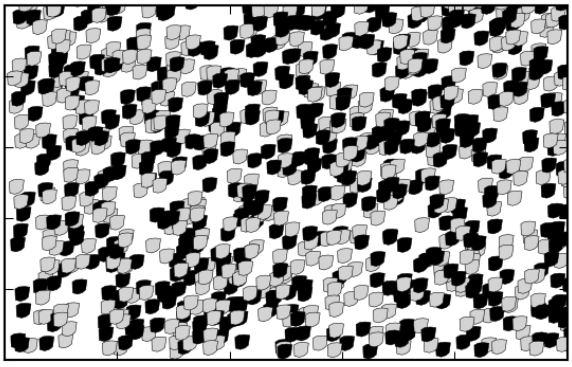

75% black

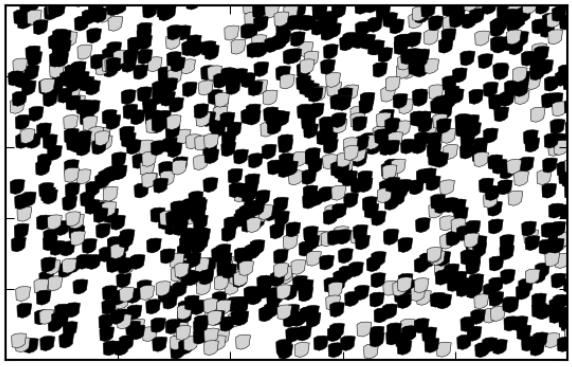

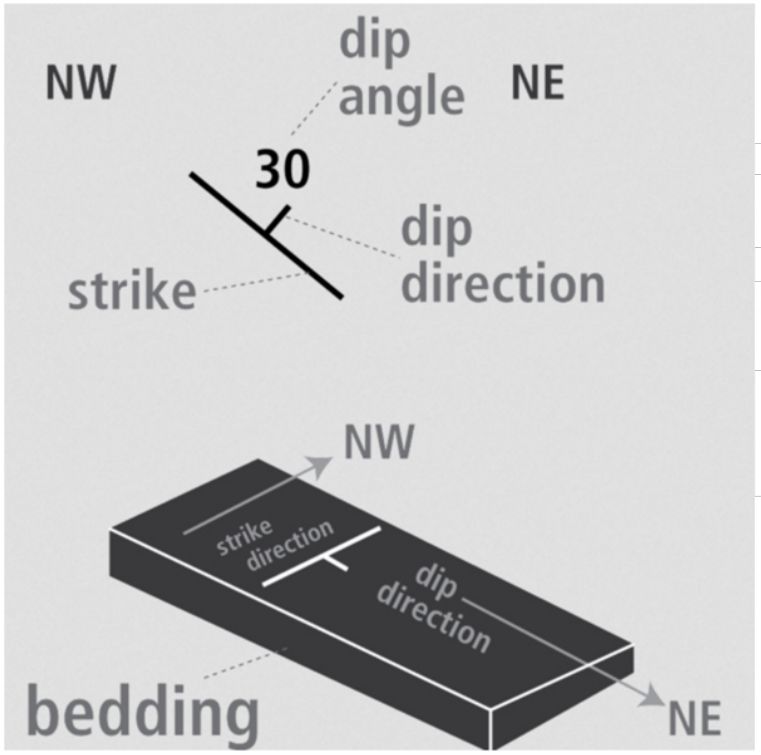
NW
dip
angle
NE
30
dip
direction
strike
NW
strike
direction
dip
direction
bedding
NE

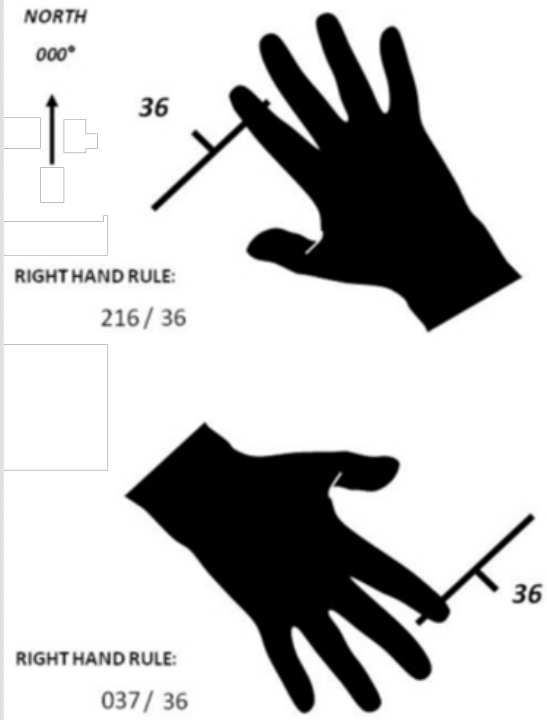
NORTH
000°
36
RIGHT HAND RULE:
216 / 36
36
RIGHT HAND RULE:
037 / 36

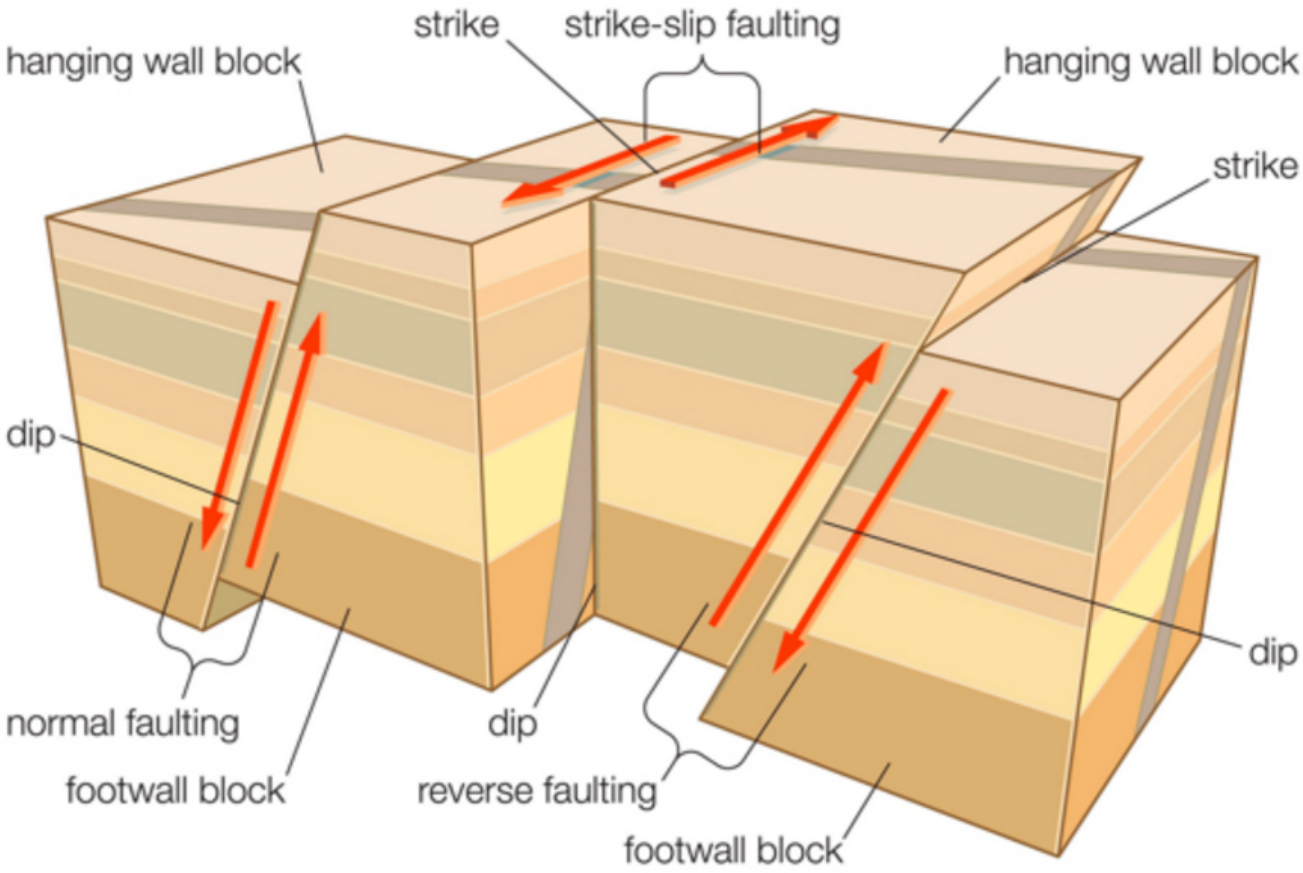
hanging wall block
strike
strike-slip faulting
hanging wall block
strike
dip
dip
normal faulting
footwall block
dip
reverse faulting
footwall block

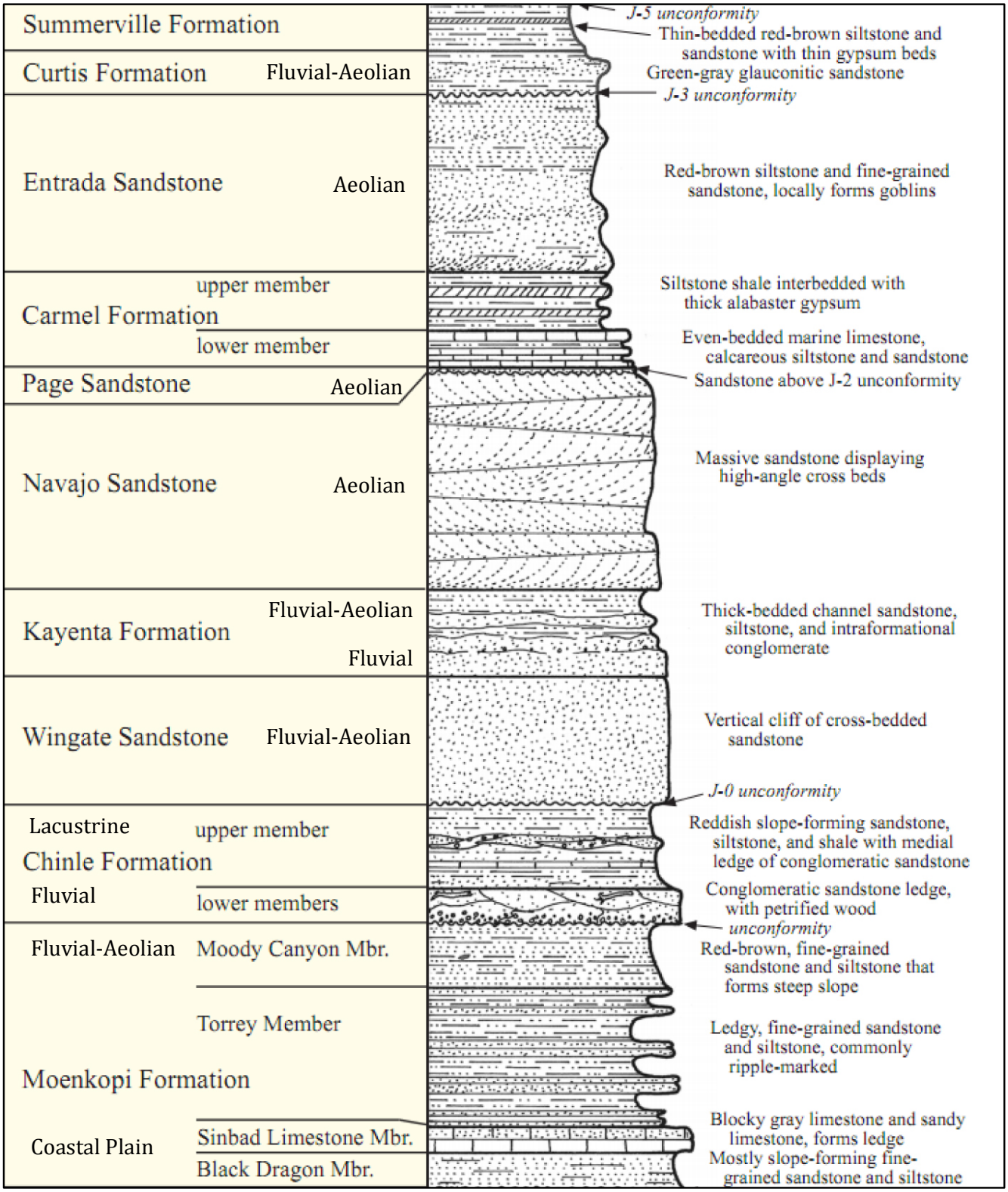
Summerville Formation
Curtis Formation
Fluvial-Aeolian
Entrada Sandstone
Aeolian
Carmel Formation
upper member
lower member
Page Sandstone
Aeolian
Navajo Sandstone
Aeolian
Kayenta Formation
Fluvial-Aeolian
Fluvial
Wingate Sandstone
Fluvial-Aeolian
Lacustrine
Chinle Formation
upper member
Fluvial
lower members
Fluvial-Aeolian
Moody Canyon Mbr.
Torrey Member
Moenkopi Formation
Coastal Plain
Sinbad Limestone Mbr.
Black Dragon Mbr.
J-5 unconformity
Thin-bedded red-brown siltstone and sandstone with thin gypsum beds
Green-gray glauconitic sandstone
J-3 unconformity
Red-brown siltstone and fine-grained sandstone, locally forms goblins
Siltstone shale interbedded with thick alabaster gypsum
Even-bedded marine limestone, calcareous siltstone and sandstone
Sandstone above J-2 unconformity
Massive sandstone displaying high-angle cross beds
Thick-bedded channel sandstone, siltstone, and intraformational conglomerate
Vertical cliff of cross-bedded sandstone
J-0 unconformity
Reddish slope-forming sandstone, siltstone, and shale with medial ledge of conglomeratic sandstone
Conglomeratic sandstone ledge, with petrified wood
unconformity
Red-brown, fine-grained sandstone and siltstone that forms steep slope
Ledgy, fine-grained sandstone and siltstone, commonly ripple-marked
Blocky gray limestone and sandy limestone, forms ledge
Mostly slope-forming fine-grained sandstone and siltstone

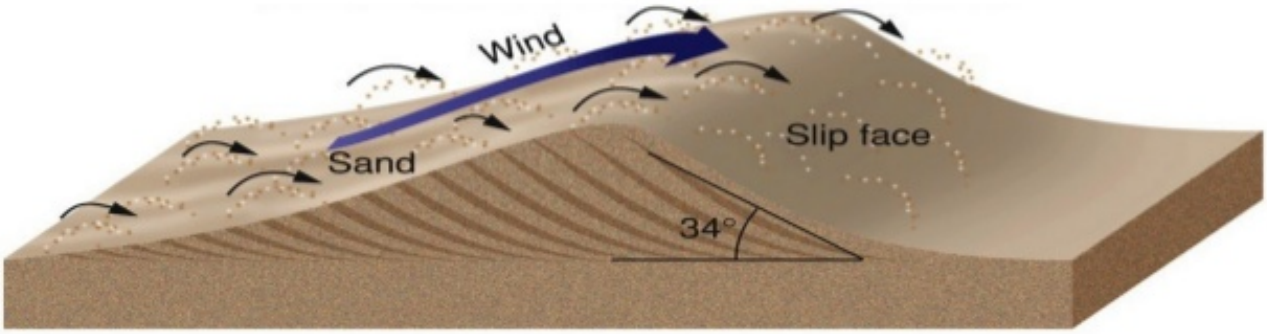
Wind
Sand
Slip face
34°

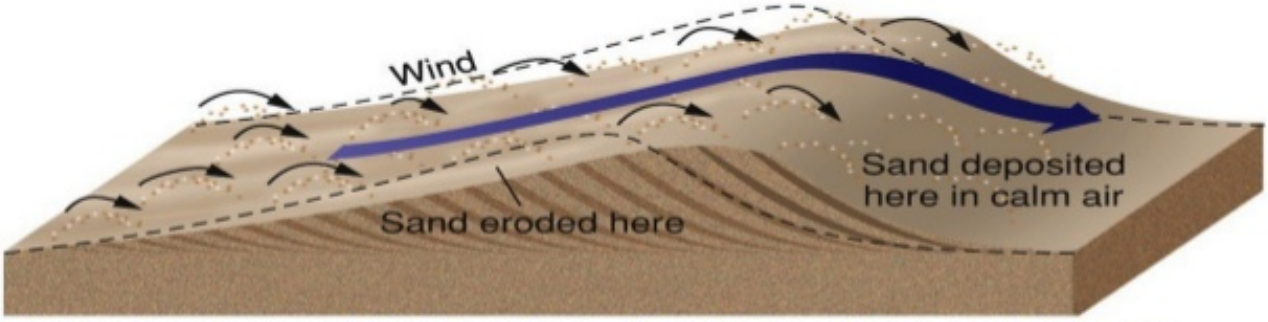
Wind
Sand deposited
here in calm air
Sand eroded here

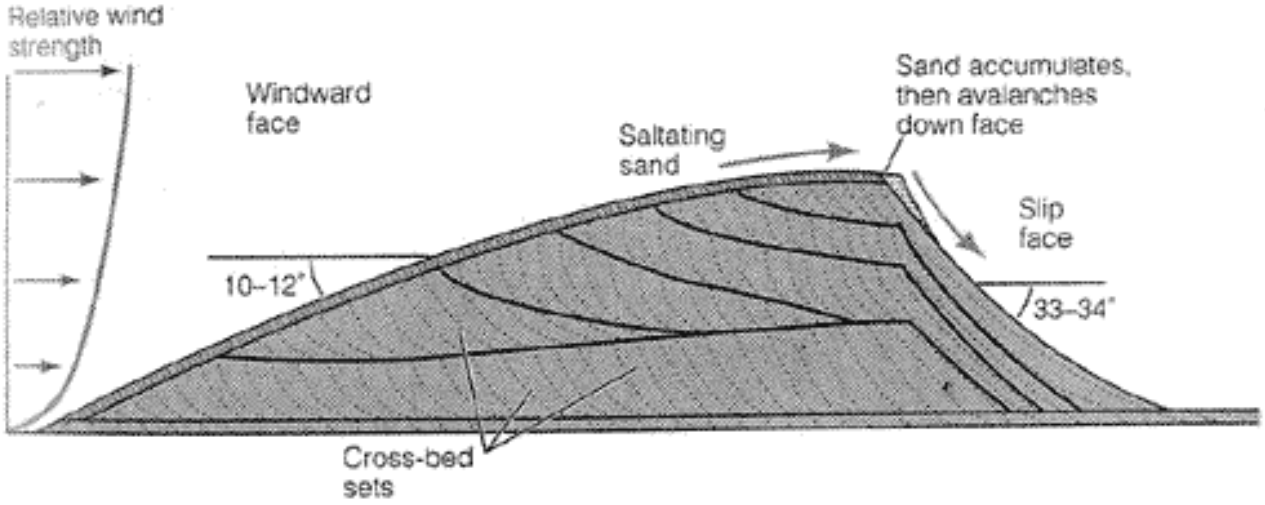
Relative wind
strength
Windward
face
Saltating
sand
Sand accumulates,
then avalanches
down face
Slip
face
10–12°
33–34°
Cross-bed
sets

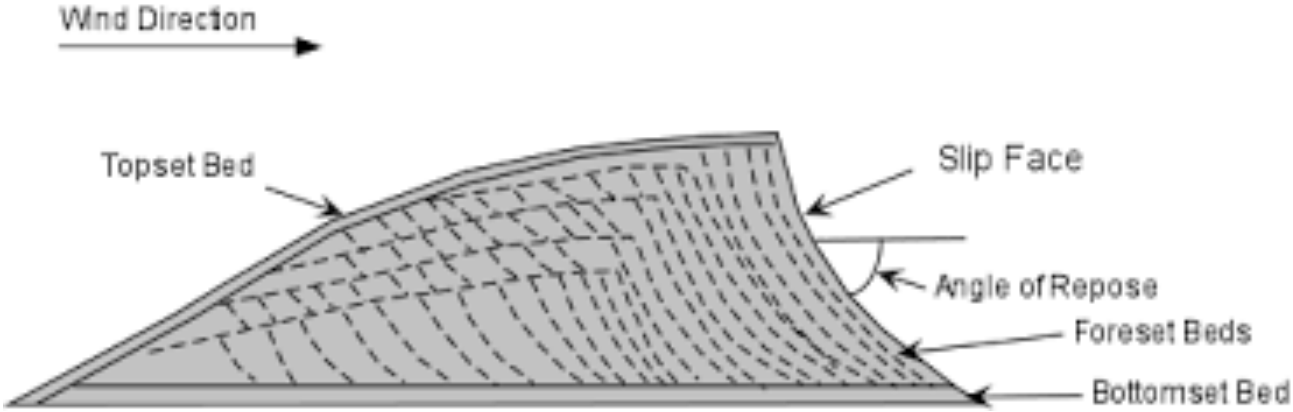
Wind Direction
Topset Bed
Slip Face
Angle of Repose
Foreset Beds
Bottomset Bed

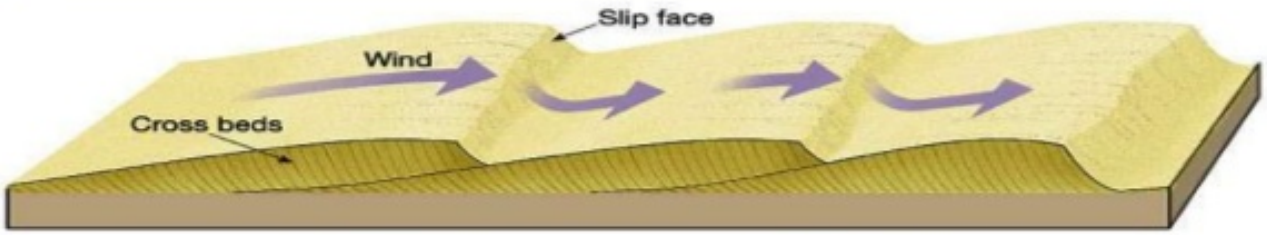
Slip face
Wind
Cross beds

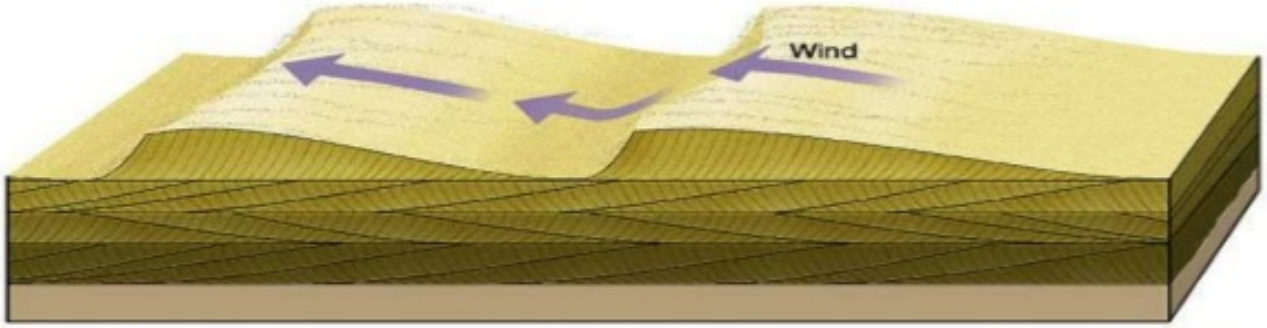
Wind

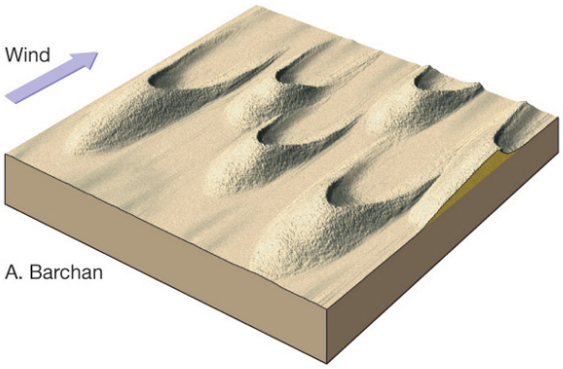
Wind
A. Barchan

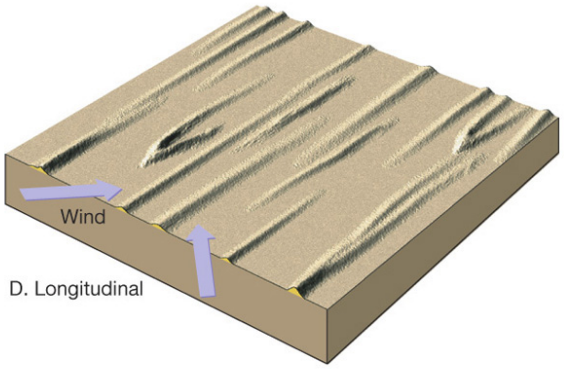
Wind
D. Longitudinal

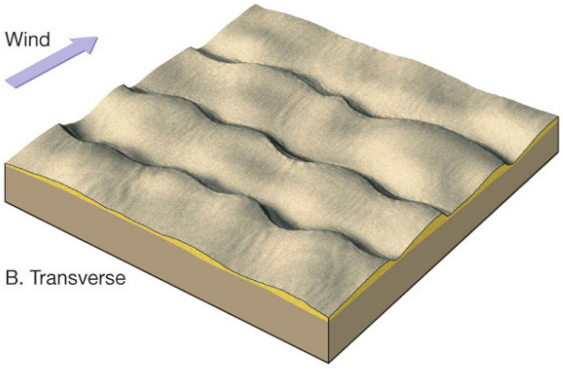
Wind
B. Transverse

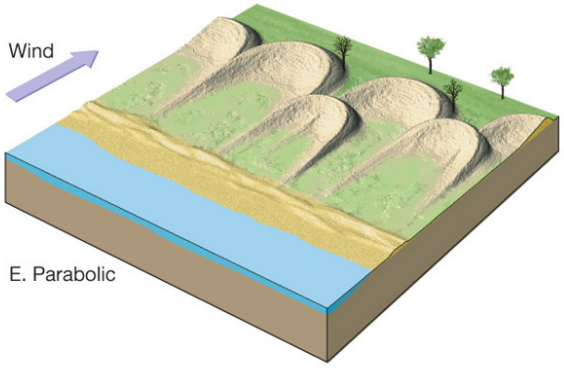
Wind
E. Parabolic

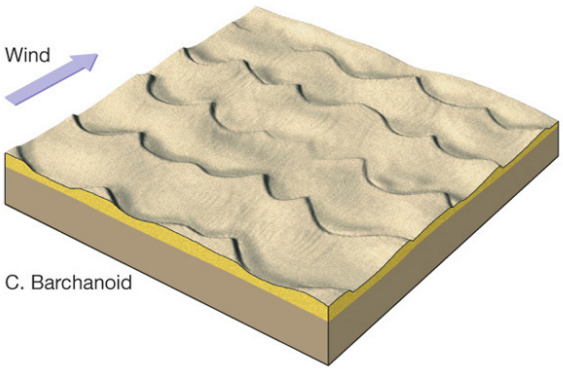
Wind
C. Barchanoid

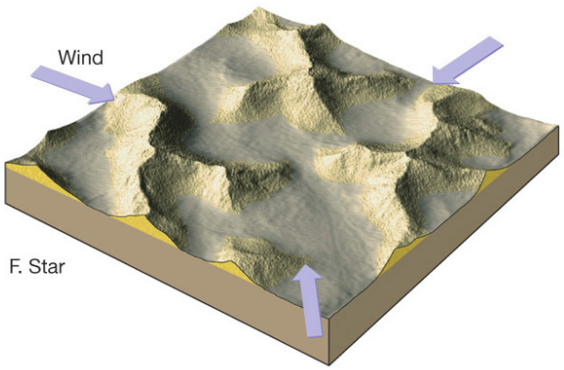
Wind
F. Star

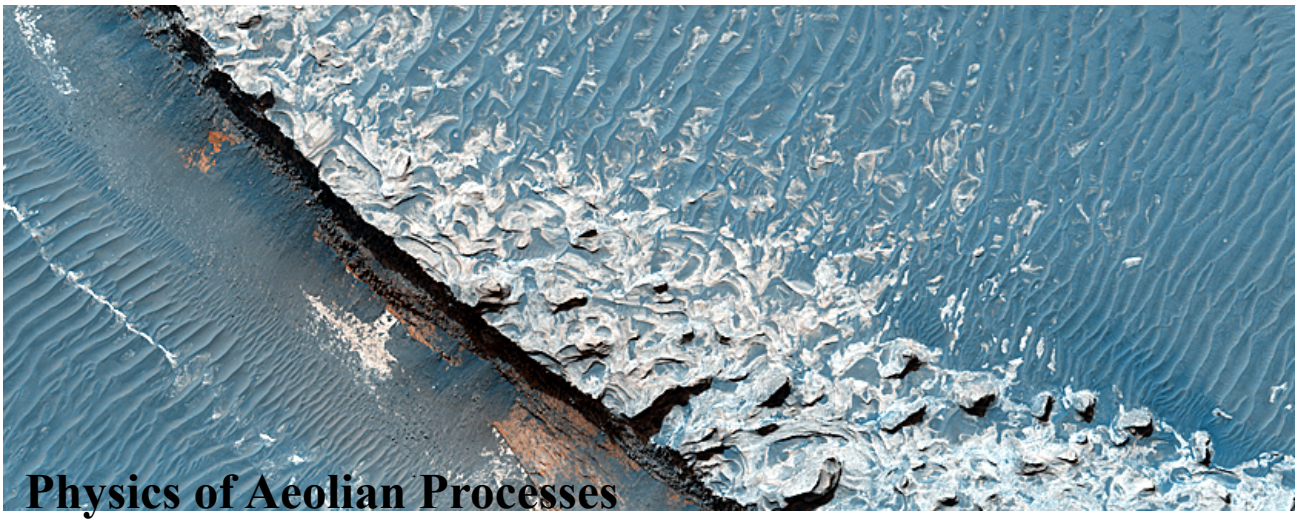

Physics of Aeolian Processes

Patrick O'Brien

Introduction (Title image – HiRISE Aeolian Theme webpage)

" Aeolian" refers broadly to geological processes resulting from the transportation, erosion, and deposition of granular material by wind. Under the right conditions, these processes can significantly shape the surfaces of Earth and other terrestrial bodies.

- Where do Aeolian processes occur?
  - Arid environments
  - Sparse vegetation
  - Dry soil
  - Large supply of loose sediment
  - Most importantly, where winds are sufficiently strong!
- What are the properties of the material involved in these processes?
  - Inorganic rock and mineral particles
  - Sand – 62.5 to ~2000 microns in size, Dust - < 62.5 microns

Transportation

Stationary particles can be mobilized through a number of different mechanisms which depend heavily on particle size and wind speed. Figure 1 summarizes the forces acting on a particle at rest in an Aeolian bedform. For a particle to be moved, the combined force of wind drag and lift must exceed the combination of the particle's weight, inter-particle cohesion, and friction between the particle and the bed.

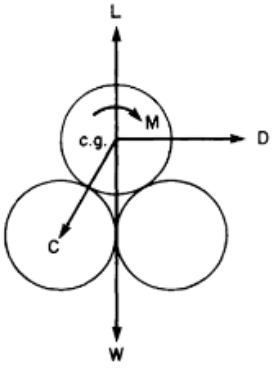

Figure 1. W is the weight of the particle, D is wind drag, L is lift, C is particle cohesion (Pye 1987)

As wind flows over a bed of particles, a shear flow velocity field develops. Above a thin layer of zero velocity, turbulent eddies form and the average speed of the wind increases logarithmically with height. At some critical velocity, the first particles begin to move from the drag force of the wind.

$v_{drag} = A\sqrt{\frac{\rho_p - \rho_a g D}{\rho_a}}$, where densities are relative densities of particles and air, respectively, g is gravitational acceleration, D is mean grain diameter, and A is a coefficient corresponding to the degree of turbulence surrounding the particle.

In desert regions on Earth, this happens first for particles ~100 microns in diameter. These particles start to hop along the surface in a fashion known as **saltation**. As they skip along, they can slam into and mobilize other particles.

For particles greater than 500 microns, these impact forces combined with wind drag forces can cause the grains to roll or slide along the surface in **creep** transport or by taking very short hops (< 1cm) which is called **reptation**.

Dust particles (<~65 microns) despite their small sizes, are rarely aerodynamically lifted from rest due to their large inter-particle cohesive forces. Once ejected by an impact, they can be become temporarily suspended in eddies or suspended for long time periods (up to weeks and months) via aerodynamic lift from velocity differentials in the wind.

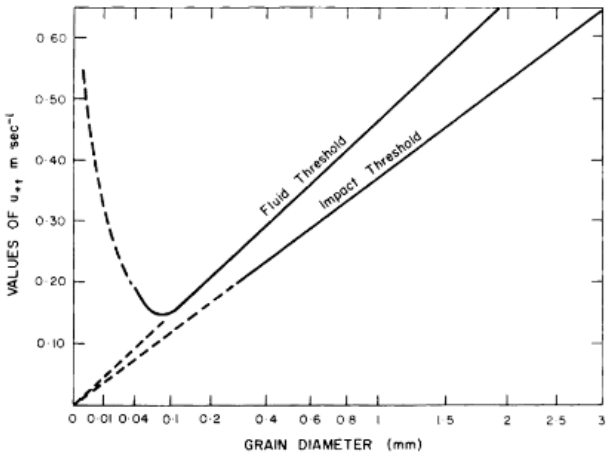

Figure 2. This plot shows the velocity at which different-sized particles can be moved fluidly by the wind and by the force of impacts from moving particles (Pye 1987)

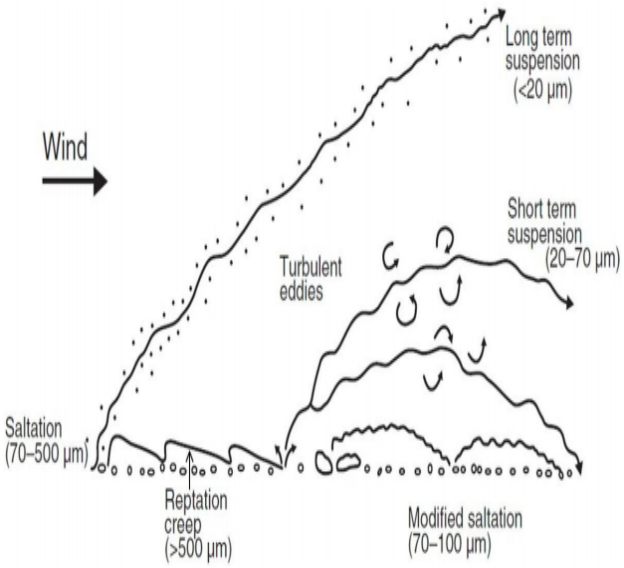

Figure 3. Summary of transportation modes for aeolian mobilized dust/sand particles (Kok et. al. 2012, Pye 1987)

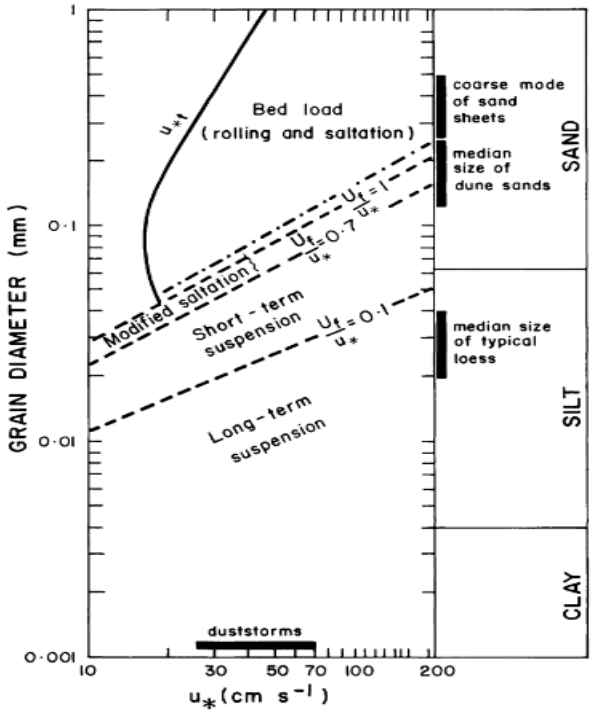

Deposition

After being mobilized by wind or interactions with wind-driven particles, deposition of grains occurs when wind lift velocity decreases or the particles interact with each other, topographic barriers, or atmospheric effects like precipitation. The total distance traveled by particles depends on their size as well as the speed and turbulence of the wind.

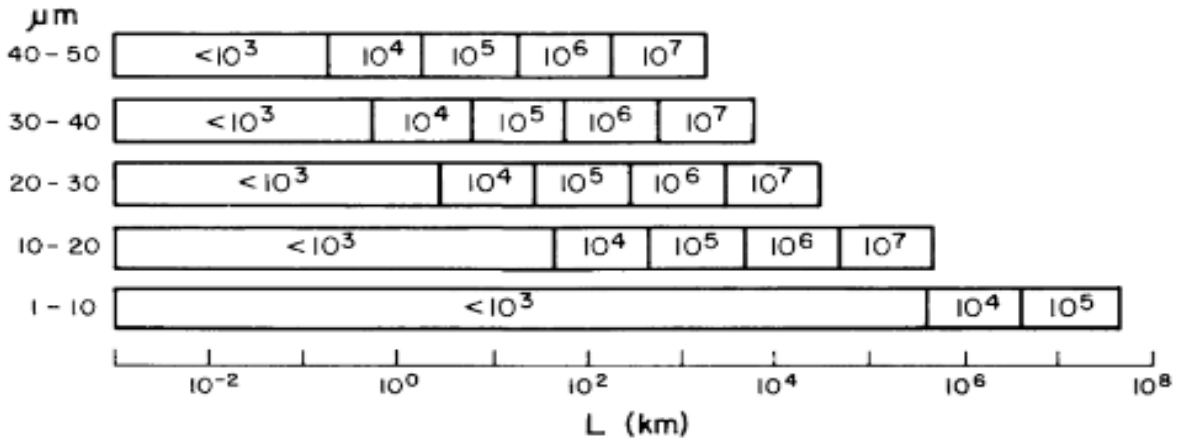

Figure 4. Maximum travel distance predicted for particles of various sizes under constant wind velocity. The powers of 10 in each bar represent varying levels of the coefficient of turbulent exchange which signifies the amount of vertical mixing in the atmosphere (Tsoar and Pye 1987)

For dust, wet-deposition dominates below ~5 microns (if there is moisture), and dry deposition for larger suspended grains as they gravitationally settle. Particles can settle if the wind velocity decreases such that the standard deviation of the vertical mixing velocity, becomes less than the settling velocity.

$$\sqrt{w'^2} = U_f \qquad \text{(suspension criterion)}$$

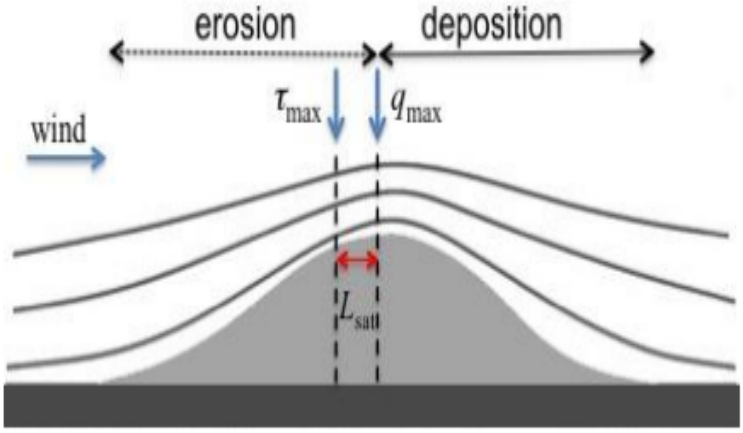

Perturbations in the logarithmic wind velocity profile can also cause deposition of lofted particles. Here, a dune introduces a nonlinear hydrodynamic effect in the shear stress of the wind which leads to maximum erosion upwind of the dune crest and deposition downwind increases the height of the dune

Figure 5. Erosion and deposition on a dune where pressure perturbations squeezing flowlines at a topographic barrier

Erosion

Aeolian processes erode planetary surfaces by **abrasion**, breaking down surfaces with windblown grains, a.k.a. "sandblasting", and **deflation**, the removal of loose particles. Soil particles at rest in a wind velocity field experience forces as outlined in Figure 1. If the threshold friction velocity is surpassed, the gravitational and inter-particle cohesive forces are overcome and the soil particles are removed and erosion occurs. For the purposes of examining erosion, this velocity is a property of the soil surface of a whole, not the individual particle, and encapsulates the surface's resistance to erosion. Together, the processes of transportation and deposition form the basis for erosion, as surfaces are weakened and particles mobilized via interactions with the wind and windborne particles. These mobilized particles may contribute to erosion of surfaces in other regions and can contribute to dust emission when they are at last deposited. Estimates of annual dust emission are as high as 3,000 Mt per year (Shao).

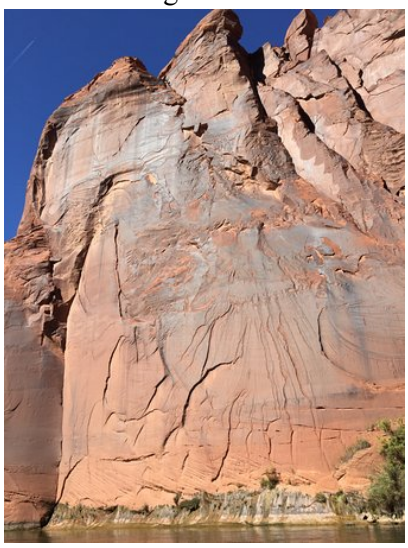

Products of Aeolian Erosion

Desert varnish – dark, shiny coating that forms on rock faces exposed to wind. Clays carried by the wind are deposited and serve as a substrate for additional materials that react in exposure to sun and dew. Desert varnishes have high concentrations of iron and manganese, which can be 50-60x greater than that of the bulk crust. At right, desert varnish along the Colorado River.s

Blowouts – areas where topography accelerates wind flow and jets maximally erode the region, removing material down to an un-erodible geomorphological layer. Can be up to km's in size.

Ventifacts – rocks shaped by the effects of sandblasting from windborne particles. Demonstrate the erosive power of aeolian processes. Also found on Mars. Right, a ventifact inside a blowout in Texas (Wikipedia image).

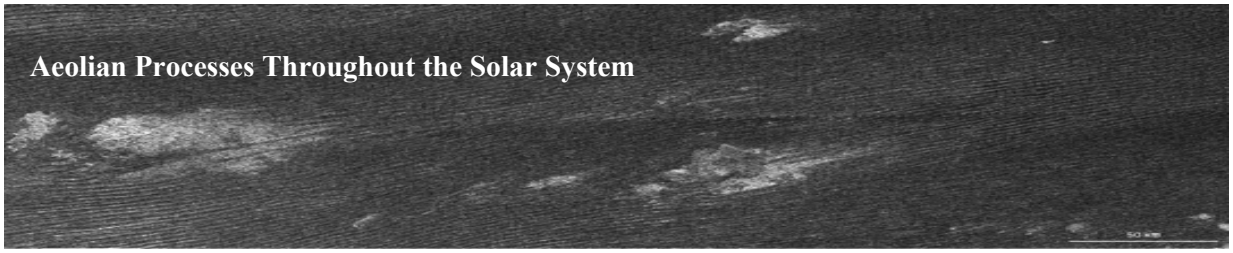

Mars

- Due to lower air density and to a lesser extent surface gravity, it is harder to physically move material. Same transport mechanisms predicted but with different particle sizes and wind speeds
- Nevertheless, with its small but significant atmosphere, Mars has a multitude of active aeolian processes that span local and planet-wide scales (dust-devils, wind streaks, dunes → global dust storms)
- Water-ice and CO2-ice condensation onto suspended dust grains → climate effects
- Magnitude of current dust/sand transport orders of magnitude less than on Earth, but more varied and exotic dune-shapes suggest high variability in wind velocity/orientation regimes on Mars
- Over 2,500 publicly available HiRISE images in the Aeolian theme. HiRISE is able to determine time variability of Martian aeolian features

Venus and Titan

- Contrary to Mars, on these bodies the air density is much greater than that of Earth and thus the terminal velocity of dust/sand is severely decreased
    - Saltating particles move more like silt agitated in water with terminal falling velocities insufficient to eject most surface particles
    - Most particles mobilized solely by aerodynamic fluid lifting
- Dunes are mostly long, parallel ridges, indicating uniform wind fields
- Whereas Earth sand is mostly SiO2 quartz, Venusian (and Martian) sand is denser basalt
    - Titan sand is an even denser combination of ice and tholins
- Image- dunes on Titan (Radebaugh et al. 2008)

References

Kok J F, Parteli E J R, Michaels T I and Bou Karam D 2012 The physics of windblown sand and dust Rep. Prog. Phys. 75 106901.

Potter, R. M., & Rossman, G. R. (1977). Desert Varnish: The Importance of Clay Minerals. Science, 196(4297), 1446-1448. doi:10.1126/science.196.4297.1446

Pye, K. (1989). Aeolian dust and dust deposits. London: Acad. Press.

Radebaugh, J., R.D. Lorenz, J.I. Lunine, S.D. Wall, G. Boubin, E. Reffet, R.L. Kirk, R.M. Lopes, E.R. Stofan, L. Soderblom, M. Allison, M. Janssen, P. Paillou, P. Callahan, C. Spencer, and Cassini Radar Team, 2008: Dunes on Titan observed by Cassini Radar. Icarus, 194, 690-703, doi:10.1016/j.icarus.2007.10.015.

Shao, Y. (2000). Physics and modelling of wind erosion. Dordrecht: Kluwer Academic.

Desert varnish image - "Desert Varnish (sheen formed by wind) on walls of Glen Canyon on Colorado River- TripAdvisor.com"

Aeolian morphology of the Colorado Plateau
Laura Seifert

Aeolian processes in the Colorado Plateau region are dominated by wind- blown dust creating ergs and dunes. An Erg is a broad, flat area of desert covered with wind swept sand with little to no vegetation and dunes are areas where this sand accumulates into visible landforms when sand supply and wind directions are right. These dunes can migrate across the surface through a process called saltation. In the southwest, the largest area of sand dunes is located in the Colorado Plateau region. This is because there is an abundant sediment/sand supply from the Colorado River and surrounding Navajo sandstone in the area. The prevailing wind direction is from the southwest. The diagram at right shows the areas of wind-blown sand and wind direction relative to the Native American reservations in the area.

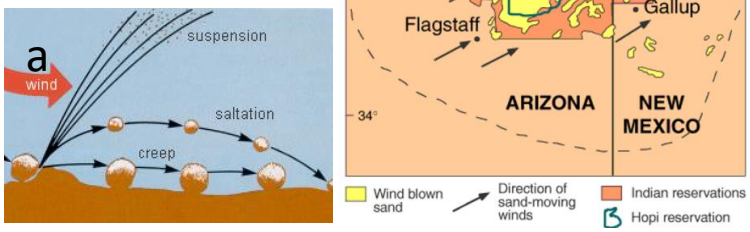

Figure 1: a) Diagram showing saltation, b) map of Colorado Plateau region showing wind-blown sand and wind direction.

Dunes in the Colorado Plateau region:

- Moenkopi dunes (AZ): Linear dunes
- Great sand dunes (CO): Star, Parabolic, Barchan, transverse dunes
- Chaco sand dunes (NM): Parabolic, barchanoid, ridge dunes
- Coral Pink sand dunes (UT): Transverse, barchan, star dunes

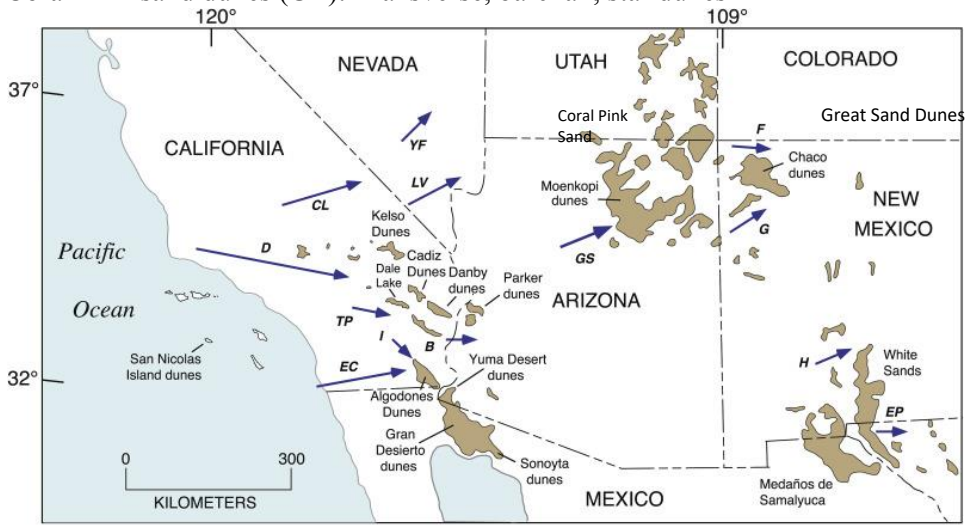

Figure 2: Map of the Southwest US dune fields.

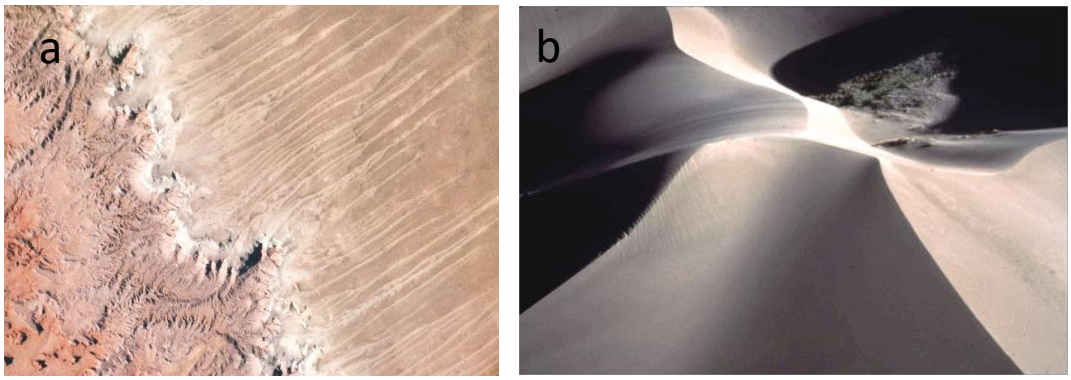

Figure 3: a) Linear dunes from the Moenkopi Plateau, b) star dune from the Great Sand Dunes.

Dune Morphology:

Dune morphology is dominated by three main factors; sand supply, wind direction and vegetation. The table below summarizes the variations in these factors for different dune morphologies:

Dune Type	Wind Direction	Sand Supply	Vegetation
Barchan	1 direction	Low/Moderate	Low
Star	Multiple Directions	High	Low
Transverse	1 direction	High	Low
Parabolic	1 direction	High	High
Linear	2 converging directions	Low/Moderate	Low

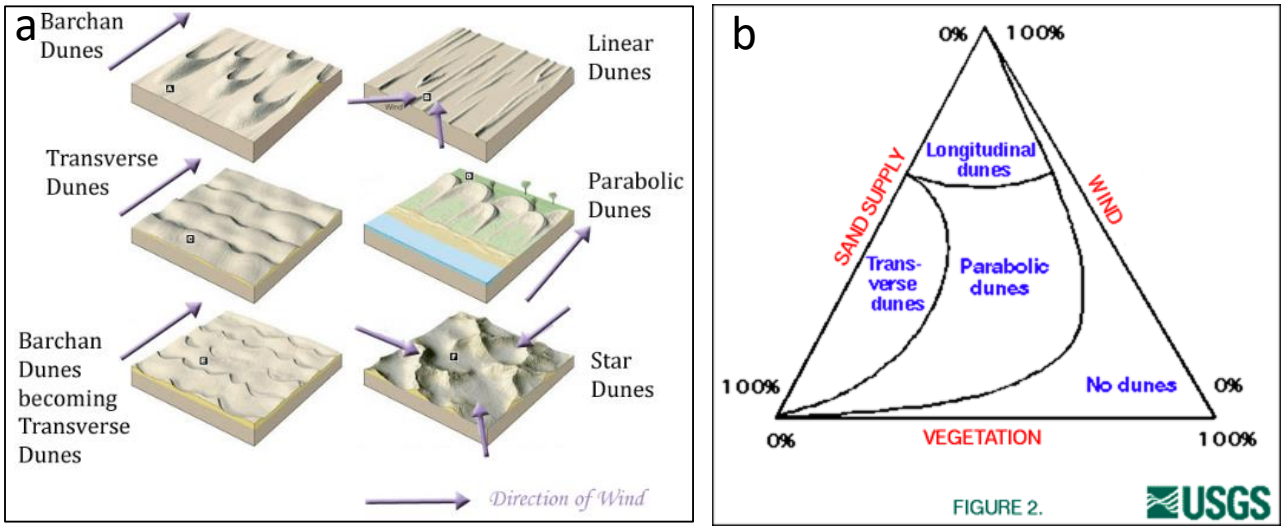

Figure 4: a) Visual of common dune morphologies with wind direction, b) Diagram (right) depicting the varying amount of sand, wind and vegetation required to form dunes.

Planetary Connection:

Mars

- Sand dunes are abundant on the surface of Mars
- This gives us important information about conditions on the surface of Mars; wind strong enough to carry the sediment supply.
- Types of dunes on Mars: Barchan/barchanoid, transverse, linear, star

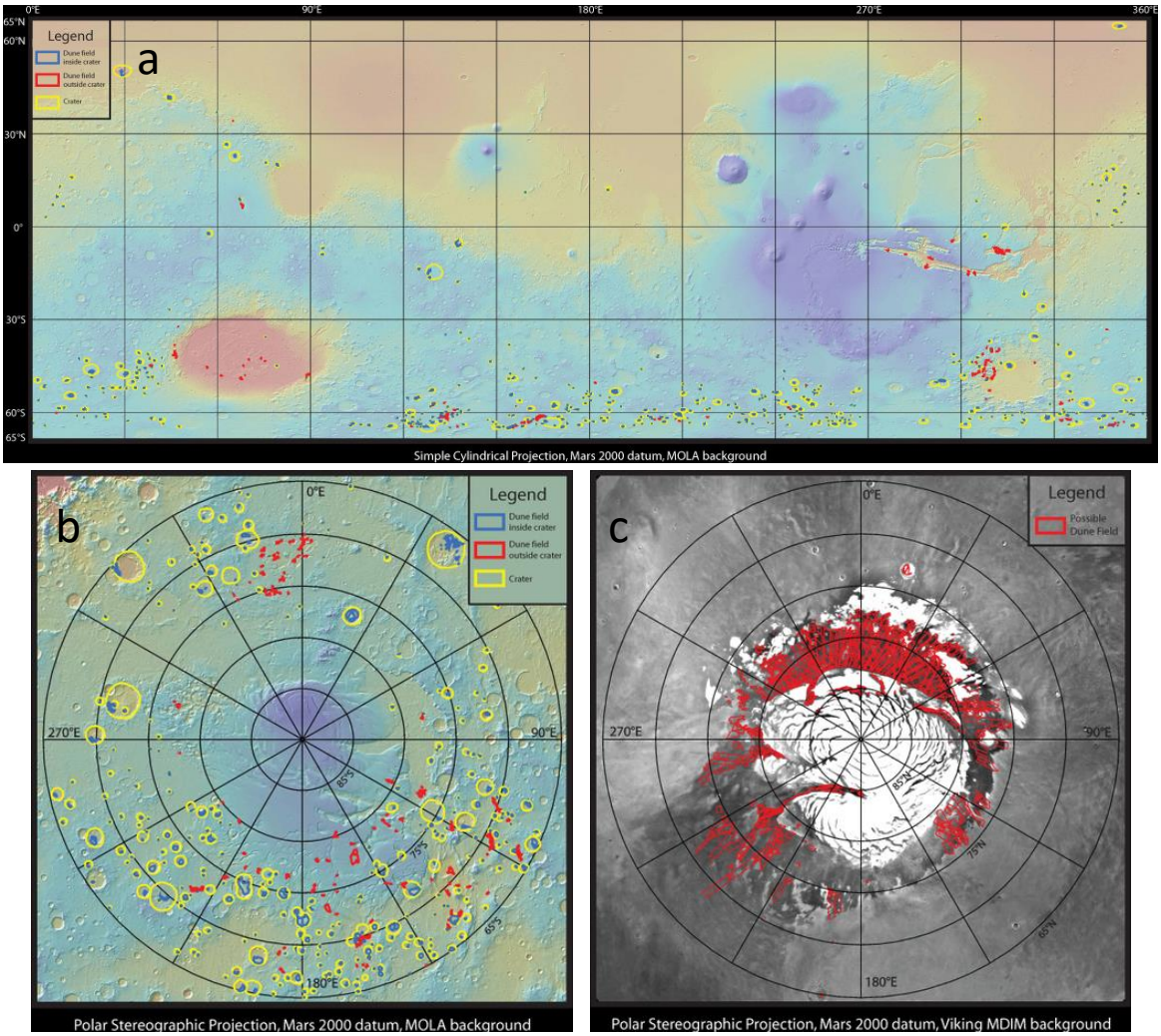

Figure 5: Maps of the martian surface showing where dune fields are located(red and blue) at the mid latitudes (a), south (b) and north pole (c).

References
https://www.nps.gov/grsa/learn/nature/dune-types.htm
http://www.usu.edu/geo/luminlab/Fordetal2010UGA.pdf
http://www.jsjgeology.net/Great-Sand-Dunes_files/image010.gif
https://astrogeology.usgs.gov/geology/mars-dunes
http://ars.els-cdn.com/content/image/1-s2.0-S0277379117300021-gr2.jpg
https://pubs.usgs.gov/bul/1672/report.pdf
https://en.wikipedia.org/wiki/Saltation_(geology)

Fluvial Process: Slot Canyons

By Kyle Pearson

A fluvial process is the physical interaction of flowing water over a bed of sediment which can result in erosion or deposition on a river bed. The movement of water across the bed exerts a shear stress directly on the bed. If the strength of the bed is lower than the shear exerted, loose sediments can be dislodged and transported downstream. The transport of sediment can occur with a pure water flow however if the river/stream has significant quantities of sediment, this material can abrade the bed. At the same time the fragments are ground down and become smaller and rounder.

A slot canyon is a narrow canyon formed by water flowing through rock. Typically, these canyons are significantly deeper than they are wide. When they start to become wider people usually just call them canyons. Many slot canyons are formed in sandstone or limestone because they erode more easily than granite and basalt. Although slot canyons in the latter are still possible. Slot canyons can be created in a matter of a few hundreds to thousands of years. Since they're created by running water, the creation timescale usually depends on environmental factors like the source of water and how fast the stream is.

Figure 1. Antelope Canyon

Some of the more famous slot canyons in Arizona are: Antelope Canyon, Canyon X, Deer Creek Narrows, Paria Canyon, Pumphouse Wash, Secret Canyon and Water Holes Canyon. Antelope Canyon is a slot canyon in the American Southwest, located on Navajo land east of Page, Arizona. The slot canyon was formed by the erosion of Navajo Sandstone primarily due to flash flooding. Rainwater, especially during monsoon season, runs into the basin above the slot canyon picking up speed and sand as it enters the narrow passageways. Over time the passages erode, making these narrow pathways with smooth edges reminiscent of flowing shapes.

Figure 2. Deer Creek Canyon with flowing water.

At the beginning of every slow canyon is a natural wash, a dry creek bed or gulch that temporarily fills with water after a heavy rain. The heavy rain is typically a result of a monsoon and then it will proceed to find cracks in the rocks and will eventually make the cracks larger. Like electricity the water tries to find the path of least resistance, which happens to be the largest crack. Over a few thousand or millions of years the water eventually erodes the walls and cuts a deep path into the rocks. Pebbles can be transported by the flow and will often be abraded down into a circular shape, if its small enough. Sometimes debris from trees and larger rocks can get picked up and carried into the canyon.

Water Holes Canyon

This canyon is a collection of drainage channels that formed several slot canyons that cut through Navajo sandstone. Water from both flash flooding and the Colorado river help cut away the walls of this slot canyon.

Sediment Transport

Motion is initiated for sediment at rest on a bed when a fluid exerts a stress that is greater than the critical shear stress of the bed. This shear stress is typically represented as a dimensionless parameter called the Shield's parameter and is defined as:

$$\tau_* = \frac{\rho u_s^2}{(\rho_s - \rho) g\ D}$$

$$\mathrm{D} - \text{characteristic sediment diameter}$$
$$\tau_* - \text{dimensionless shear stress}$$
$$\mathrm{g} - \text{acceleration due to gravity}$$
$$\mathrm{u}_s - \text{sediment velocity}$$
$$\rho_s - \text{density of sediment}$$
$$\rho - \text{density of fluid}$$

This equation is valid for granular sediment (composed of distinguishable pieces or *grains*) however this will not work for muds or clays. Also, keep in mind this equation is only for one type of particle, typical flows will usually have a heterogenous size distribution.

WARNING: Slot canyons can kill! Be careful of flash floods when traversing a slot canyon. Remember slot canyons are created from water and the canyon makes an easy drainage route for local reserves or run offs. There may not be an exit for you to escape to either.

Mars

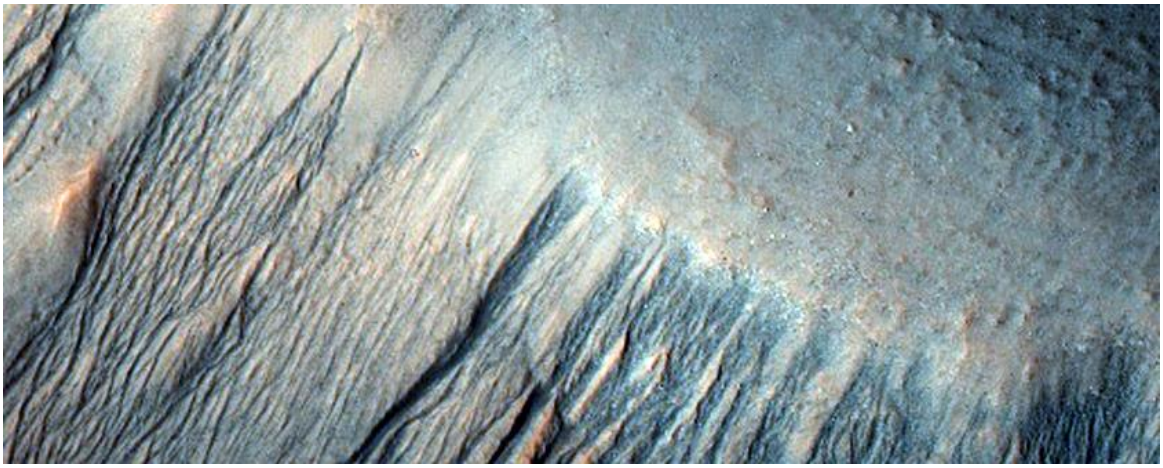

Figure 3. Small gullies on a equator facing slope. The image was taken by HIRISE on 11 Jan 2009 at 15:37 Local Mars time. The geolocation is 49.8N 288.8E. The image scale is roughly 30.4cm/pixel. NASA/ JPL/ University of Arizona

Titan

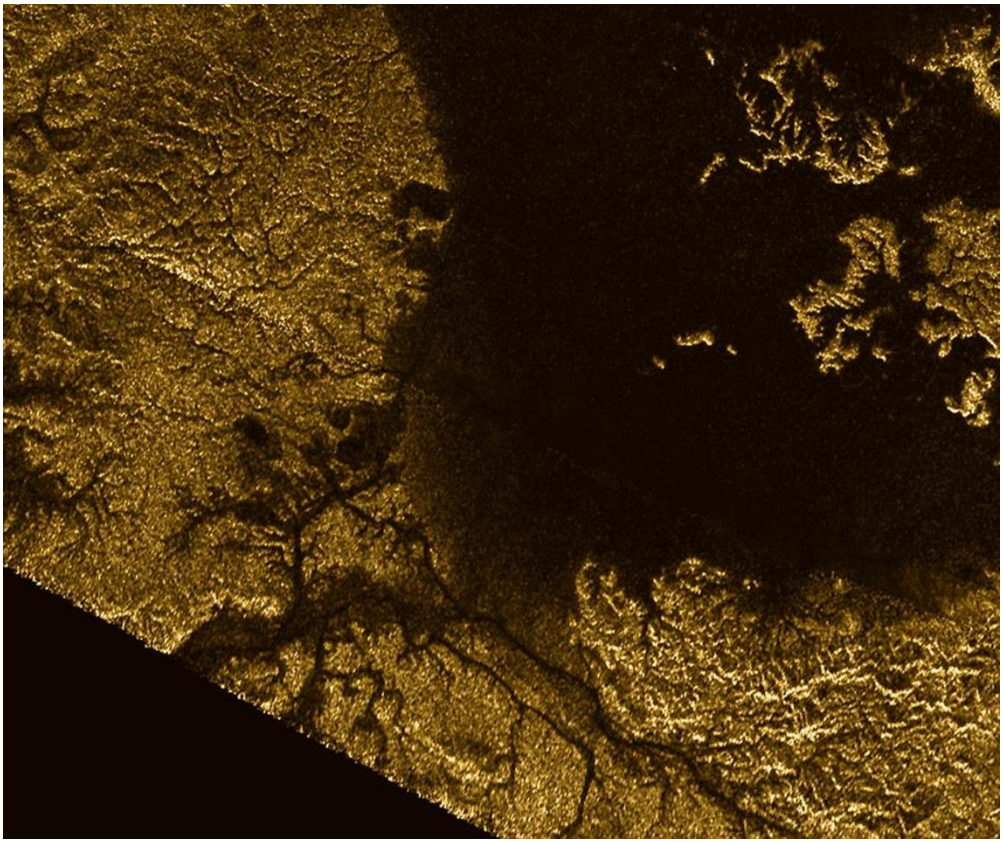

Figure 4. Radar Image from NASA's Cassini spacecraft reveal a large lake on Titan's surface. NASA/JPL/JPL-Caltech/ASI/USGS . It looks like there are dendritic drainage channels leading away from the lake. On Earth, these patterns usually form in horizontal sedimentary rock as fluid drains away from a tributary. However, the lakes and seas on Titan are composed of liquid hydrocarbons (methane and ethane) which can erode part of the surface rock and ice as it flows over it.

Strike and Dip

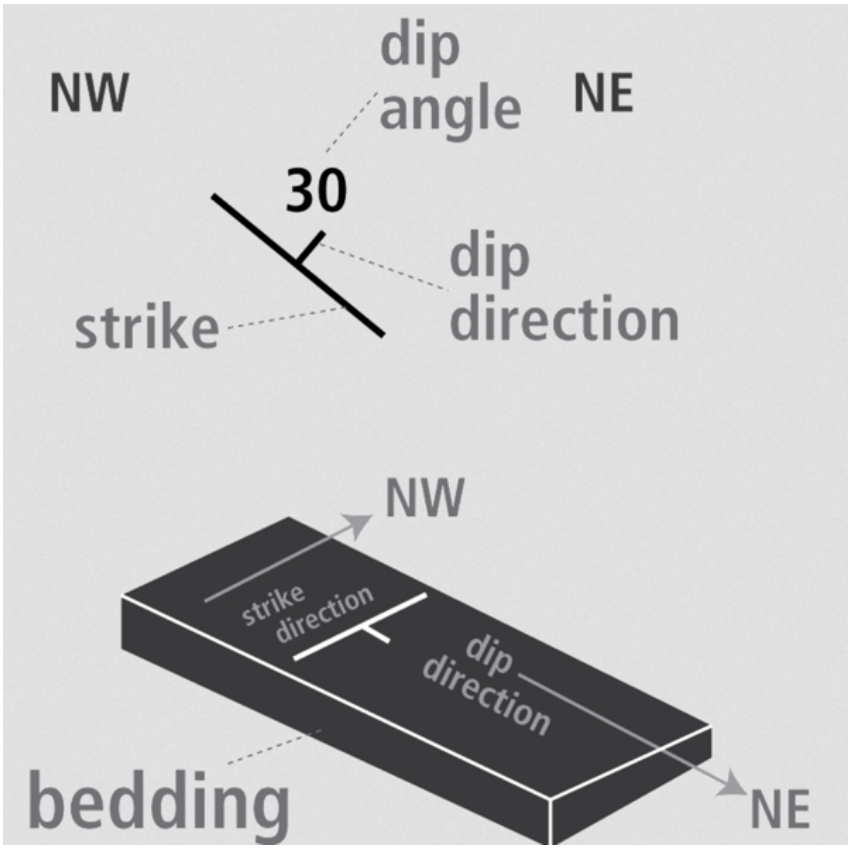

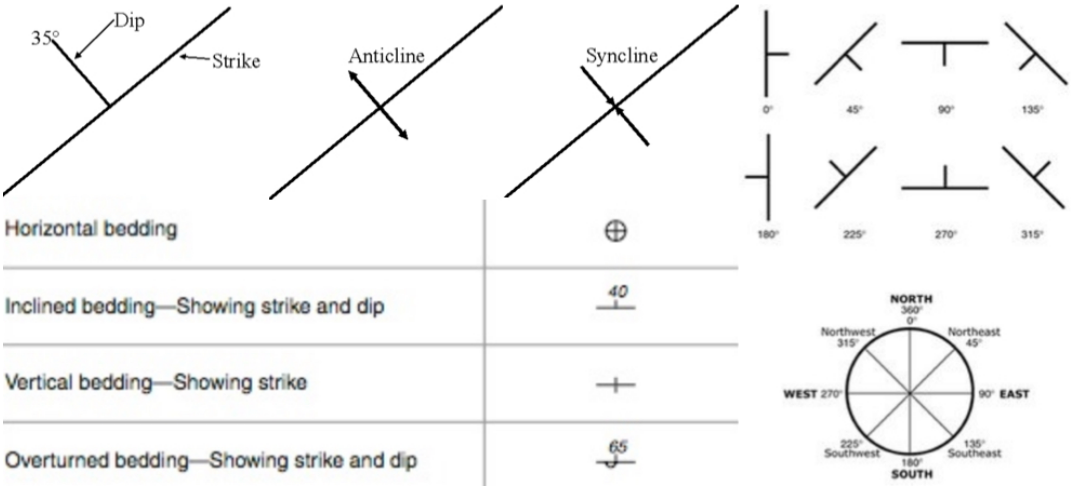

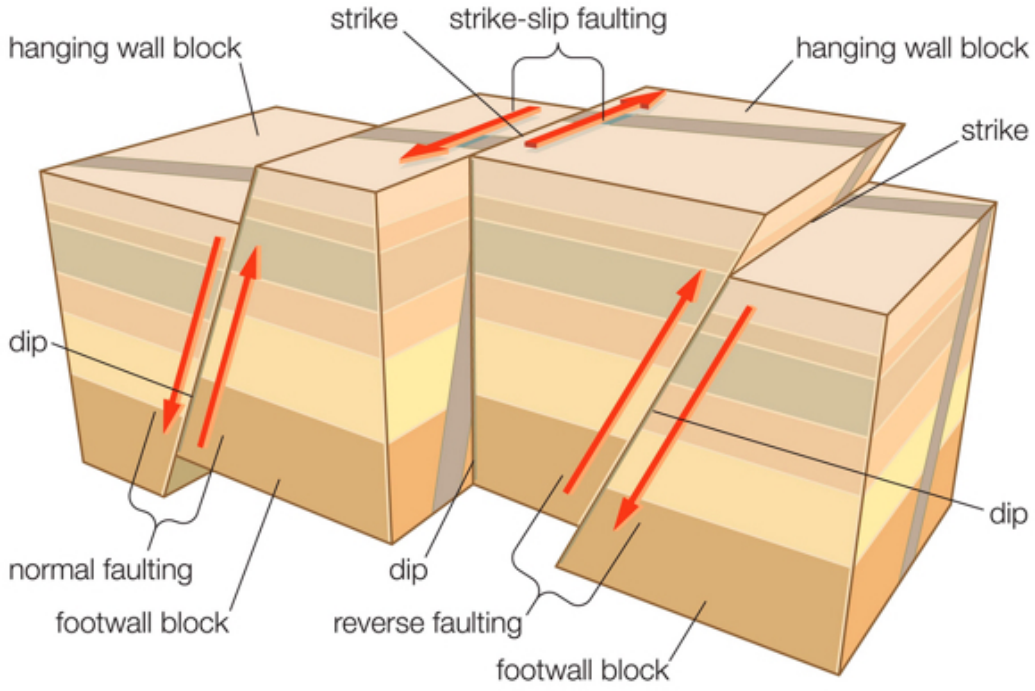
strike
strike-slip faulting
hanging wall block
hanging wall block
strike
dip
dip
normal faulting
dip
footwall block
reverse faulting
footwall block

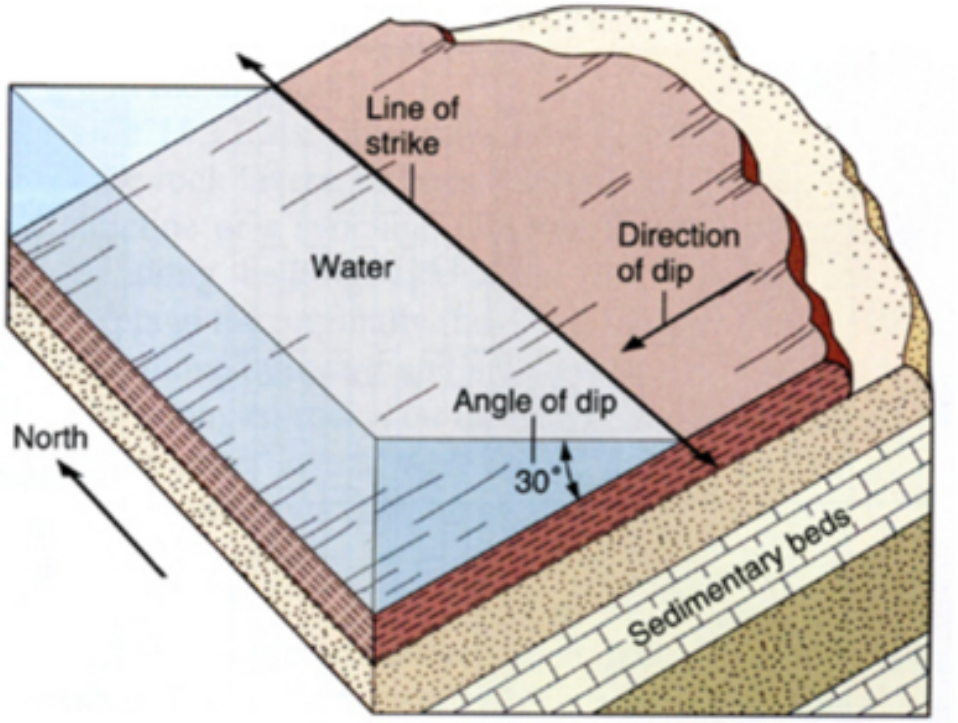
Line of strike
Water
Direction of dip
Angle of dip
North
30°
Sedimentary beds

The right hand rule:
If the fingers of your RIGHT hand point DOWN the dip, then your THUMB points in the direction of strike.
Ignore this rule, and the strike could be interpreted as EAST rather than WEST, and another person reading your map could think the strata dip the other direction: down to the NORTH rather than to the SOUTH.
That would completely mess up the interpretation of the geologic structure.

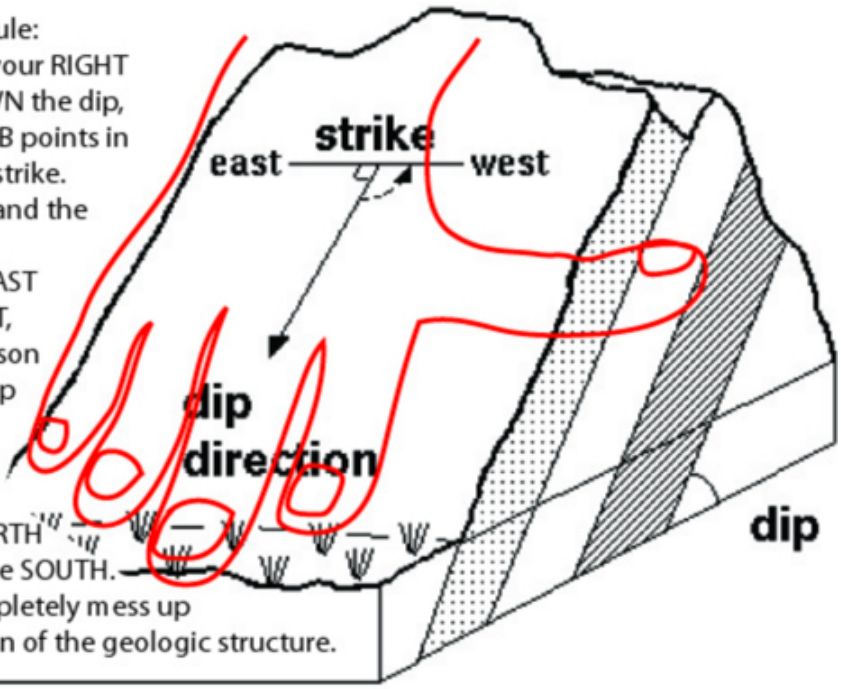

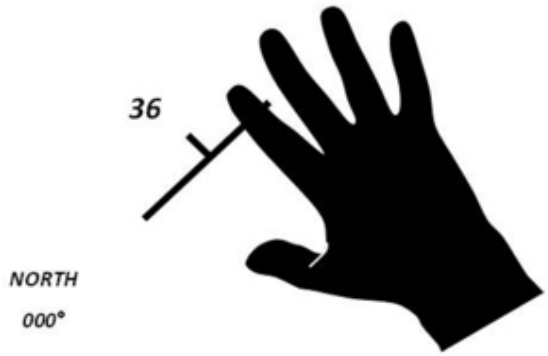

RIGHT HAND RULE:
216 / 36

NORTH
000°

RIGHT HAND RULE:
037 / 36

Contacts: Unconformities, Nonconformities, and Disconformities

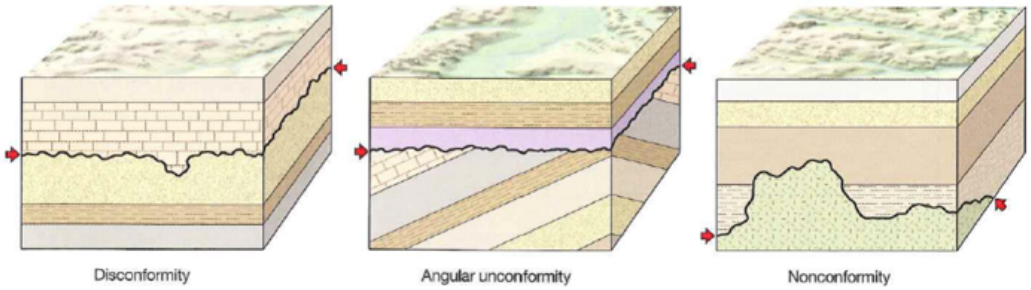

FIGURE 10.5 Unconformities. Arrows point to the unconformity surface (black line). A *disconformity* is an unconformity between relatively *parallel* strata. An *angular unconformity* is an unconformity between *nonparallel* strata. A *nonconformity* is an unconformity between sedimentary rock/sediment and igneous or metamorphic rock.

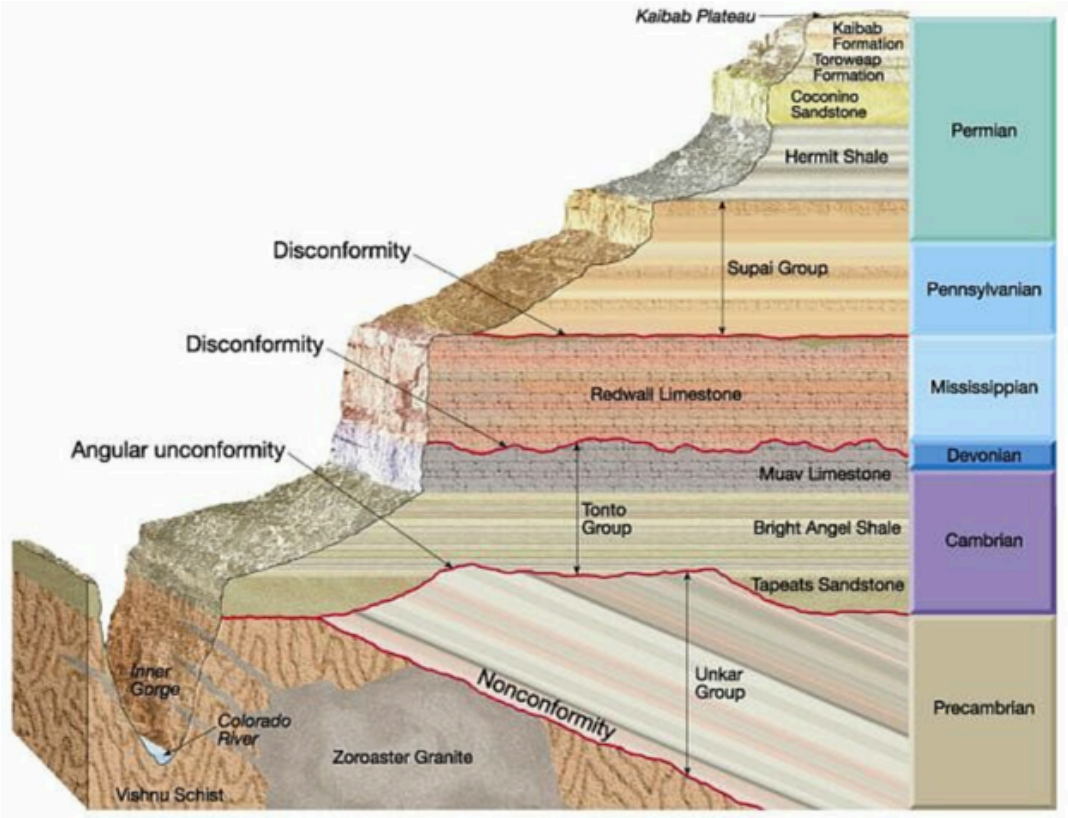

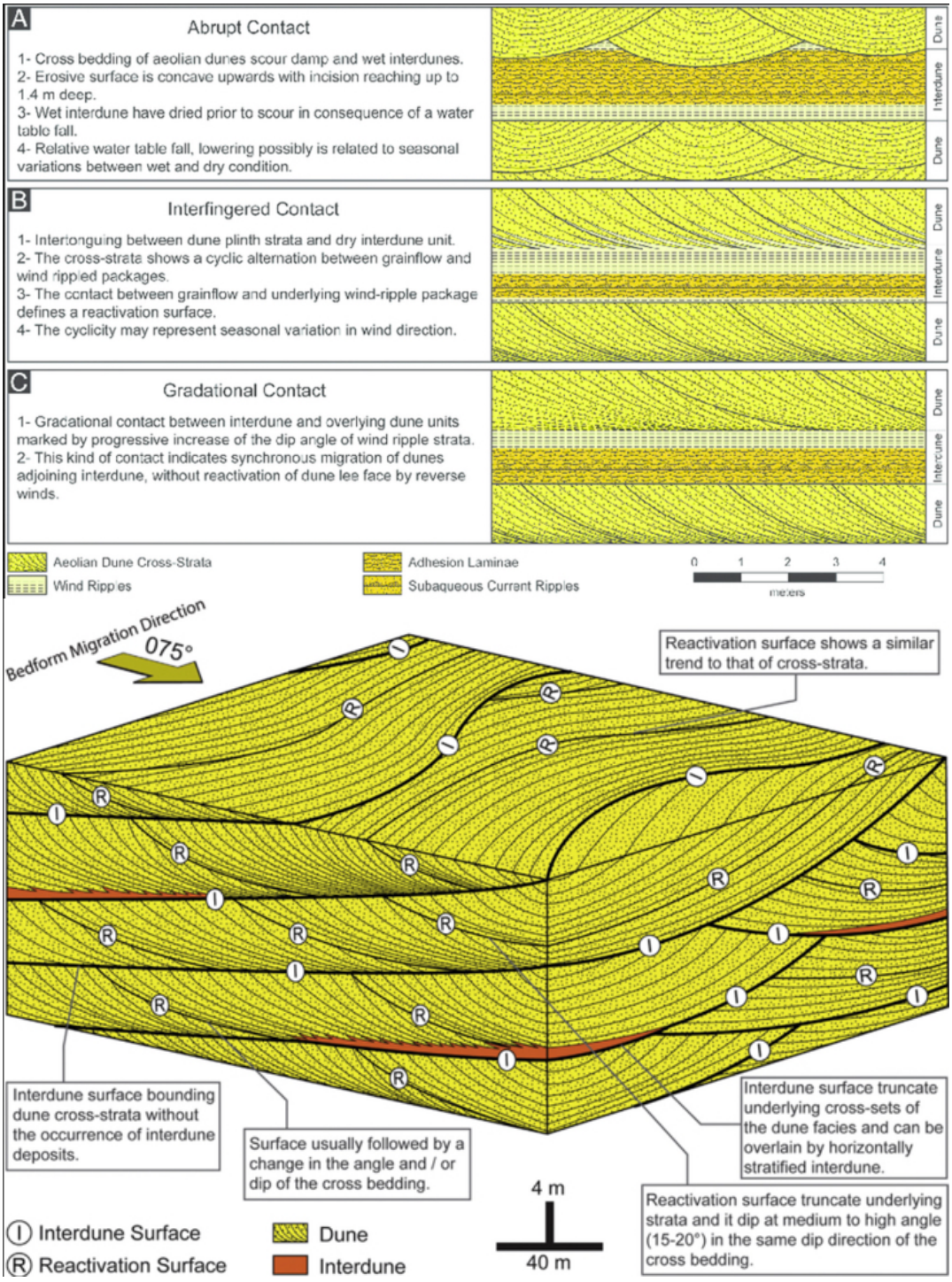
A
Abrupt Contact
1- Cross bedding of aeolian dunes scour damp and wet interdunes.
2- Erosive surface is concave upwards with incision reaching up to 1.4 m deep.
3- Wet interdune have dried prior to scour in consequence of a water table fall.
4- Relative water table fall, lowering possibly is related to seasonal variations between wet and dry condition.
Dune
Interdune
Dune
B
Interfingered Contact
1- Interfonguing between dune plinth strata and dry interdune unit.
2- The cross-strata shows a cyclic alternation between grainflow and wind rippled packages.
3- The contact between grainflow and underlying wind-ripple package defines a reactivation surface.
4- The cyclicity may represent seasonal variation in wind direction.
Dune
Interdune
Dune
C
Gradational Contact
1- Gradational contact between interdune and overlying dune units marked by progressive increase of the dip angle of wind ripple strata.
2- This kind of contact indicates synchronous migration of dunes adjoining interdune, without reactivation of dune lee face by reverse winds.
Dune
Interdune
Dune
Aeolian Dune Cross-Strata
Wind Ripples
Adhesion Laminae
Subaqueous Current Ripples
0 1 2 3 4
meters
Bedform Migration Direction
075°
Reactivation surface shows a similar trend to that of cross-strata.
Interdune surface bounding dune cross-strata without the occurrence of interdune deposits.
Surface usually followed by a change in the angle and / or dip of the cross bedding.
Interdune surface truncate underlying cross-sets of the dune facies and can be overlain by horizontally stratified interdune.
Reactivation surface truncate underlying strata and it dip at medium to high angle (15-20°) in the same dip direction of the cross bedding.
4 m
40 m
I Interdune Surface
R Reactivation Surface
Dune
Interdune

Common Rock Forming Minerals

Dark-Colored minerals			
Hardness	**Cleavage**	**Physical Properties**	**Name**
Hardness >5	Excellent or good	Dark gray, Blue-gray or black. May be iridescent. Cleavage in 2 planes at nearly right angles, Striations. Hardness-6	**Plagioclase Feldspar**
		Brown, gray, green or red. Cleavage in 2 planes at nearly right angles. Exsolution Lamellae. Hardness-6	**Potassium Feldspar**
		Opaque black. 2 cleavage planes at 60°and 120°. Hardness- 5.5	**Hornblende (Amphibole)**
	Poor or absent	Opaque red, gray, hexagonal prisms with striated flat ends. Hardness- 9	**Corrundum**
		Gray, brown or purple. Greasy luster. Massive or hexagonal prisms and pyramids. Transparent or translucent. Hardness- 7	**Quartz Black or brown-Smoky , Purple-Amethyst**
		Opaque red or brown. Waxy luster. Hardness-7. Conchoidal Fracture	**Jasper**
		Opaque black. Waxy luster. Hardness- 7	**Flint**
		Transparent- translucent dark red to black. Hardness- 7	**Garnet**
Hardness < 5	Excellent or good	Colorless, purple, green, yellow, blue. Octahedral cleavage. Hardness- 4	**Flourite**
		Green. Splits along 1 excellent cleavage plane. Hardness- 2-3	**Chlorite**
		Black to dark brown. Splits along 1 excellent cleavage plane. Hardness- 2.5-3	**Biotite mica**
	Poor or absent	Opaque green, yellow or gray. Silky or greasy luster. Hardness- 2-5	**Serpentine**
		Opaque white, gray or green. Can be scratched with fingernail. Soapy feel. Hardness- 1	**Talc**
		Opaque earthy red to light brown. Hardness- 1.5-6	**Hematite**

Light-colored minerals			
Hardness	**Cleavage**	**Physical Properties**	**Name**
Hardness >5	Excellent or good	White or gray, Cleavage in 2 planes at nearly right angles, Striations. Hardness-6	**Plagioclase Feldspar**
		Orange, brown, white, gray, green or pink. Cleavage in 2 planes at nearly right angles. Exsolution Lamellae. Hardness-6	**Potassium Feldspar**
		Pale brown, white or gray. Long slender prisms. Cleavage in 1 plane. Hardness- 6-7	**Sillimanite**
	Poor or absent	Opaque red, gray, white hexagonal prisms with striated flat ends. Hardness- 9	**Corrundum**
		Colorless, white, gray or other colors. Greasy luster. Massive or hexagonal prisms and pyramids. Transparent or translucent. Hardness- 7	**Quartz White-Milky, Yellow-Citrine, Pink- Rose**
		Opaque gray or white. Waxy luster. Hardness-7. Conchoidal Fracture	**Chert**
		Colorless, white, yellow, light brown. Translucent opaque. Laminated or massive. Cryptocrystalline. Hardness- 7	**Chalcedony**
		Pale olive green. Conchoidal fracture. Transparent or translucent. Hardness- 7	**Olivine**
Hardness < 5	Excellent or good	Colorless, white, yellow, blue, green. Excellent cleavage in 3 planes. Breaks into rhombohedrons. Effervesces in HCl. Hardness- 3	**Calcite**
		Colorless, white, yellow, blue, green. Excellent cleavage in 3 planes. Breaks into rhombohedrons. Effervesces in HCl only if powdered. Hardness- 3.5-4	**Dolomite**
		White with tints of brown. Short tabular crystals or roses. Very heavy. Hardness- 3-3.5	**Barite**
		Colorless, white or gray. Massive or tabular crystals, blades or needles. Can be scratched by fingernail. Hardness- 2	**Gypsum**
		Colorless, white. Cubic crystals. Salty taste. Hardness- 2.5	**Halite**
		Colorless, purple, green, yellow, blue. Octahedral cleavage. Hardness- 4	**Flourite**
		Colorless, yellow, brown. Splits along 1 excellent cleavage plane. Hardness- 2-2.5	**Muscovite mica**
	Poor or absent	Yellow crystals or earthy masses. Hardness 1.5-2.5	**Sulfur**
		Opaque green, yellow or gray. Silky or greasy luster. Hardness- 2-5	**Sepentine**
		Opaque white, gray or green. Can be scratched with fingernail. Soapy feel. Hardness- 1	**Talc**
		Opaque earthy white to light brown. Hardness- 1-2	**Knolinite**

Metallic			
	Streak	**Physical Properties**	**Name**
Hardness > 5	Dark Gray	Brass yellow	**Pyrite**
		Dark gray-black, attracted to magnet	**Magnetite**
Harness < 5	Brown	Silvery black to black tarnishes gray	**Chromite**
	Red Red-Brown	Silvery gray, black, or brick red	**Hematite**
	Dark Gray	Brass yellow, tarnishes dark brown or purple	**Chalcopyrite**
		Iridescent blue, purple or copper red, tarnishes dark purple	**Bornite**
		Silvery gray, tarnishes dull gray Cleavage good to excellent	**Galena**
		Dark gray to black, can be scratched with fingernail	**Graphite**

Sedimentary Rocks

McBride, 1963 & Dott, 1964 Classification Scheme for Clastic Sedimentary Rocks

Scheme based on the normalized percentages of the visible grains: quartz and chert(Q), feldspar (F), and lithic rock fragments (R) – as well as the percent composed of matrix (mud & silt)

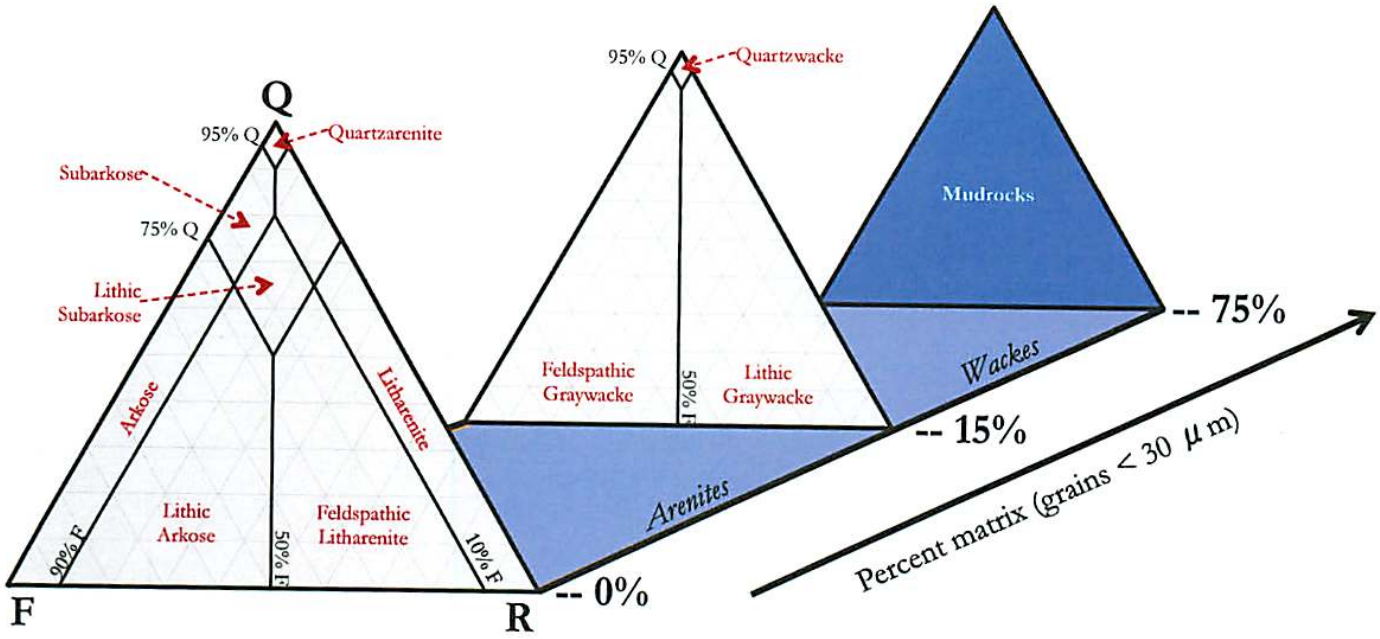

Tectonic Setting for Clastic Sedimentary Rocks

Scheme based on the normalized percentages of the visible grains: quartz and chert(Q), feldspar (F), and lithic rock fragments (R) – as well as the percent composed of matrix (mud & silt). Regions based upon field data.

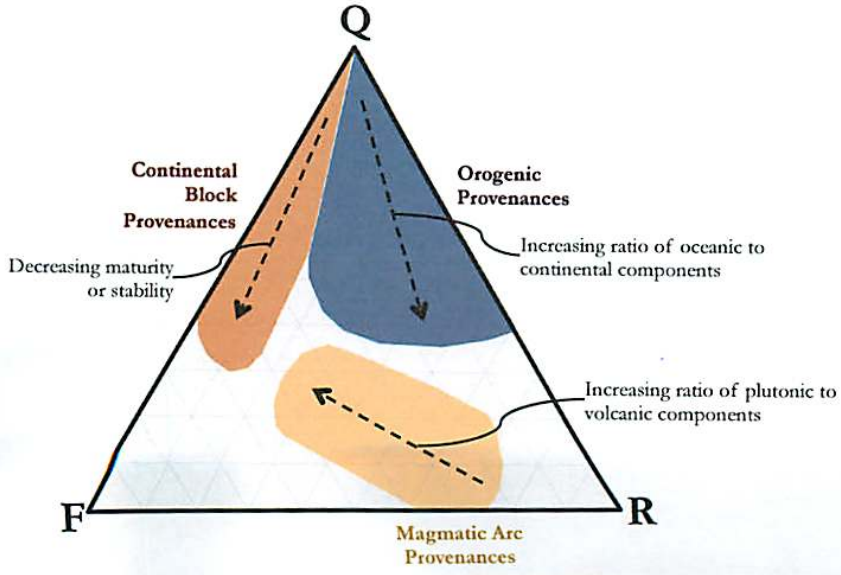

Sedimentary Rocks

	Mudrocks (containing > 50% mud)			Rocks with <50%mud
	Silt dominant (> 2/3 of rock)	Clay and Silt	Clay dominant (> 2/3 of rock)	Sand-sized or larger grains dominant
Non-laminated	Siltstone	Mudstone	Claystone	Conglomerates, Breccias, Sandstones, etc.
Laminated	Laminated Siltstone	Mudshale	Clayshale	

Classification Scheme for Mudrocks

Scheme based on clay/silt content, and whether the rock is laminated (layered) or not.

Classification Scheme for Sub-Conglomerates and Sub-Breccias

Scheme based on percent of a rock composed of: gravel or pebbles (size >2 mm), sand (2 mm > size > 1/16 mm), and mud (size < 1/16 mm).

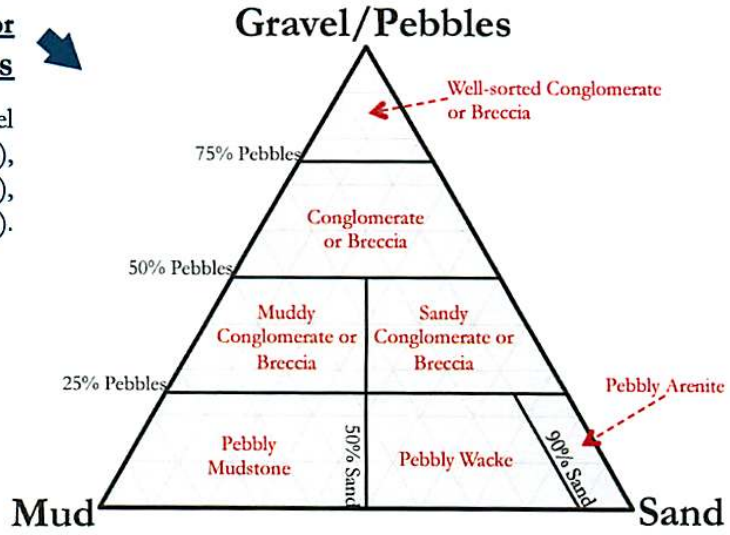

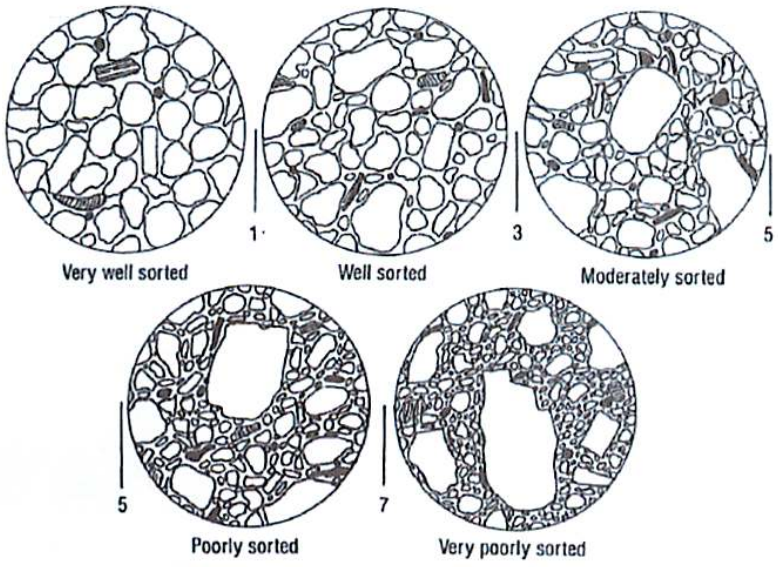

Estimating Sorting

Example hand-lens view of detritus. From Compton, 1985

Sedimentary Rocks

Degrees of Rounding

Example hand-lens view of detritus of varying degrees of roundedness. The top row are equidimensional (spherical) grains, while the lower row are elongated grains. From Compton, 1985 and Davis & Reynolds, 1996, respectively.

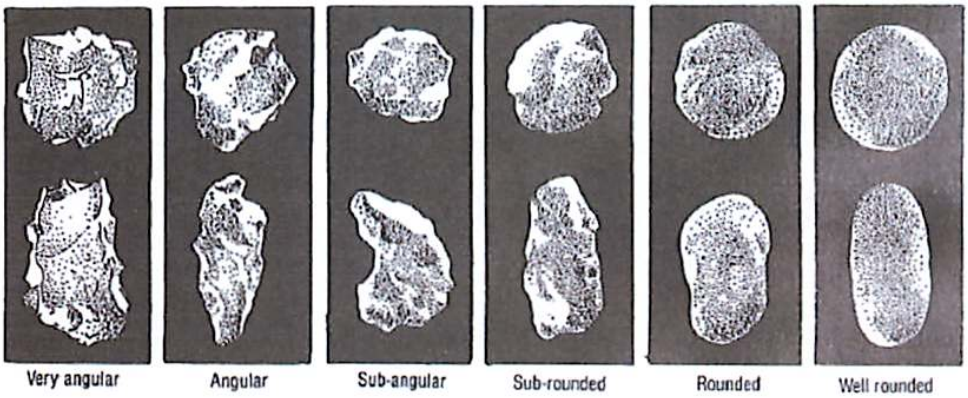

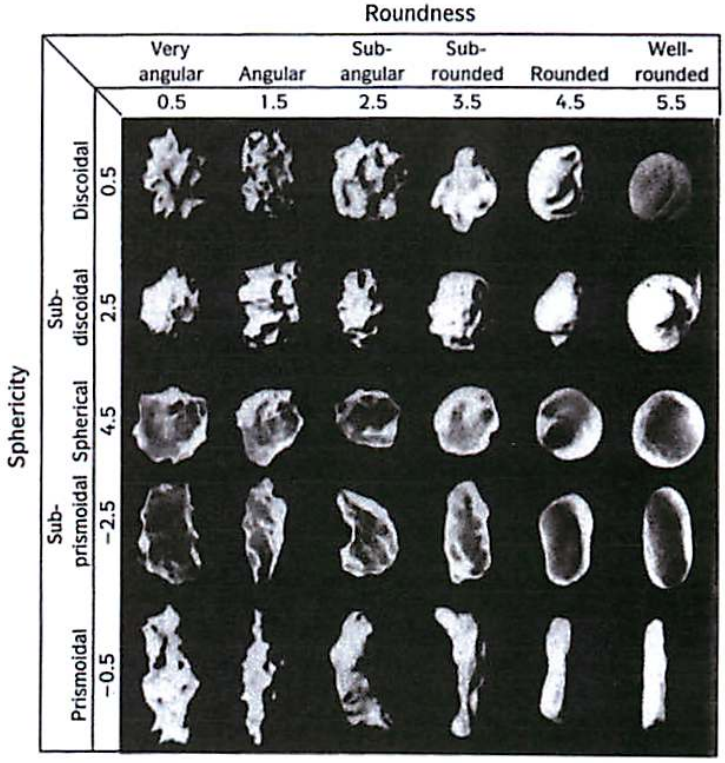

Sedimentary Rocks

Percentage Diagrams for Estimating Composition by Volume

Example hand-lens view of rocks with varying composition. To find weight percents, simply multiply each volume percent by the specific gravity of that mineral, and re-normalize. Compton, 1985

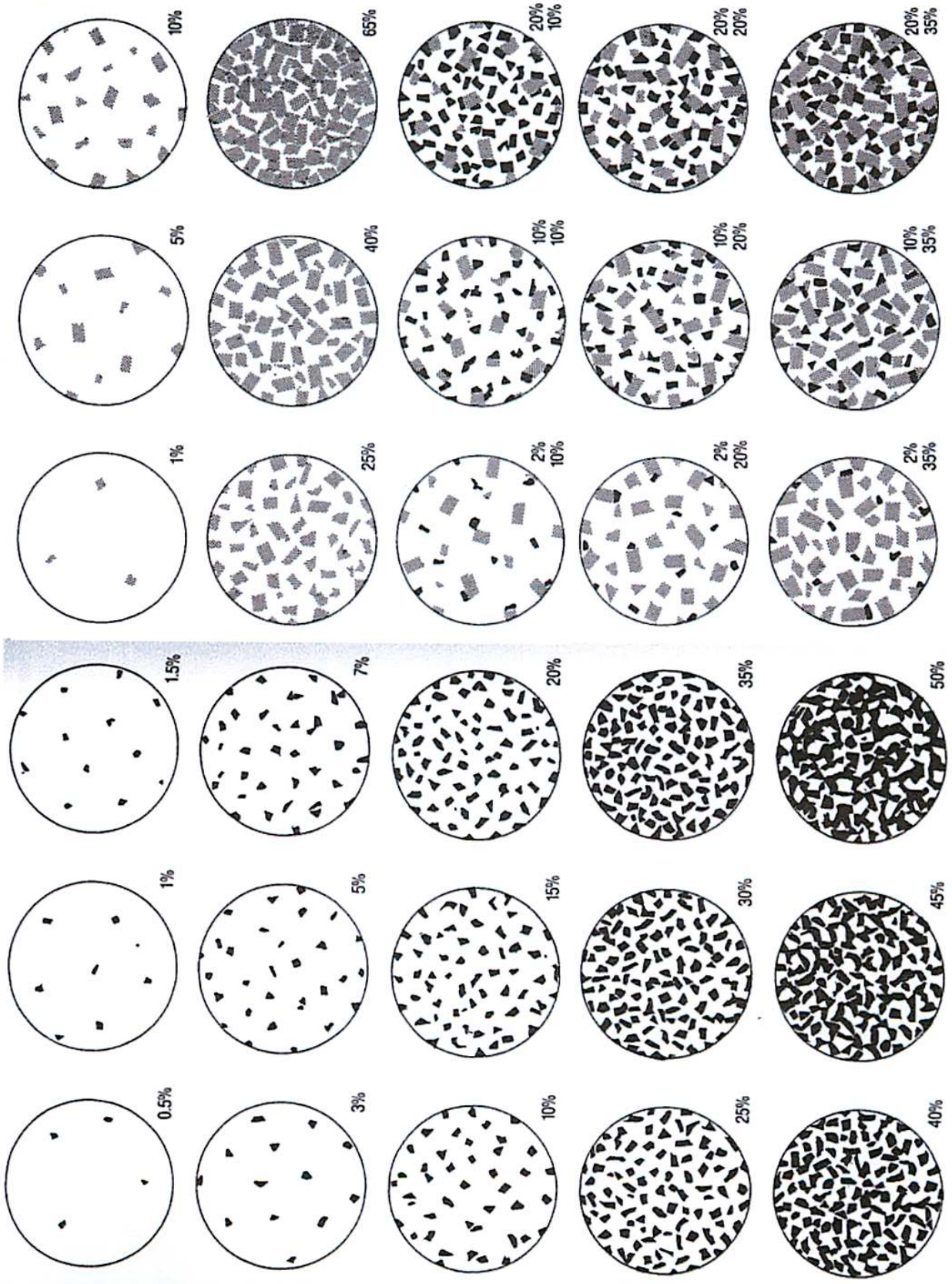

Sedimentary Rocks

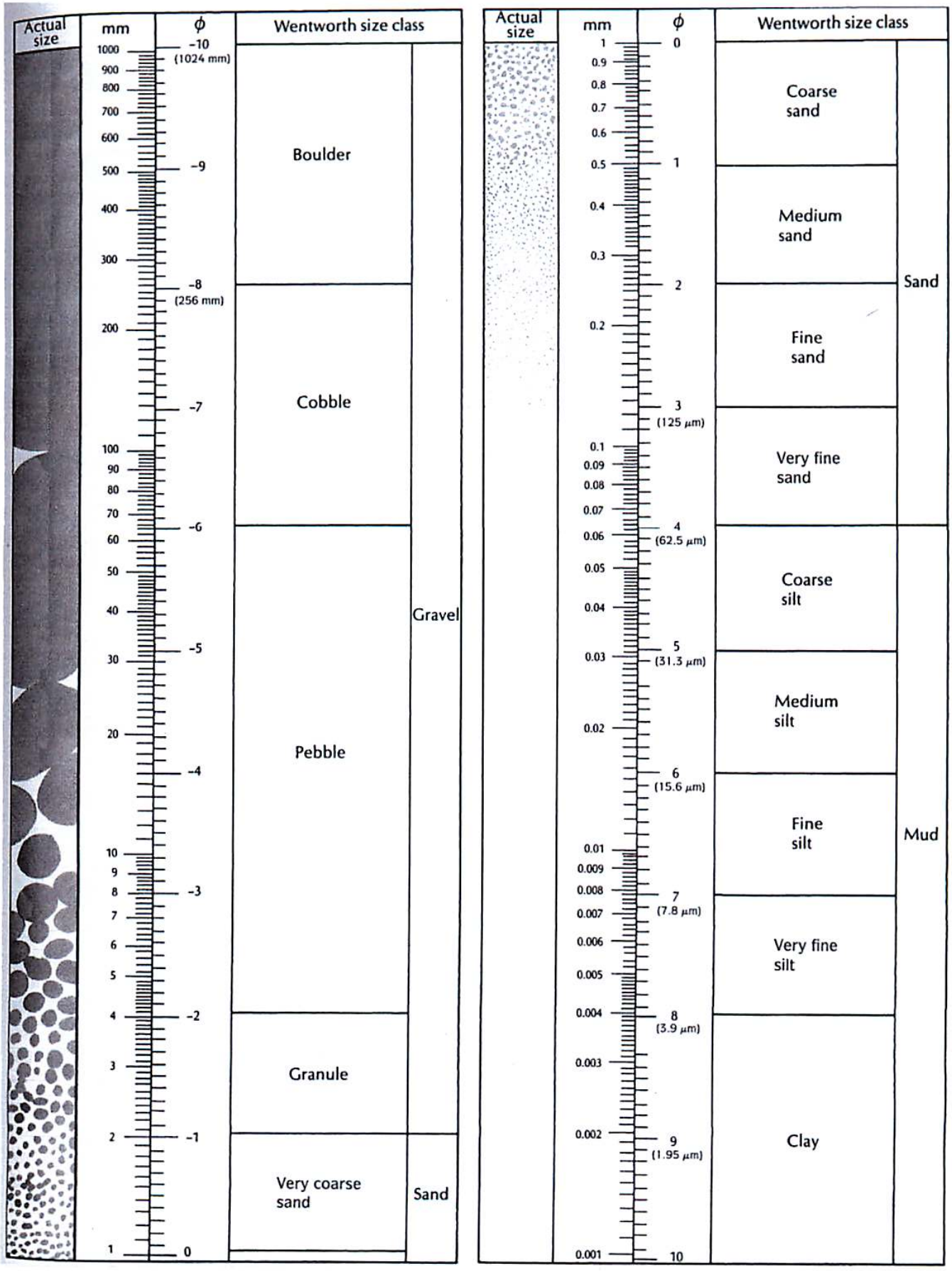

From Prothero and Schwab, 200

Sedimentary Rocks: Carbonates

Folk Classification Scheme for Carbonate Rocks

Folk's classification scheme is based upon the composition (and type of allochems) within a limestone. Figures from Prothero and Schwab, 2004

Principle Allochems in Limestone	Limestone Type			
	Cemented by Sparite		Cemented by Micritic Matrix	
Skeletal Grains (Bioclasts)	Biosparite	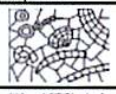	Biomicrite	
Ooids	Oosparite		Oomicrite	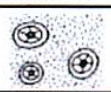
Peloids	Pelsparite		Pelmicrite	
Intraclasts	Intrasparite		Intramicrite	
Limestone formed in place	Biolithite		Terrestrial Limestone	

Dunham Classification Scheme for Carbonate Rocks

Dunham's classification scheme is based upon depositional textures within a limestone.

Allochthonous Limestone (original components not organically bound during deposition)						Autochthonous Limestone (original components organically bound during deposition; reef rocks)		
Of the allochems, less than 10% are larger than 2 mm				Of the allochems, greater than 10% are larger than 2 mm				
Contains carbonate mud			No mud	Matrix supported	Grain supported	Organisms acted as baffles	Organisms are encrusting and binding	Organisms building a rigid framework
Grain supported		Grain supported						
Less than 10% grains	More than 10% grains							
Mudstone	Wackestone	Packstone	Grainstone	Floatstone	Rudstone	Bafflestone	Bindstone	Framestone

Igneous Rocks

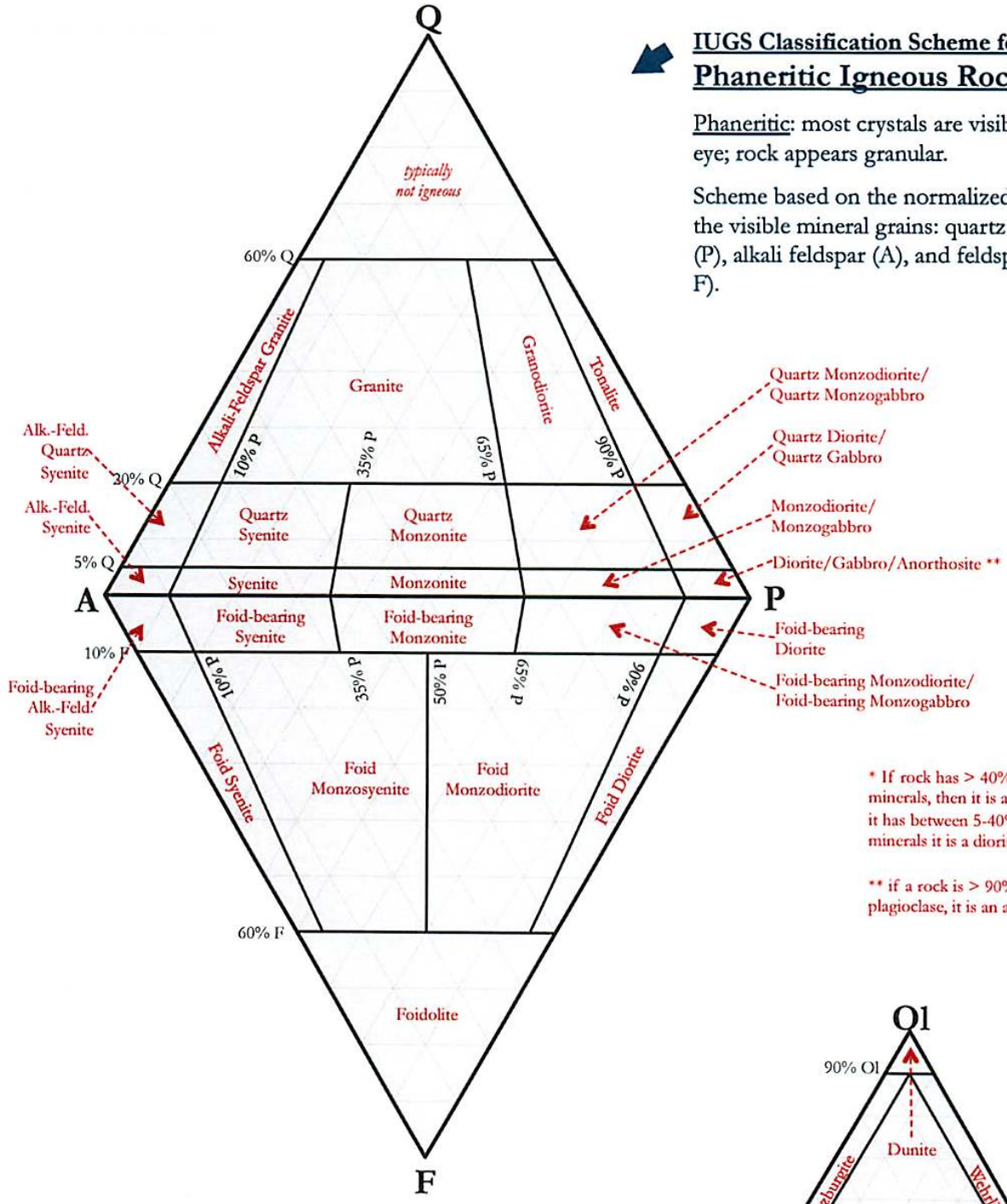

IUGS Classification Scheme for Phaneritic Igneous Rocks

Phaneritic: most crystals are visible to the naked eye; rock appears granular.

Scheme based on the normalized percentages of the visible mineral grains: quartz (Q), plagioclase (P), alkali feldspar (A), and feldspathoids (foids, F).

* If rock has > 40% mafic minerals, then it is a gabbo. If it has between 5-40% mafic minerals it is a diorite.

** if a rock is > 90% plagioclase, it is an anorthosite

IUGS Classification Scheme for Phaneritic Ultramafic Igneous Rocks (1)

Ultramafic: more than 90% of the total minerals are mafic.

Scheme based on the normalized percentages of the visible minerals: olivine (Ol), orthopyroxene (Opx), and clinopyroxene (Cpx).

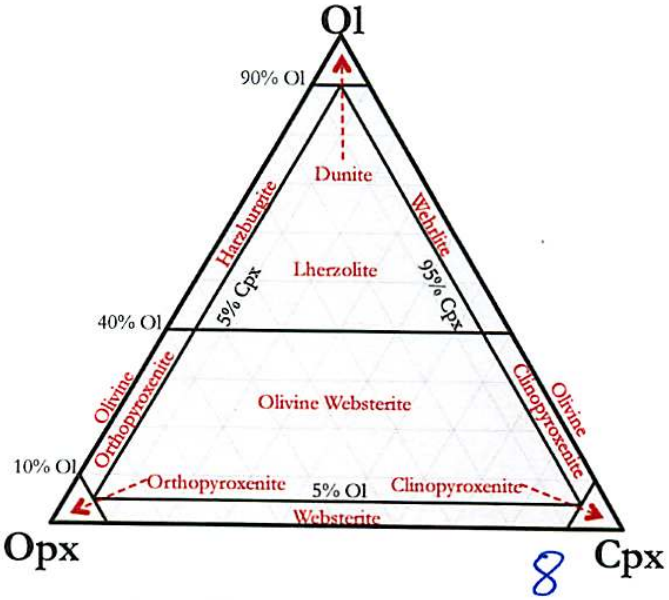

Igneous Rocks

IUGS Classification Scheme for Aphanitic Igneous Rocks

Aphanitic: the majority of crystals are not visible to the naked eye.

Aphanetic rocks are hard to classify due to the lack of visible minerals. However, you may still be able identify them based on phenocryst content, if phenocrysts are present. Scheme based on the normalized percentages of the visible phenocrysts: quartz (Q), plagioclase (P), alkali feldspar (A), and feldspathoids (foids, F).

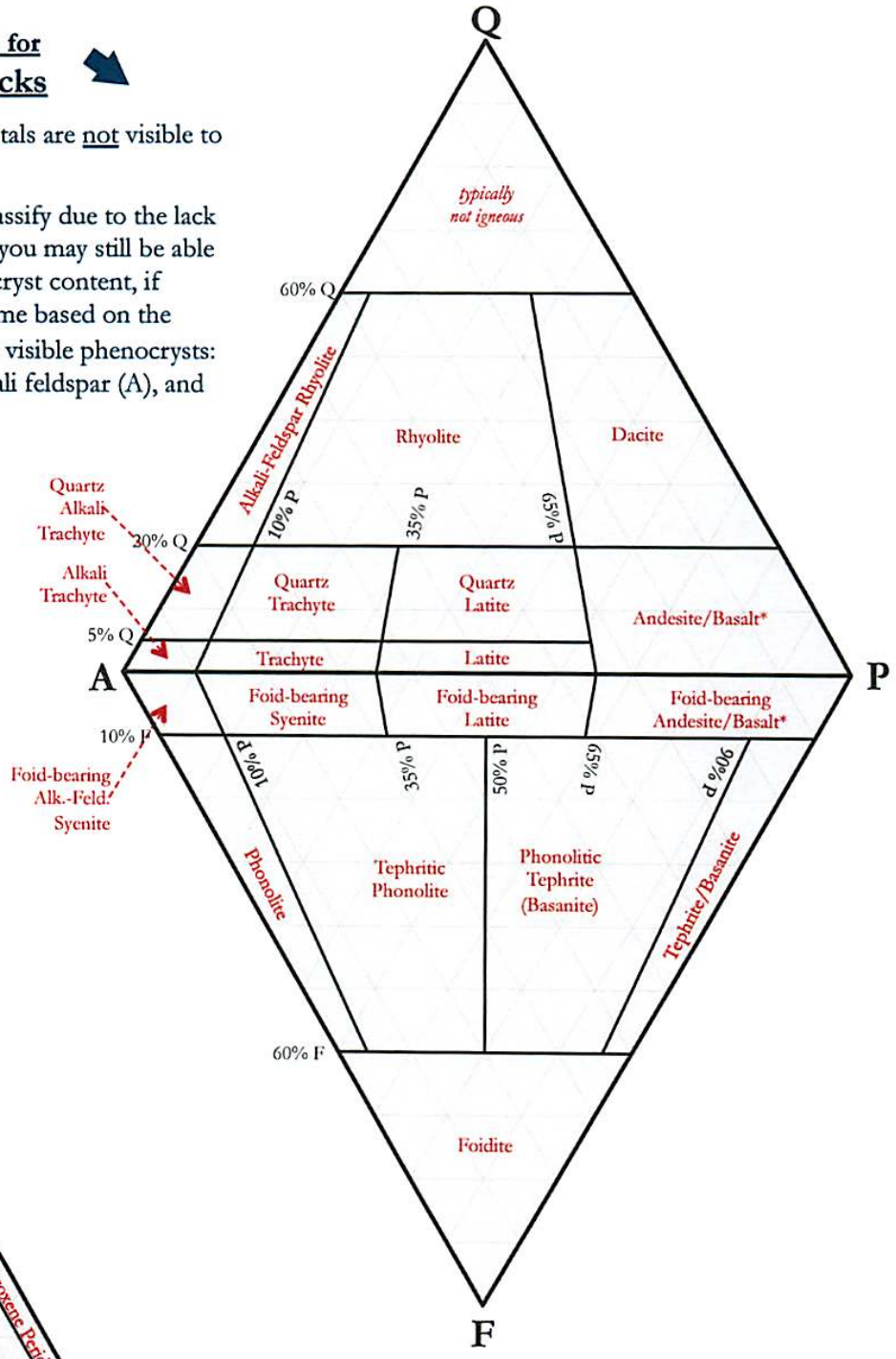

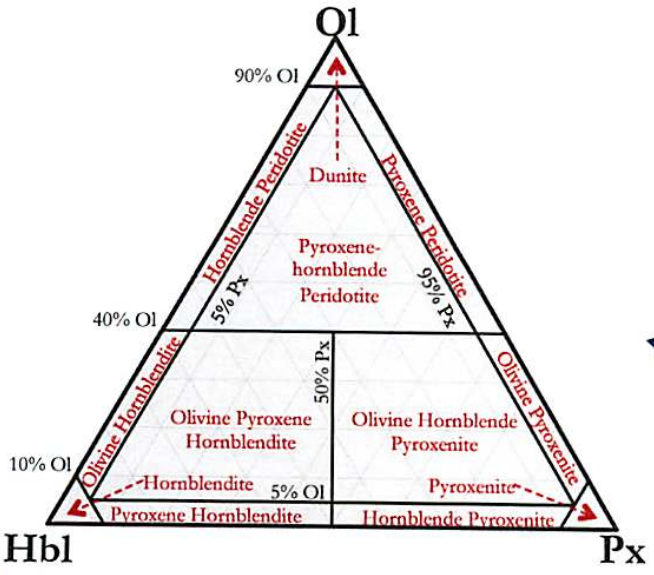

IUGS Classification Scheme for Phaneritic Ultramafic Igneous Rocks (2)

Ultramafic: more than 90% of the total minerals are mafic.

Scheme based on the normalized percentages of the visible minerals: olivine (Ol), hornblende (Hbl), and pyroxene (Px).

Igneous Rocks

Classification Scheme for Pyroclastic Igneous Rocks

Pyroclastic rocks are formed via the accumulation of fragments of volcanic rock scattered by volcanic explosions. They are frequently classified based upon the size distribution of clasts.

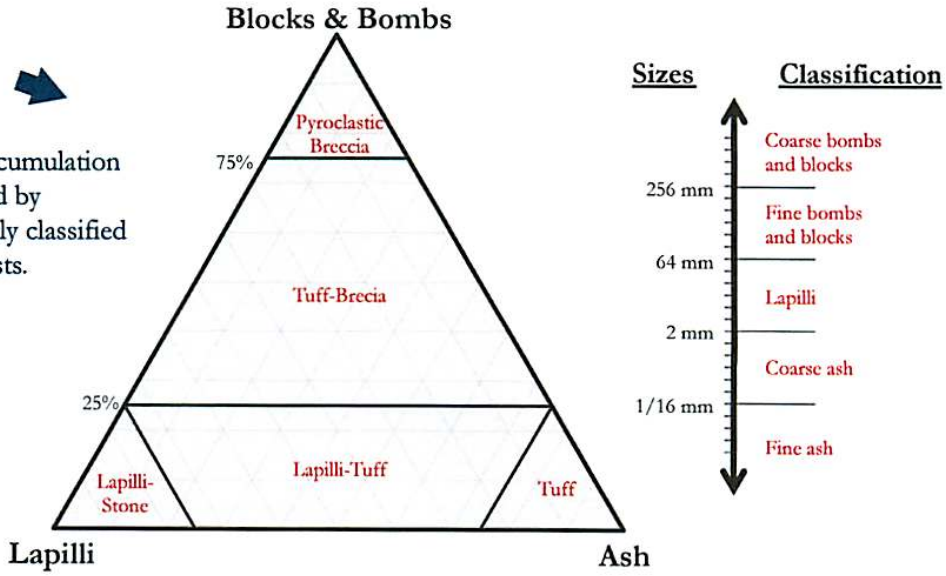

Types of Tephra (Pyroclasts)

In each row, the viscosity of the lava increases to the right. From Compton, 1985.

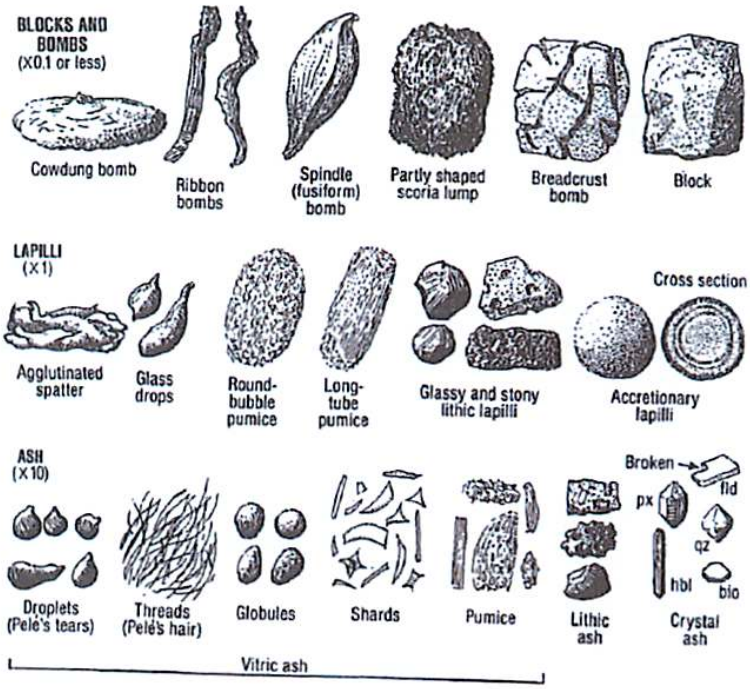

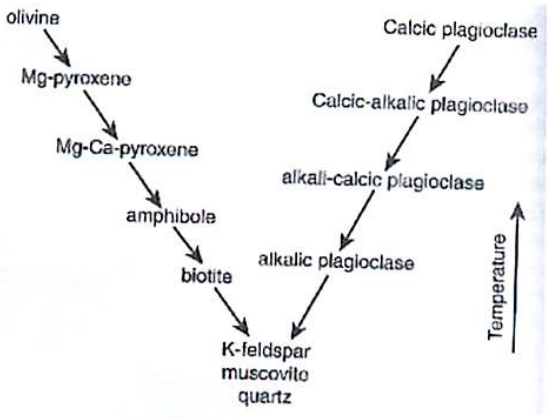

Bowen's Reaction Series

From Winter, 2010.

Metamorphic Rocks

Classification Scheme for Metamorphic Rocks

Based upon texture and mineralogical composition.

Structure &Texture	Characteristic Properties	Characteristic Mineralogy	Rock Name
Foliate (layered) (Increasing grain size, and degree of metamorphism ↓)	Dull luster; very flat fracture surface; grains are too small to readily see; more dense than shale	No visible minerals	Slate
	Silky sheen; Crenulated (wavy) fracture structure; A few grains visible, but most are not	Development of mica and/or hornblende possible	Phyllite
	Sub-parallel orientations of individual mineral grains; wavy-sheet like fracture; often contains porphyroblasts; thinly foliated	Abundant feldspar; Quartz and mica are common; hornblende possible	Schist
	Sub-parallel, alternating bands or layers of light and dark material; coarsely foliated; blocky fracture	Abundant feldspars; Quartz, mica, and hornblende are common	Gneiss
Foliate (layered)	Interlocking crystals; effervesces in dilute HCl; softer than glass	Calcite	Marble
	Nearly equigranular grains; fracture across grains (not around them); sub-vitreous appearance; smooth feel compared to sandstone	Quartz	Quartzite

Mineralogy for Metamorphic Rock Facies

Facies	Definitive Mineral Assemblages in Mafic Rocks
Zeolite	zeolites: especially laumontite, wairakite, analcime (in place of other Ca-Al silicates such as prehnite, pumpellyite and epidote)
Prehnite-Pumpellyite	prehnite + pumpellyite (+ chlorite + albite)
Greenschist	chlorite + albite +epidote (or zoisite) + actinolite ± quartz
Amphibolite	hornblende + plagioclase (oligoclase, andesine) ± garnet
Granulite	orthopyroxene + clinopyroxene + plagioclase ± garnet
Blueschist	glaucophane + lawsonite or epidote/zoisite (± albite ± chlorite ± garnet)
Eclogite	pyralspite garnet + omphacitic pyroxene (± kyanite ± quartz), no plagioclase
Contact Facies	mineral assemblages in mafic rocks of the facies of contact metamorphism do not differ substantially from those of the corresponding regional facies at higher pressure

Metamorphic Rocks

Metamorphic Rock Facies, P vs. T diagram

From Winter, 2010

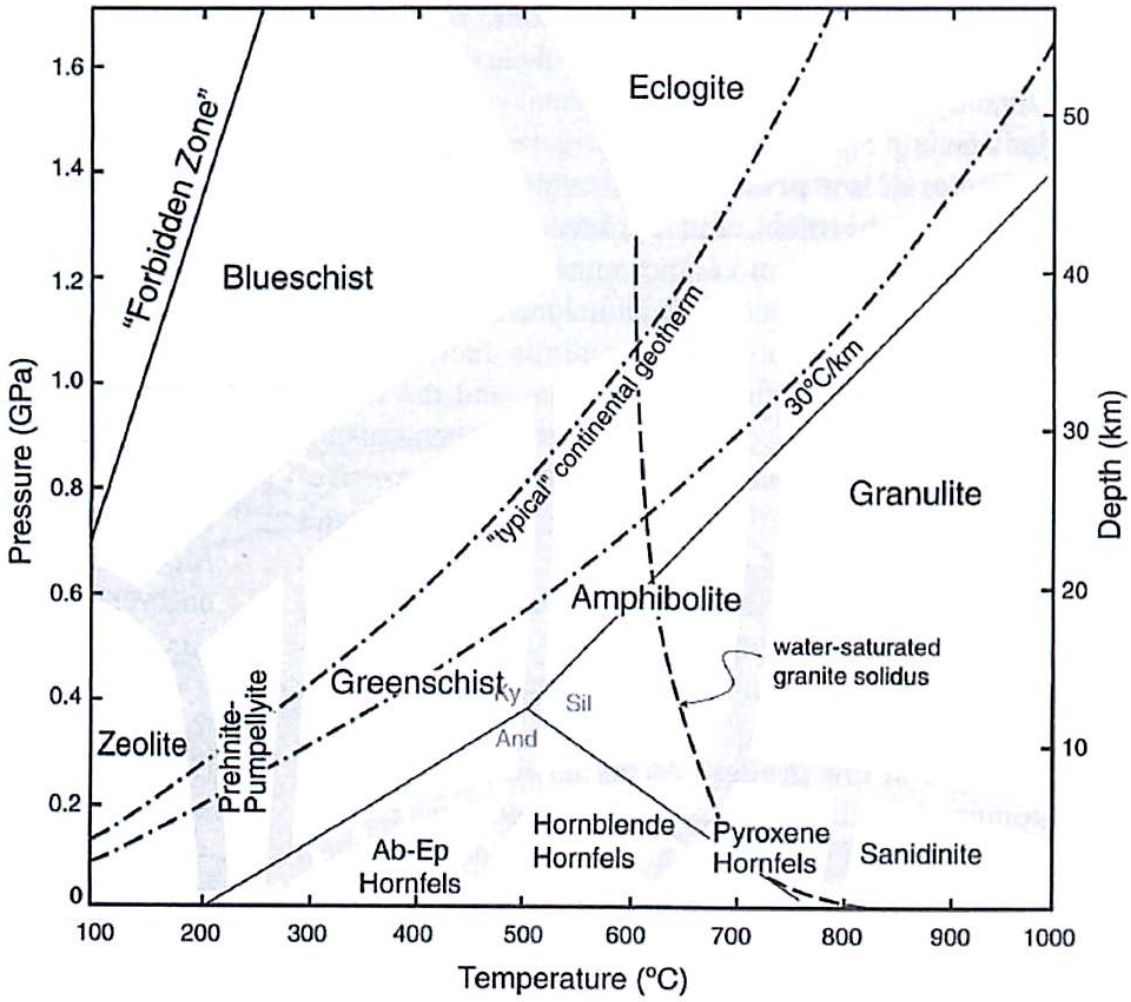

Schematic of Island Arc, and the origins of Metamorphic Facies

A schematic cross section of an island arc. Light gray lines are isotherms. From Winter, 2010

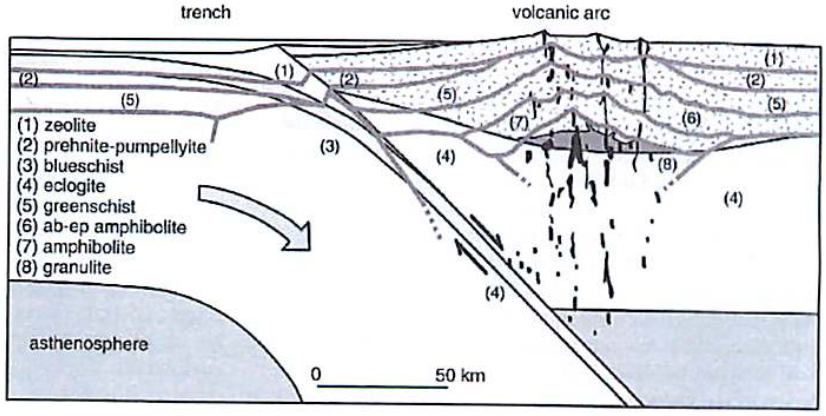

Structural Geology: Normal Faults

Normal Faults

In normal faults, the footwall goes up with respect to the hanging wall. Normal faults are indicative of extension. Figures from Davis & Reynolds, 1996.

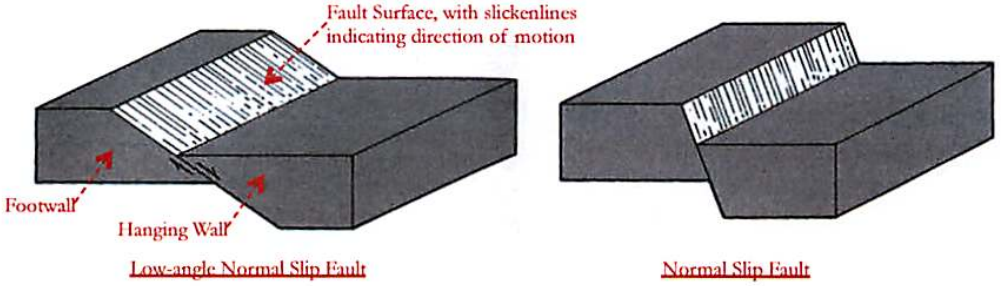

Effects of Brittle or Ductile Shear in Normal Faults

The block diagrams below illustrate the effects of changing the nature of deformation, between brittle deformation (which results in clear fault planes, fractures and fault rocks), ductile deformation (which causes deformation over a larger shear zone). Often, strata of different rheologies will behave differently, as is shown in the figure at right. The dashed layer was weak and deformed ductilely, while the middle grey layer was rigid and formed boudins. Figures from Davis & Reynolds, 1996.

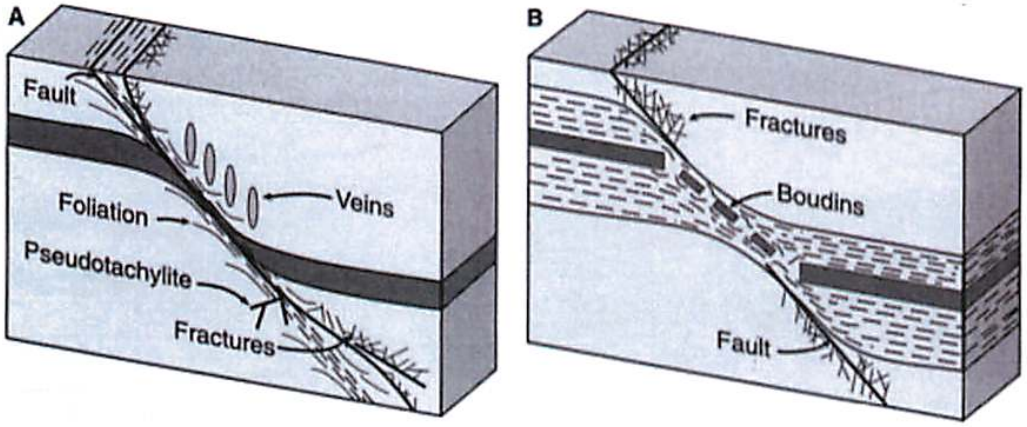

Inversion Tectonics

If the regional stresses change, previously inactive faults can reactivate, and change their sense of motion. In the figure at left, layer-A was formed prior to the formation of a normal fault. Layer-B and layer-C were deposited after the formation, and shut down of the fault. In the figure at the right, the fault has reactivated, though as a reverse fault. The resulting stratigraphic sequence is a combination of effects one would expect from both normal and reverse faults. Figures from Davis & Reynolds, 1996.

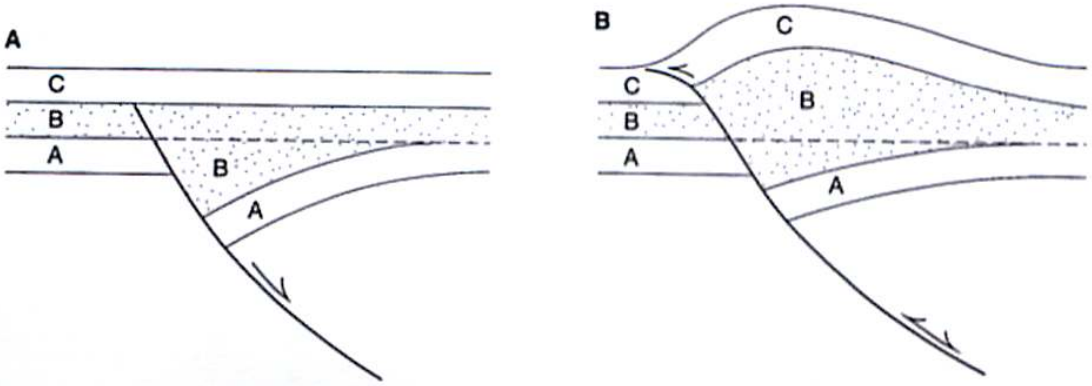

Structural Geology: Normal Faults

Normal Faults Geometries

Various normal fault geometries are possible. They all allow for lithospheric extension. (A) Domino style faulting. (B) Listric normal faulting with reverse drag. (C) Imbricate listric normal faulting. Note that listric faulting can cause extreme rotation of faulted blocks. (D) Listric normal faulting bounding a family of planar normal faults. Figures from Davis & Reynolds, 1996.

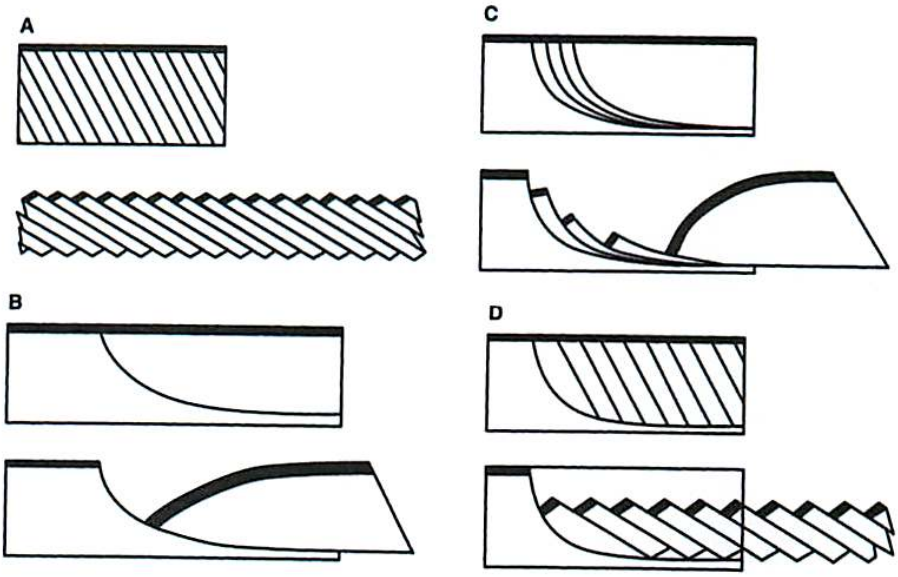

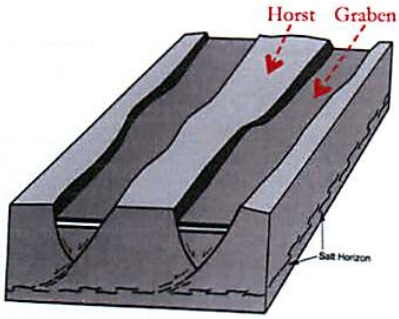

Horsts & Grabens

Classical formation describing fault-bounded uplifted (horsts) and down-dropped blocks (grabens). Figures from Davis & Reynolds, 1996.

Drag Folds, Reverse Drag, and Step Faulting

Faulting does not always produce clean displacement along the fault surface. Fault blocks are frequently folded or fractured, and the nature of these deformations are non-trivial. Figures from Davis & Reynolds, 1996.

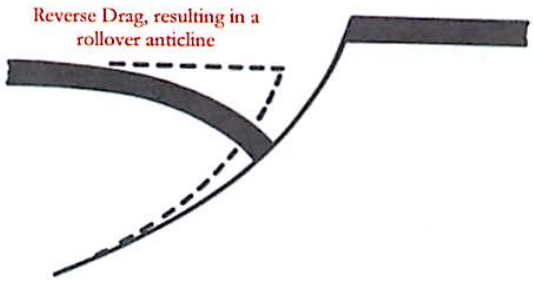

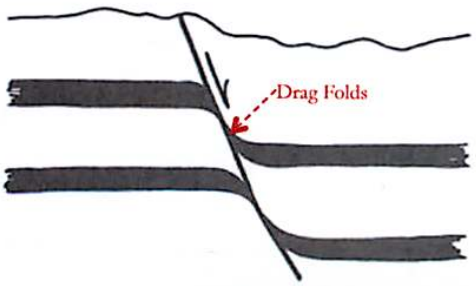

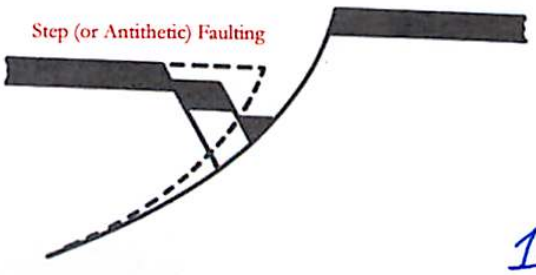

Structural Geology: Reverse & Thrust Faults

Reverse Faults

In reverse faults, the footwall goes down with respect to the hanging wall. Normal faults are indicative of compression. Thrust faults are reverse faults with fault dips <45 degrees. Figures from Davis & Reynolds, 1996.

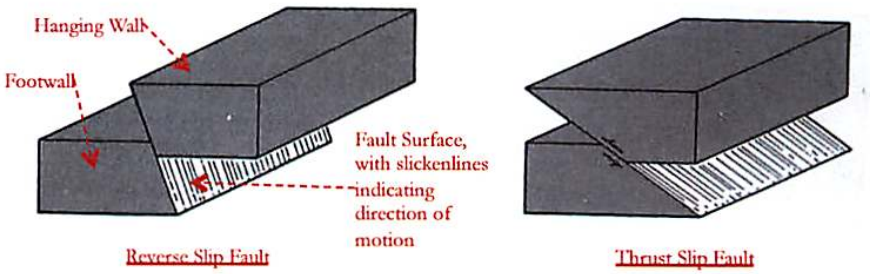

"Ramp-Flat" Geometry of Typical Thrust Fault Systems

In a regional thrust, faulted blocks are "thrust" on top of younger strata. The exact geometry of these thrust systems can vary significantly. Figures from Davis & Reynolds, 1996.

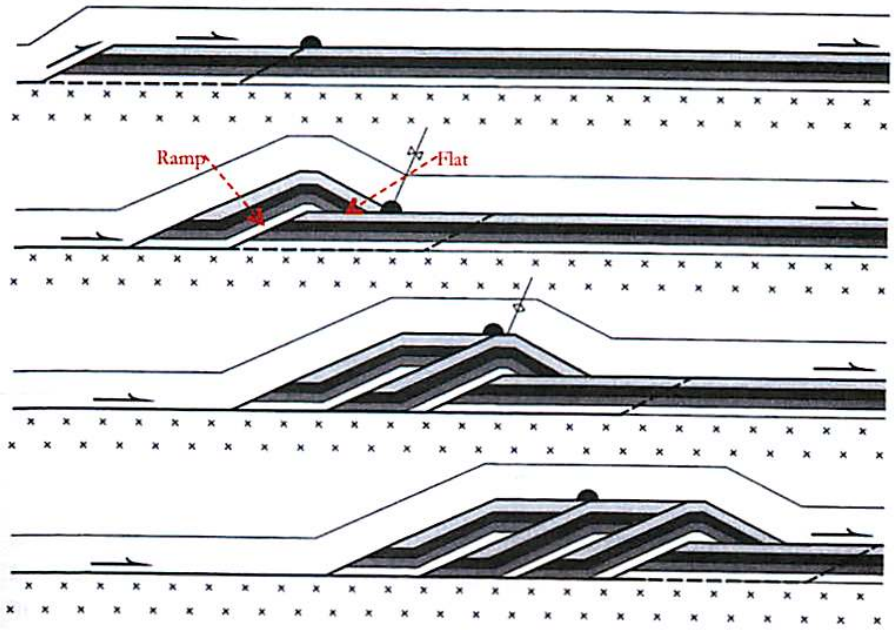

Klippe & Windows

Thrust faults move large blocks of non-indigenous rock (referred to as "allochthonous" rock) over emplaced rock (referred to as "autochthonous" rock). If the overlying allochthonous rock is eroded, it can create windows into the lower underlying autochthonous rock. Erosion can also create islands of isolated allochthonous rock, called klippe. Figures from Davis & Reynolds, 1996.

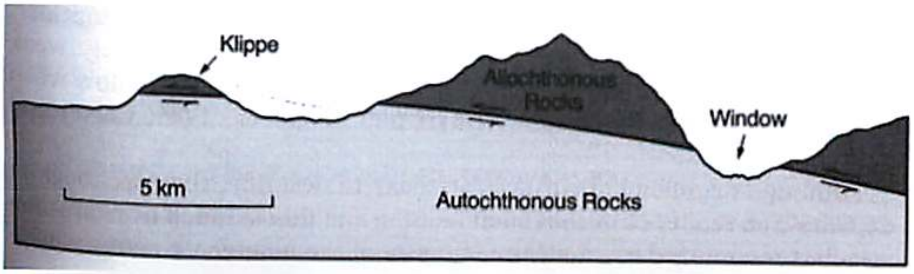

Structural Geology: Reverse & Thrust Faults

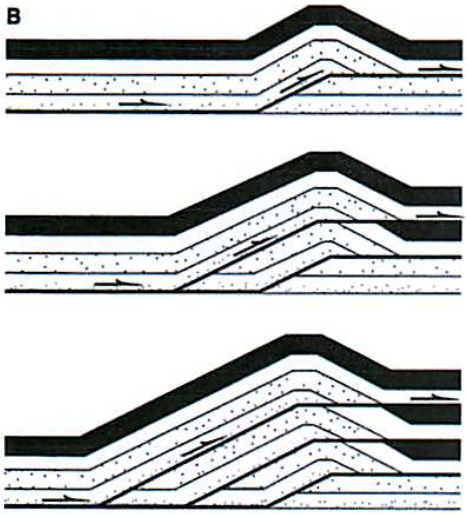

Out-of-Sequence Thrust Fault System

Unlike "in-sequence" thrust fault systems (as shown on the previous page, the "roof" of the thrust block in an out-of-sequence system becomes the "flat" for subsequent fault blocks. Figures from Davis & Reynolds, 1996.

Imbricate Fans vs. Duplexes

Two thrust fault geometries: imbricate fans (top) and duplexes (bottom). Figures from Davis & Reynolds, 1996.

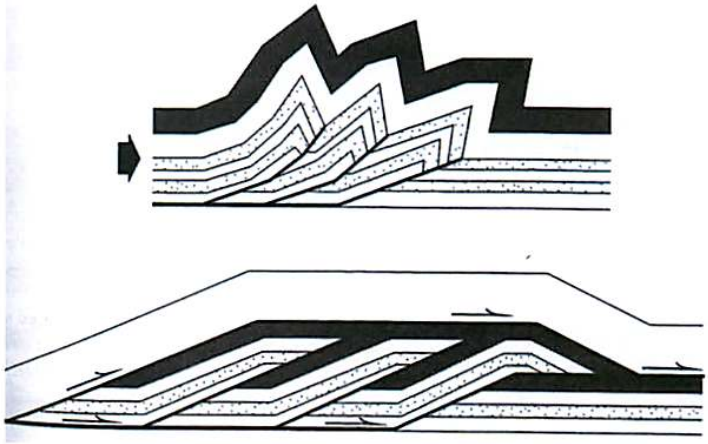

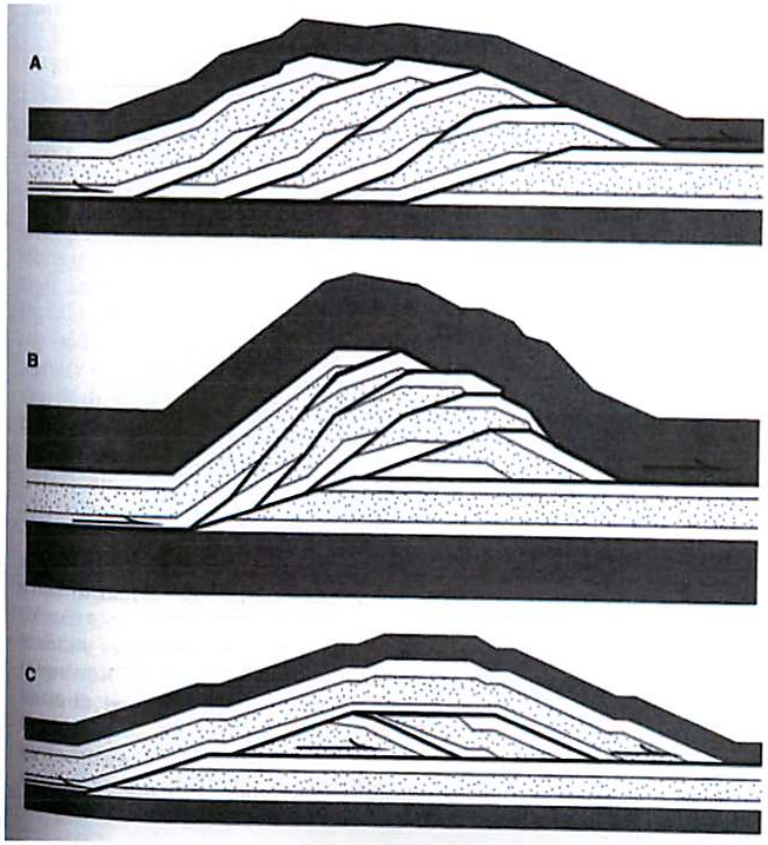

Forms of Duplexes

The exact form of a duplex or imbricate fan depends on the spacing of ramps and the amount of slip. (A) A normal duplex develops when slice length exceeds the fault slip. (B) An antiformal duplex develops when slice length and fault slip are effectively equal. (C) A forward-dipping duplex develops when the fault slip is greater than the slice length. Figures from Davis & Reynolds, 1996.

Structural Geology: Strike-Slip or Transform Faults

Strike-Slip Faults

In reverse faults, the footwall goes down with respect to the hanging wall. Normal faults are indicative of compression. Thrust faults are reverse faults with fault dips <45 degrees. Figures from Davis & Reynolds, 1996.

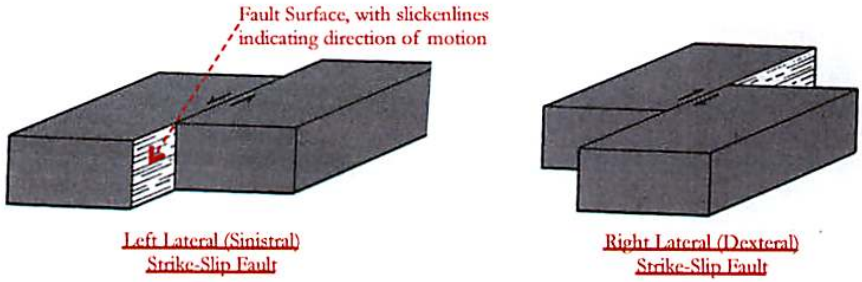

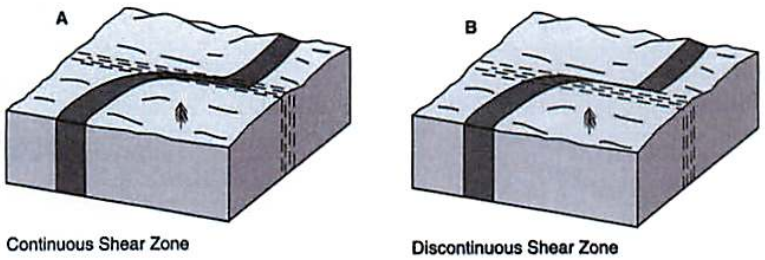

Ductile Shear Zones

Shear in a strike-slip fault is not always located in a single plane. Sometimes, shear takes place over an extended region. Figures from Davis & Reynolds, 1996.

Brittle Shear Zones

Figures from Davis & Reynolds, 1996.

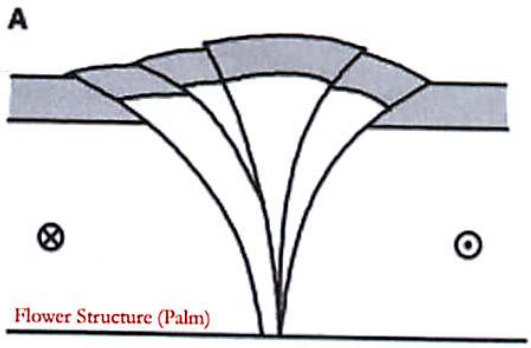

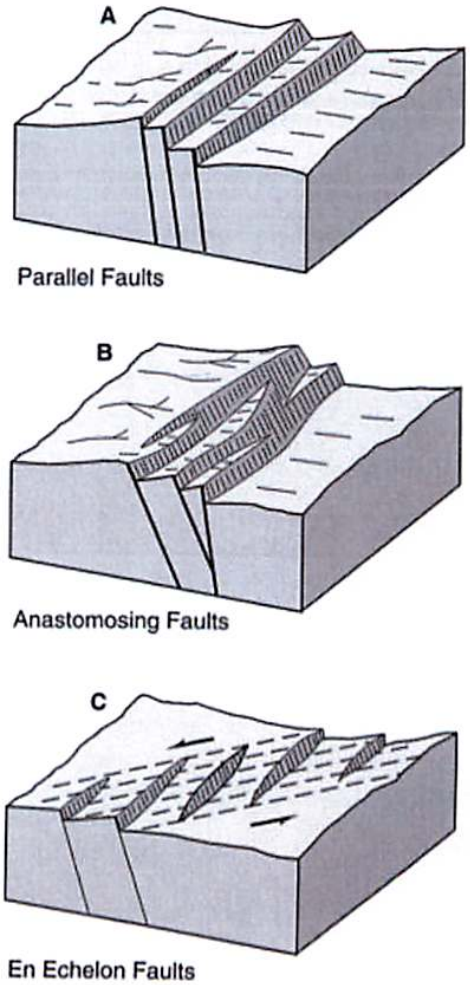

Structural Geology: Strike-Slip or Transform Faults

Bends in Strike-Slip Faults

Strike-slip faults along irregularly curved faults creates localized regions of extension and compression. Figures from Davis & Reynolds, 1996.

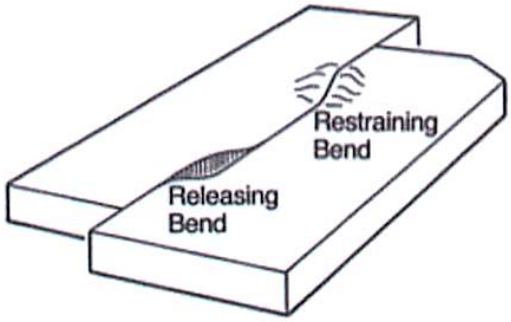

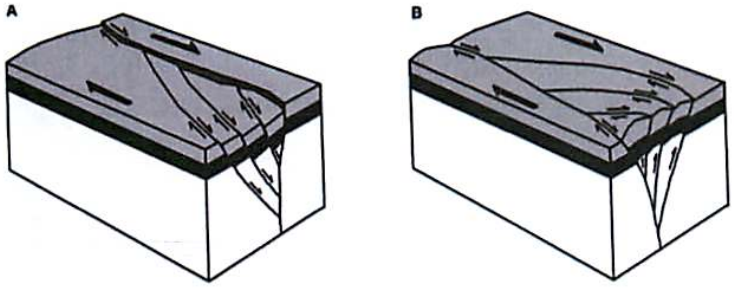

Strike-Slip Duplexes

(A) Extensional duplexes can form at releasing bends. (B) Compressional duplexes can form at restraining bends. Figures from Davis & Reynolds, 1996.

Slip Indicators in Strike-Slip Systems

In strike-slip systems, the maximum (S_1) and minimum compressional stresses (S_3) are at an angle with respect to the sense of shear. This can lead to the formation of both large scale folds and faults, or small scale fractures or veins, which are indicative to the sense of motion. Figures from Davis & Reynolds, 1996.

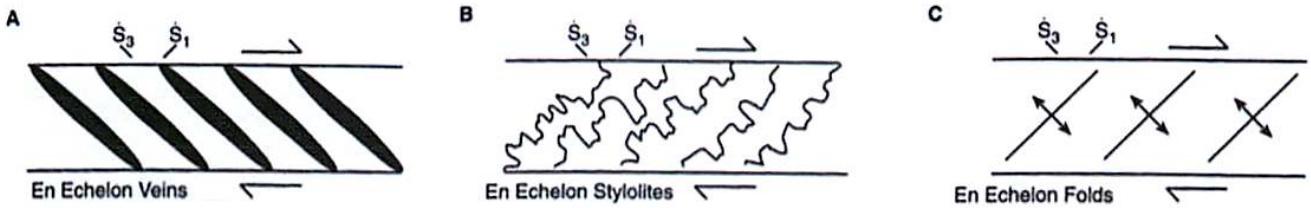

Even more Geometric Arrangements of Strike-Slip Faults

Figures from Davis & Reynolds, 1996.

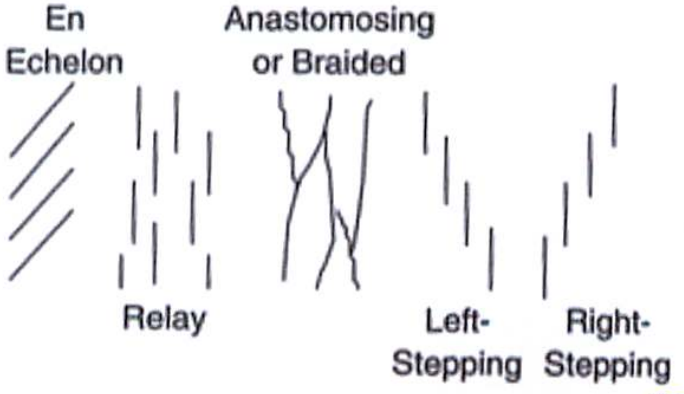

Structural Geology: Strike-Slip or Transform Faults

Riedel Shears

When under compression, rocks tend to form fail with faults forming 30° from the primary compressional stress. In a strike-slip fault, the primary compressional stress (σ_1) is 45° away from the plane of strike-slip shearing. The combination of these two facts results in fractures at interesting angles with respect to the motion of shear. These are called Riedel shears. The figure below shows a left-handed strike-slip zone. Figures from Davis & Reynolds, 1996.

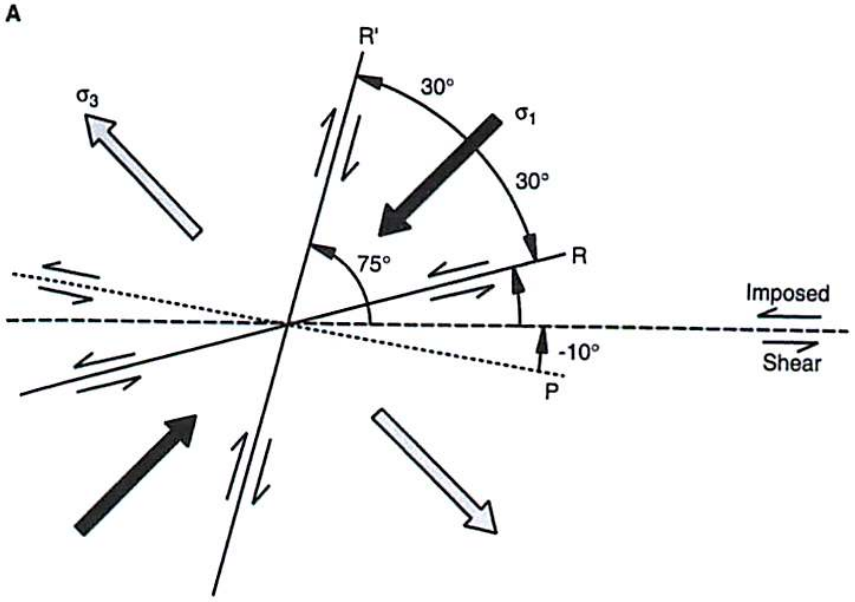

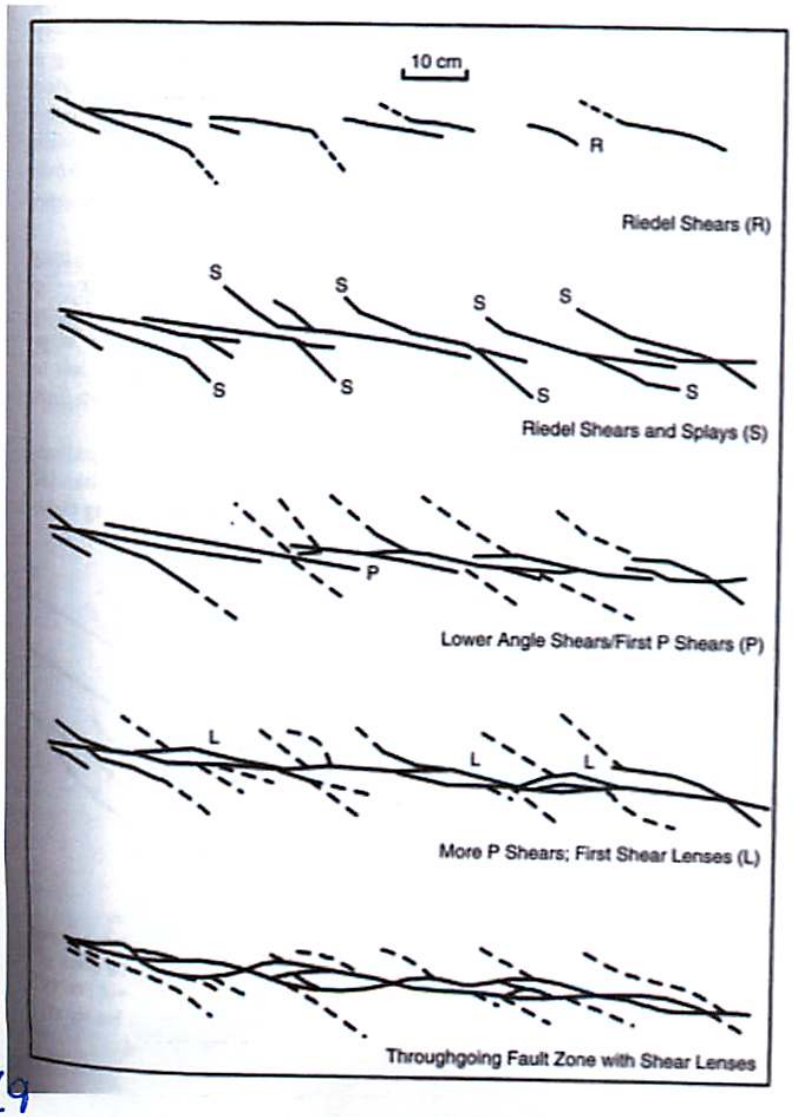

The figure at left illustrate the formation sequence of Riedel shears and other splays and shears in a right-handed strike-slip zone. Figures from Davis & Reynolds, 1996.

Structural Geology: Folds

Anticlines & Antiforms, and Synclines & Synforms

Antiforms are concave-down folds, while Synforms are concave-up folds. Anticlines are antiforms were we know that the younger strata lie on top of older strata. Similarly, Synclines are antiforms where younger strata lie on top of older strata. Figures from Davis & Reynolds, 1996.

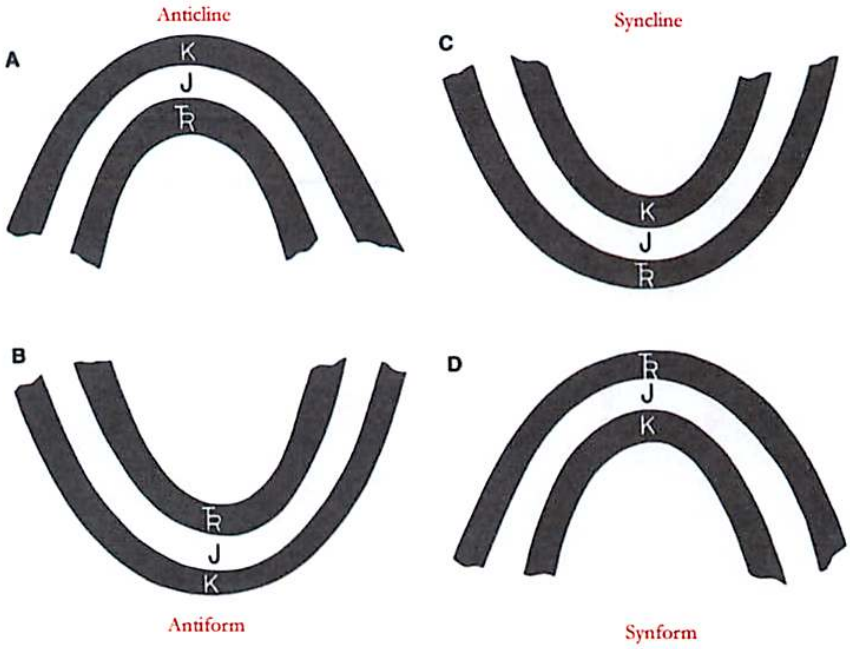

Plunging Folds

Folds (defined by hinge lines and axial surfaces) are not necessarily perpendicular to the Earth's surface. They can be dipping into or out of the surface. This can create interesting patterns of exposed surface rock, or even topography. Figures from Jones, 2001.

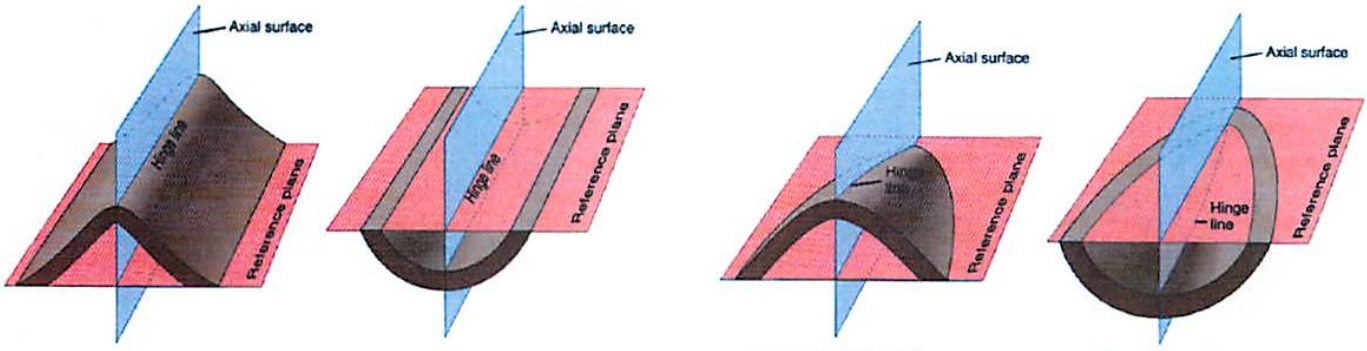

Fold Shapes

Folds can come in a variety of shapes. Davis & Reynolds, 1996.

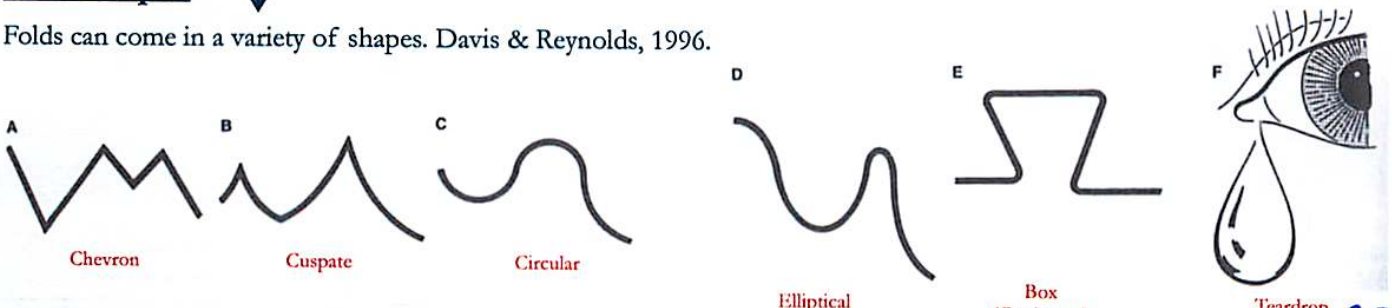

Structural Geology: Folds

Fold Tightness

Fold tightness is based upon the size of the inter-limb angle. Figures from Davis & Reynolds, 1996.

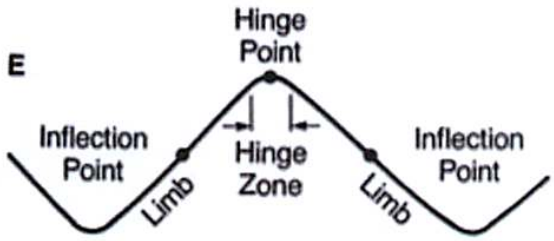

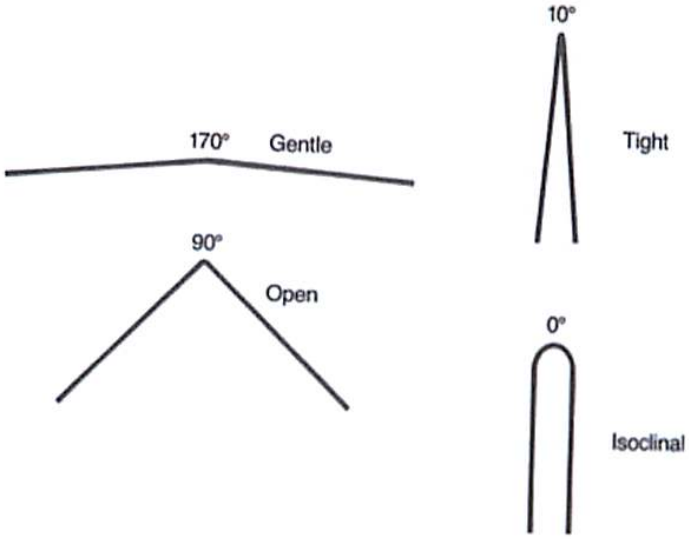

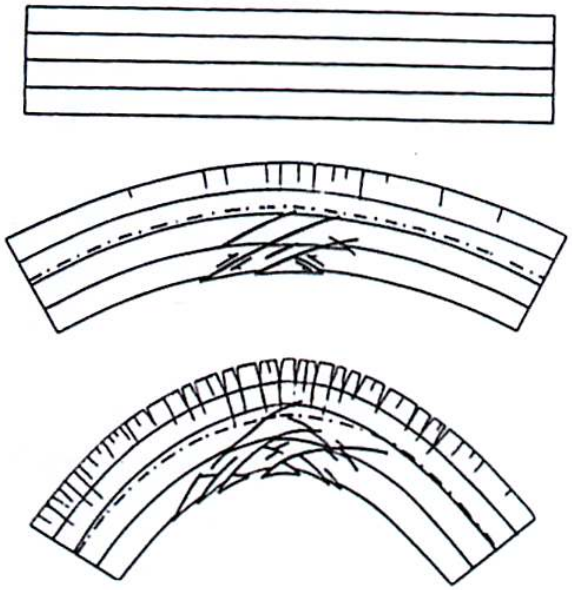

Minor Structures in Folds

When folding layers of strata, layer-parallel stretching occurs in the outer arc of a folded layer, while layer-parallel shortening occurs in the inner arc. Figures from Davis & Reynolds, 1996.

Boudins

Layer-parallel stretching can pinch off layers of strata, depending on the ductility contrast between layers. This can result in pinch-and-swell structures or boudins (where the pinching completely pinches off portions of a given strata). Figures from Davis & Reynolds, 1996.

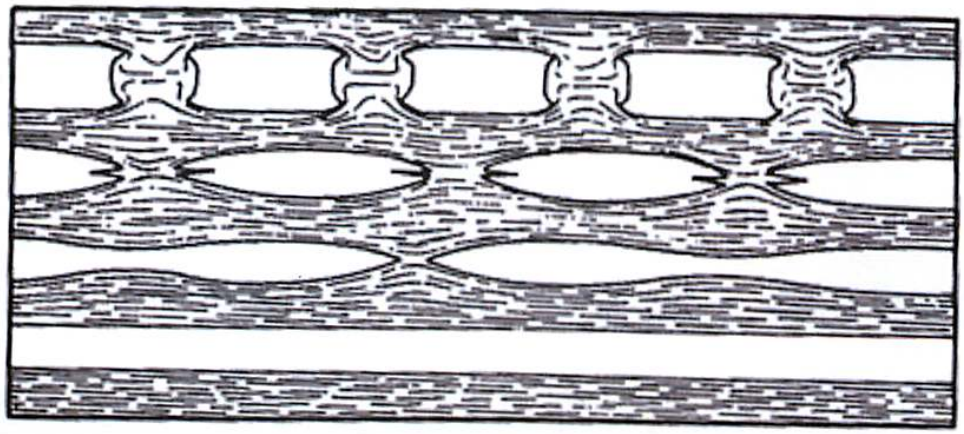

Geologic Map Symbols

1 

Contact, showing dip where trace is horizontal, and strike and dip where trace is inclined

2 Contact, located approximately (give limits)

3 Contact, located very approximately, or conjectural

4 Contact, concealed beneath mapped units

5 Contact, gradational (optional symbols)

6 Fault, nonspecific, well located (optional symbols)

7 Fault, nonspecific, located approximately

8 Fault, nonspecific, assumed (existence uncertain)

9 Fault, concealed beneath mapped units

10 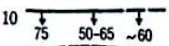

Fault, high-angle, showing dip (left) and approximate dips

11 

Fault, low-angle, showing approximate dip and strike and dip

12 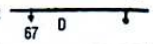

Fault, high-angle normal (D or ball and bar on downthrown side)

13 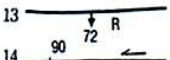

Fault, reverse (R on upthrown side)

14 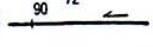

Fault, high-angle strike-slip (example is left lateral)

15 

Fault, thrust (T on overthrust side)

16 

Fault, low-angle normal or detachment (D on downthrown side)

17 Fault, low-angle strike-slip (example is right lateral)

18 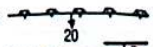

Fault, low-angle, overturned (teeth in direction of dip)

19 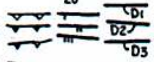

Optional sets of symbols for different age-groups of faults

20 Fault zone or shear zone, width to scale (dip and other accessory symbols may be added)

21 

Faults with arrows showing plunge of rolls, grooves or slickensides

22 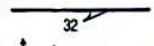

Fault showing bearing and plunge of net slip

23 Point of inflection (bar) on a high-angle fault

24 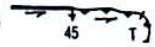

Points of inflection on a strike-slip fault passing into a thrust

25 Fault intruded by a dike

26 Faults associated with veins

27 

Anticline, showing trace and plunge of hinge or crest line (specify)

28 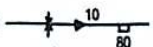

Syncline (as above), showing dip of axial surface or trough surface

29 Folds (as above), located approximately

30 Folds, conjectural

31 Folds beneath mapped units

32 Asymmetric folds with steeper limbs dipping north (optional symbols)

33 Anticline (top) and syncline, overturned

34 Antiformal (inverted) syncline

35 Synformal (inverted) anticline

36 Antiform (top) and synform (stratigraphic sequence unknown)

37 Separate dome (left) and basin

38 Culmination (left) and depression

40 Vertically plunging anticline and syncline

41 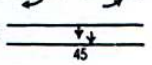

Monocline, south-facing, showing traces of axial surfaces

42 

Steeply plunging monocline or flexure, showing trace in horizontal section and plunge of hinges

43 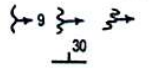

Plunge of hinge lines of small folds, showing shapes in horizontal section

44 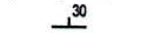

Strike and dip of beds or bedding

45 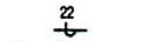

Strike and dip of overturned beds

46 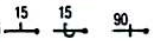

Strike and dip of beds where stratigraphic tops are known from primary features

47 Strike and dip of vertical beds or bedding (dot is on side known to be stratigraphically the top)

48 Horizontal beds or bedding (as above)

49 Approximate (typically estimated) strike and dip of beds

50 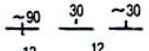

Strike of beds exact but dip approximate

51 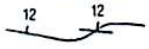

Trace of single bed, showing dip where trace is horizontal and where it is inclined

52 

Strike and dip of foliation (optional symbols)

53 Strike of vertical foliation

54 Horizontal foliation

55 

Strike and dip of bedding and parallel foliation

56 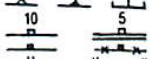

Strike and dip of joints (left) and dikes (optional symbols)

57 Vertical joints (left) and dikes

58 Horizontal joints (left) and dikes

59 Strike and dip of veins (optional symbols)

60 Vertical veins

61 Horizontal veins

62 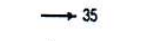

Bearing (trend) and plunge of lineation

63 Vertical and horizontal lineations

64 

Bearing and plunge of cleavage-bedding intersection

65 Bearing and plunge of cleavage-cleavage intersections

66 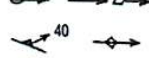

Bearings of pebble, mineral, etc. lineations

67

Bearing of lineations in plane of foliation

68 

Horizontal lineation in plane of foliation

69 Vertical lineation in plane of vertical foliation

70 Bearing of current from primary features; from upper left: general; from cross-bedding; from flute casts; from imbrication

71 Bearing of wind direction from dune forms (left) and cross-bedding

72 Bearing of ice flow from striations (left) and orientation of striations

73 Bearing of ice flow from drumlins

74 Bearing of ice flow from crag and tail forms

75 Spring

76 Thermal spring

77 Mineral spring

78 Asphaltic deposit

79 BIT Bituminous deposit

80 Sand, gravel, clay, or placer pit

From Compton, 198

Geologic Map Symbols

81		Mine, quarry, or open pit
82		Shafts: vertical, inclined, and abandoned
83		Adit, open (left) and inaccessible
84	x	Trench (left) and prospect
85		Water wells: flowing, nonflowing, and dry
86		Oil well (left) and gas well
87		Well drilled for oil or gas, dry
88		Wells with shows of oil (left) and gas
89		Oil or gas well, abandoned (left) and shut in
90		Drilling well or well location
91		Glory hole, open pit, or quarry, to scale
92		Dump or fill, to scale

Fossil and Structural Symbols for Stratigraphic Columns

Algae	Tree trunk fallen	Foraminifers, general	Scour casts
Algal mats	Trilobites	Foraminifers, large	Convolution
Ammonites	Vertebrates	Fossils	Slumped beds
Belemnites	Wood	Fossils abundant	Paleosol
Brachiopods	Beds distinct	Fossils sparse	Mud cracks
Bryozoans	Beds obscure	Gastropods	Salt molds
Corals, solitary	Unbedded	Graptolites	Burrows
Corals, colonial	Graded beds	Leaves	Pellets
Crinoids	Planar cross-bedding	Ostracodes	Oolites
Echinoderms	Trough cross-bedding	Pelecypods	Pisolites
Echinoids	Ripple structures	Root molds	Intraclasts
Fish bones	Cut and fill	Spicules	Stylolite
Fish scales	Load casts	Stromatolites	Concretion
		Tree trunk in place	Calcitic concretion

From Compton, 198

Lithologic Patterns for Stratigraphic Columns & Cross Sections

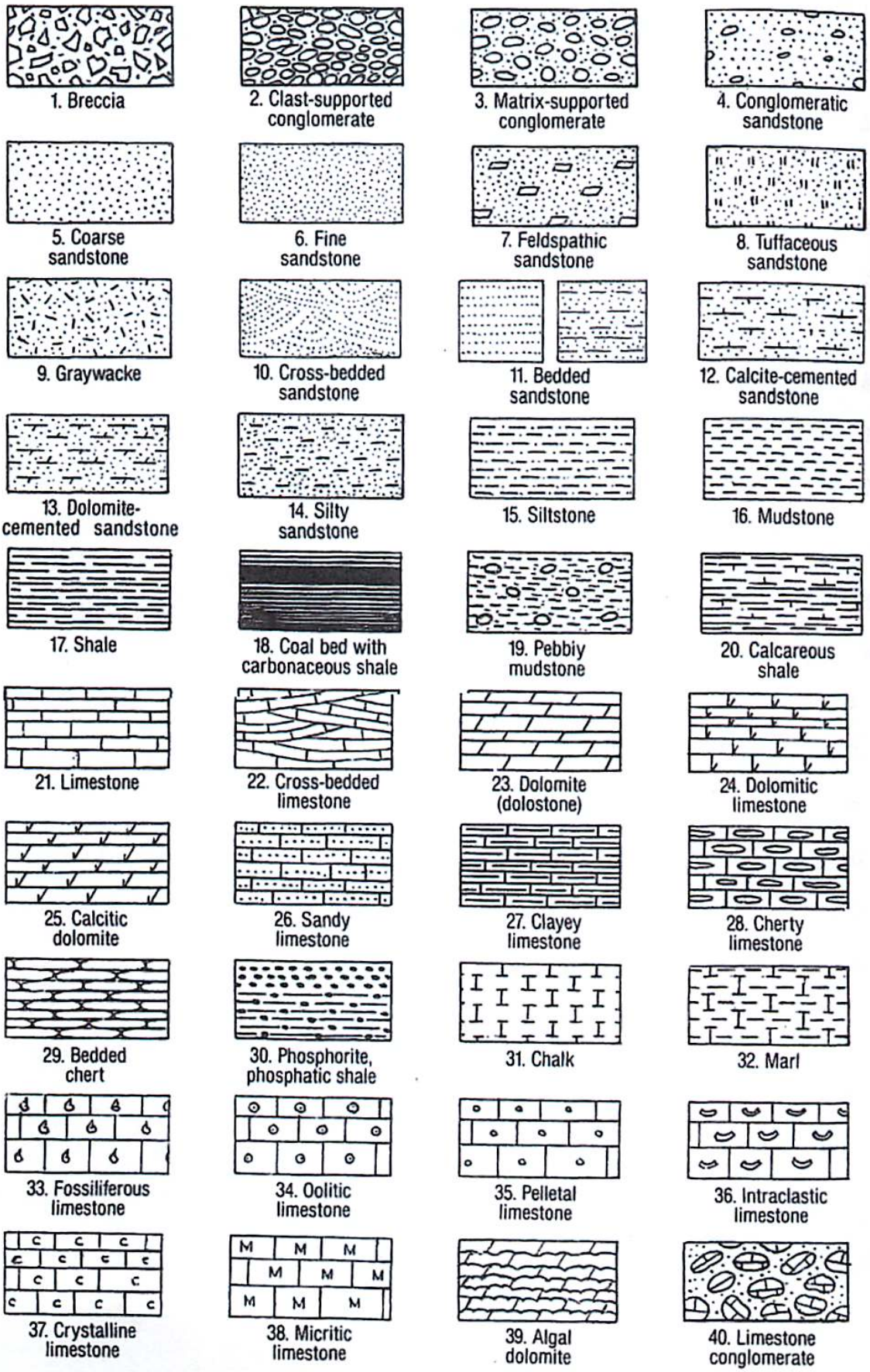

From Compton, 198

Lithologic Patterns for Stratigraphic Columns & Cross Sections


41. Limestone breccia


42. Algal dolomite breccia


43. Gypsum bed, gypsiferous shale

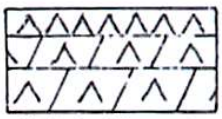
44. Anhydrite, anhydritic dolomite


45. Rock salt, salty mudstone

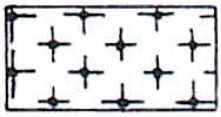
46. Peridotite

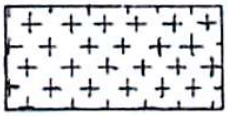
47. Gabbro

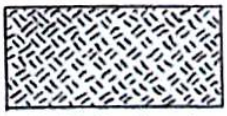
48. Mafic plutonic rock


49. Coarse granitic rock

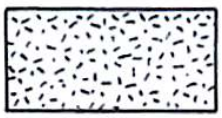
50. Fine granitic rock

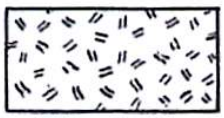
51. Porphyritic plutonic rock

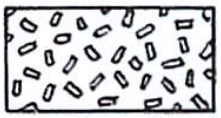
52. Porphyritic plutonic rock


53. Mafic lava


54. Silicic lava

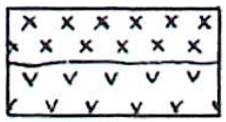
55. Intrusive volcanic rocks

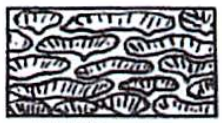
56. Pillow lava


57. Hyaloclastite

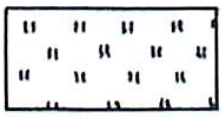
58. Tuff

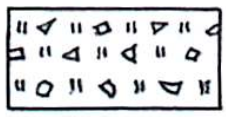
59. Tuff-breccia

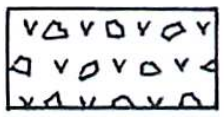
60. Volcanic breccia


61. Massive serpentinite


62. Foliated serpentinite

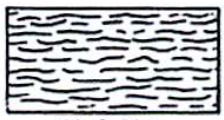
63. Schist

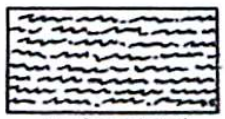
64. Crenulated schist


65. Folded schist

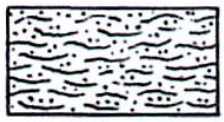
66. Semischistose sandstone

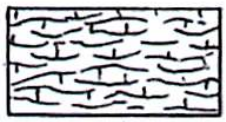
67. Semischistose limestone

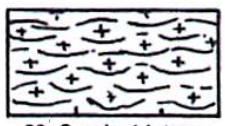
68. Semischistose gabbro


69. Greenstone


70. Silicic gneiss

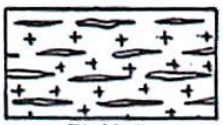
71. Mafic gneiss

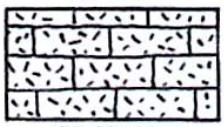
72. Marble

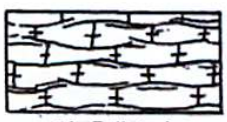
73. Foliated marble

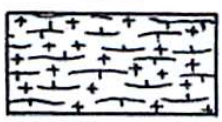
74. Foliated calc-silicate rock

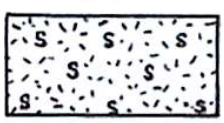
75. Massive skarn

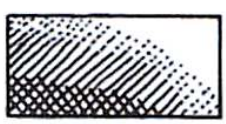
76. Alteration zones

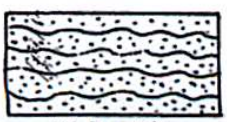
77. Quartzite


78. Quartzite


79. Silicic migmatite


80. Mafic migmatite

From Compton, 1985

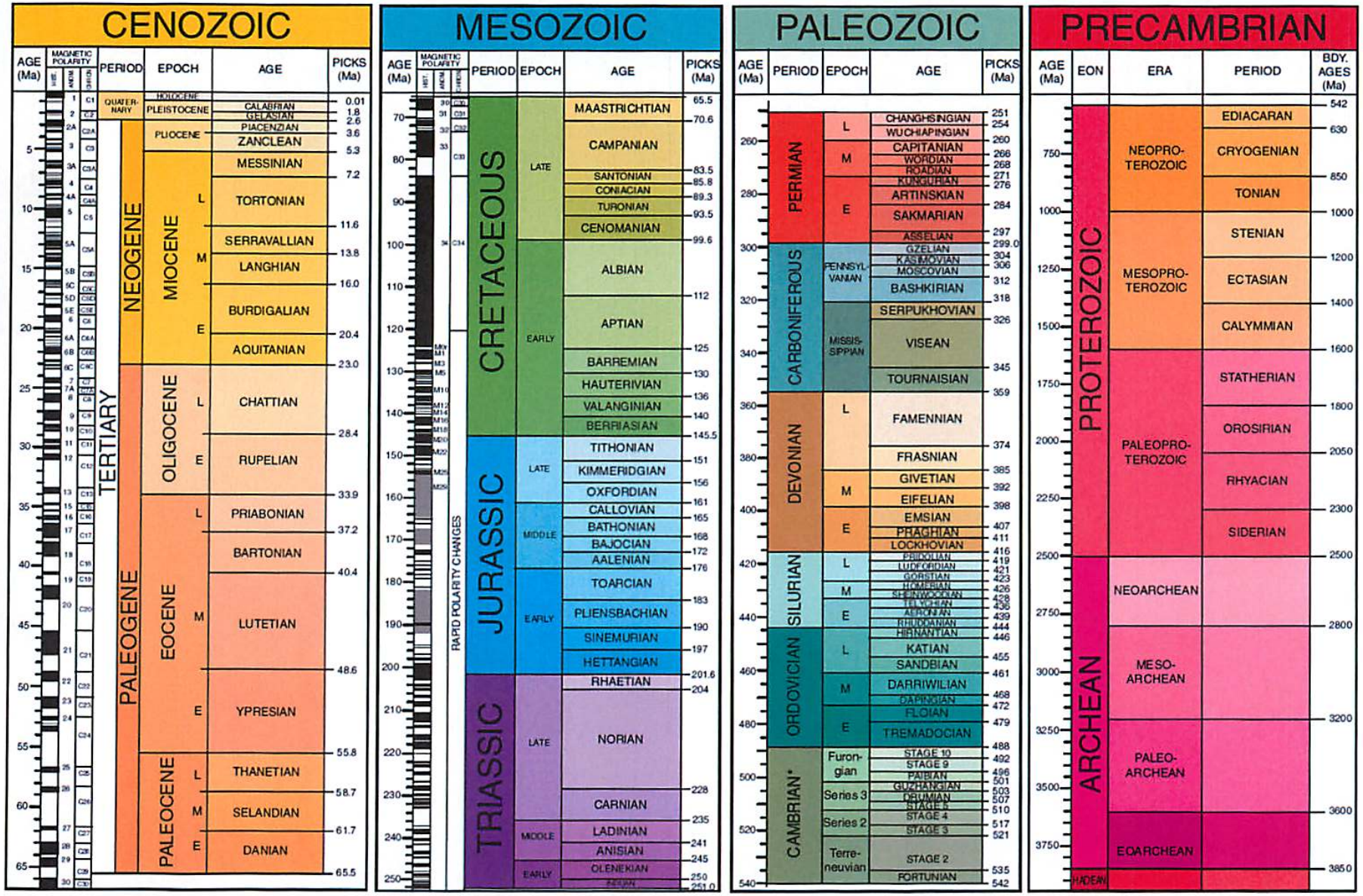

Geologic Timescale

2009 version, from the Geologic Society of A

Sudoku #337 (Medium)

		2					9	
8		5	1					
	3						2	
	1				6			
				9	2		6	
5					4			7
						5	7	2
4								
	8		3		7			

Sudoku #333 (Hard)

		3			4		5	7
	9	5		6		8		3
						4		1
			4			6		2
			5				9	
	3	2			9		7	4
8						3		6
		1	7					
							4	5

Sudoku #338 (Medium)

						9	3	
	7				4			
		9		7		8		6
	6		5					4
					2			
	1			4			7	
6	5		2					
								2
4		8		3		5		

Sudoku #334 (Hard)

						9		
6	7		2	9				4
			1	3			5	
			6		7			
	4						2	
	9					6		
								8
1			4			7		
2							1	9


END
START

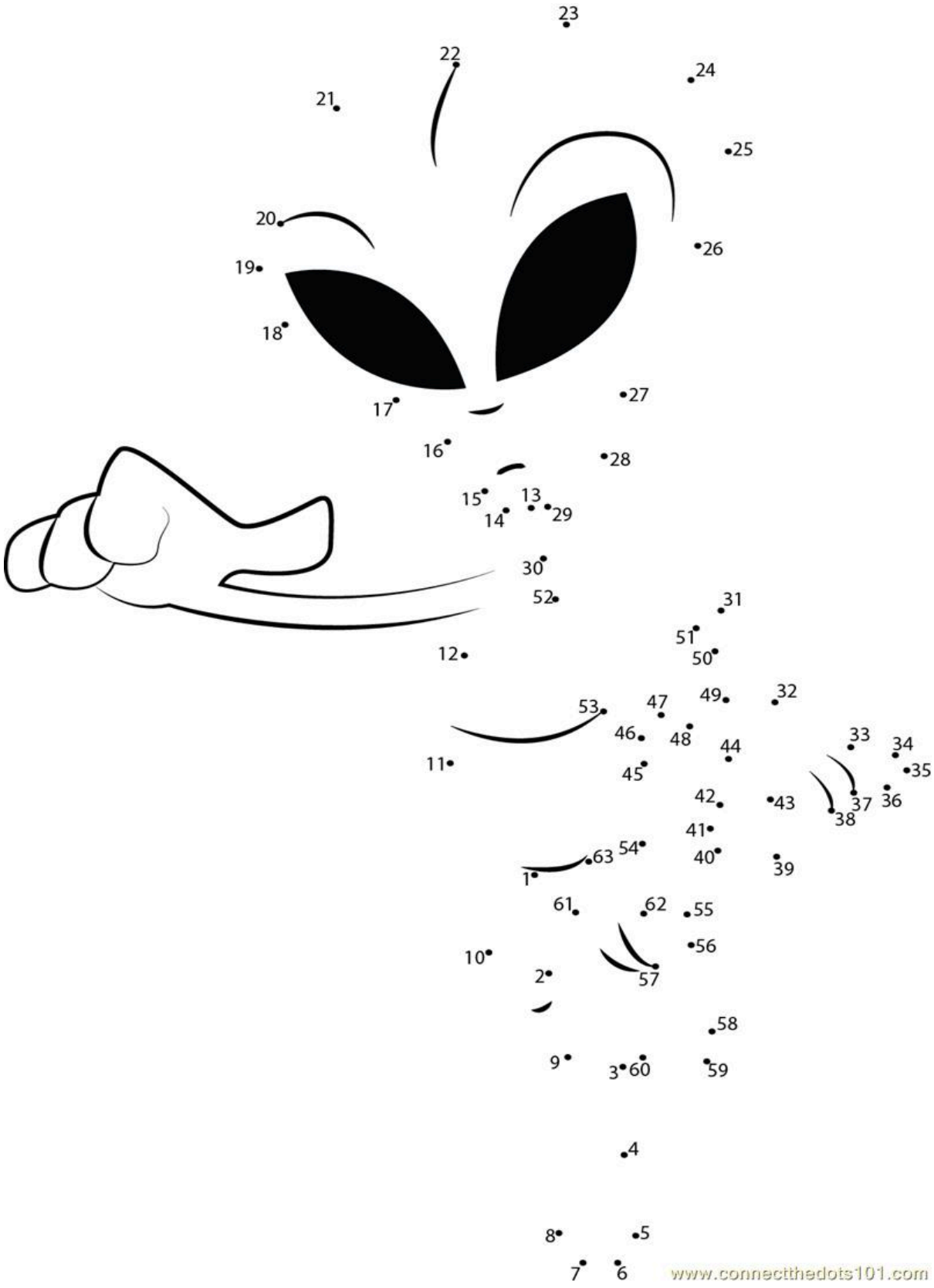
23
22
24
21
25
20
26
19
18
27
17
16
28
15
13
14
29
30
52
31
51
12
50
49
32
53
47
46
48
44
33
34
11
45
35
42
43
37
36
38
41
54
63
40
39
1
61
62
55
56
10
57
2
58
9
3
60
59
4
8
5
7
6
www.connectthedots101.com

HORSE

1.

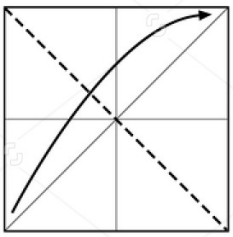

2.

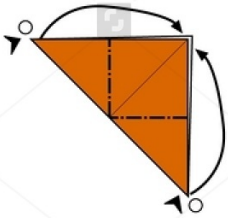

The corners to the inside..

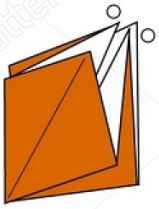

Step **2.** in process..

3.

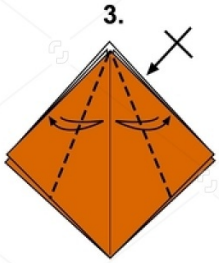

Make the marks in the two sides, front and back..

4.

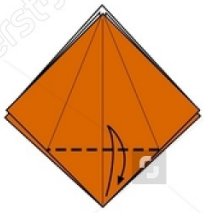

5.

Cut the top layer until the line of the previous step..

6.

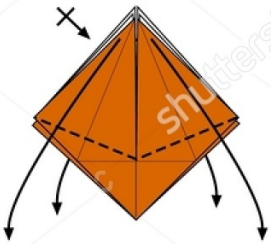

7.

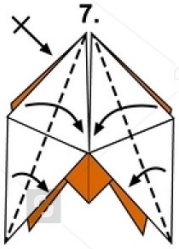

8.

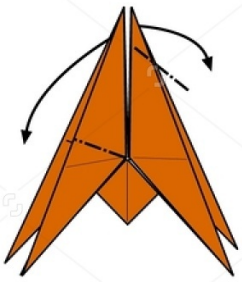

9.

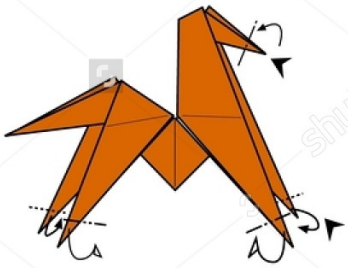

The tips of the legs and the head to the inside..

10.

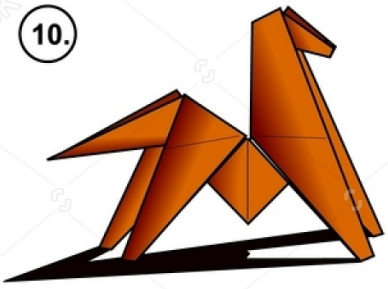

MANDALA
Carla

8 units
rectangles 1:2
/5x10 cm for 12 cm mandala/

DESIGN BY **Maria Sinayskaya**

GoOrigami.com